Eigenmode Distortion Analysis for Motion Cueing Evaluation

In Fixed-Wing Aircraft Simulators

Stanimir Stoev

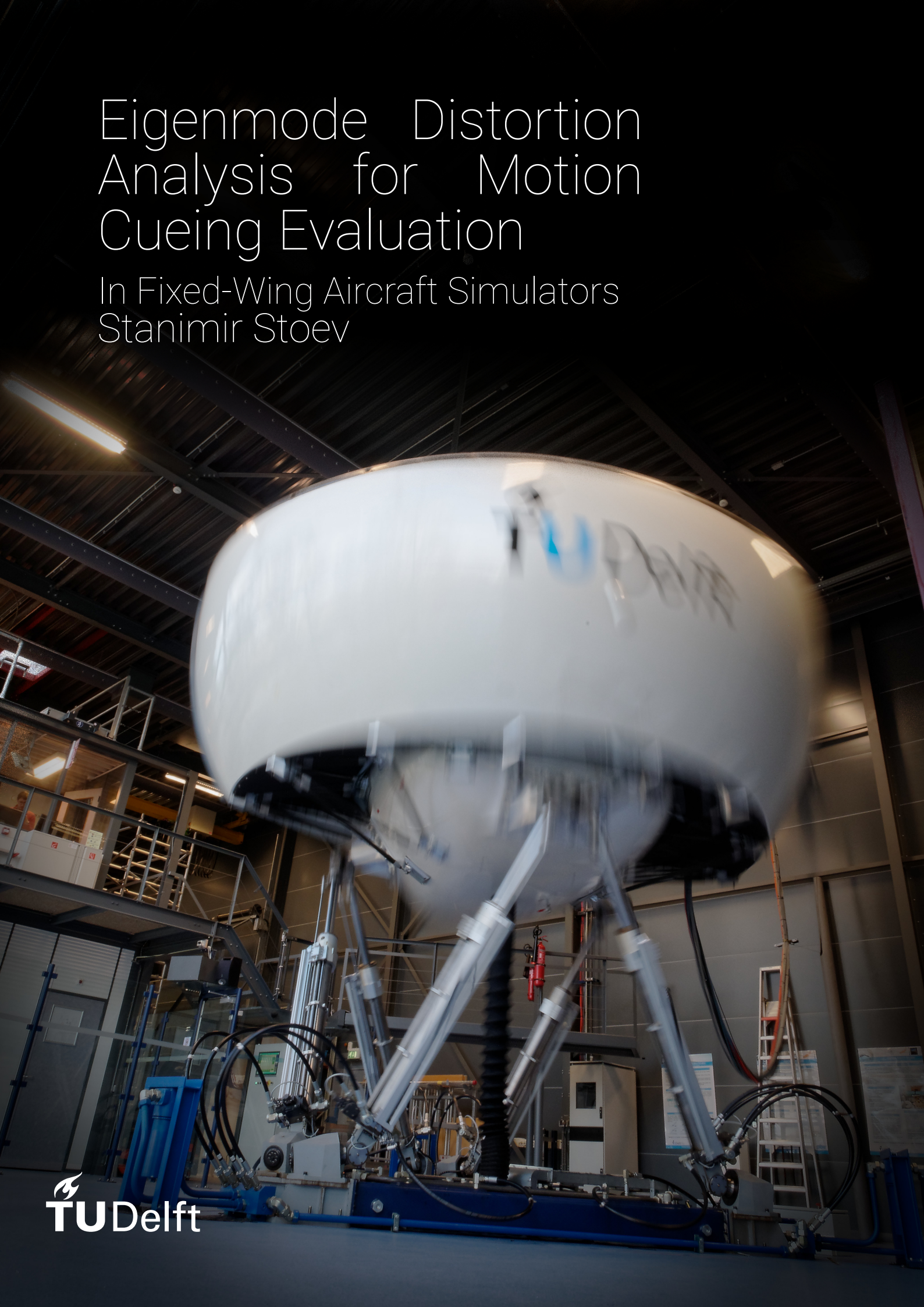

TU Delft

Eigenmode Distortion Analysis for Motion Cueing Evaluation

In Fixed-Wing Aircraft Simulators

MASTER OF SCIENCE THESIS

For obtaining the degree of Master of Science in Aerospace Engineering at Delft University of Technology

Stanimir Stoev

January 14, 2019

Faculty of Aerospace Engineering · Delft University of Technology

DELFT UNIVERSITY OF TECHNOLOGY
DEPARTMENT OF
CONTROL AND SIMULATION

The undersigned hereby certify that they have read and recommend to the Faculty of Aerospace Engineering for acceptance a thesis entitled **"Eigenmode Distortion Analysis for Motion Cueing Evaluation in Fixed-Wing Aircraft Simulators"** by **S. Stoev** in partial fulfilment of the requirements for the degree of **Master of Science**.

Dated: January 14, 2019

Readers:

prof.dr.ir. M. Mulder

dr.ir. M. M. van Paassen

ir. O. Stroosma

dr. B. Shyrokau

Acknowledgments

The process of completing this Master thesis would not have been possible without the help and support from a number of people, to whom I must give my biggest gratitude. I would like to begin with Olaf Stroosma, who suggested the thesis topic to me in the first place. It would be safe to say that he had a major role in piquing my interest in the field of flight simulation and, more specifically, motion research. This is likely to shape the early stages of my professional career. Olaf was always quick to respond to my numerous questions, which occasionally led to long, fruitful discussions. Last but not least, he provided invaluable help with preparing the SIMONA Research Simulator for the piloted experiments.

I would also like to thank Rene van Paassen for his guidance during this thesis project, regarding both its theoretical aspect and my working approach towards the project. The latter was especially helpful in the early stages of the thesis, when he occasionally advised me to take a more 'Zen' approach to my work. Another person responsible for the existence of this project is Ivan Miletović, who is responsible for creating the Eigenmode Distortion analysis method. My discussions with him helped me gain a better understanding of the methodology and were thus an important part of the completion of my project. I must also thank Max Mulder for providing me with an exhaustive feedback on the conference paper that was subsequently submitted to AIAA SciTech conference.

Credit must also be given to my friends and colleagues from 'Control and Simulation', particularly the group of FlexRoom 2.50/2.56, who made the whole experience of working on my thesis a lot more enjoyable than it would otherwise have been. Thank you for all the barbecues, dinners, and beach volleyball games that we had in the scourging hot summer of 2018.

Finally I must express my gratitude to my family and Maggy, who always believed in me and supported me in pursuing my passion for aviation. I would not have made it this far without you.

Stanimir Stoev

Delft University of Technology,

January 14, 2019

Contents

List of Figures

List of Tables

List Of Symbols

Acronyms

CWA	Classical Washout Algorithm
EMD	Eigenmode Distortion
GUI	Graphical User Interface
HP	High Pass
ICAO	International Civil Aviation Organization
LGP	Lower Gimbal Point
LP	Low Pass
LT	Lower Threshold
MCA	Motion Cueing Algorithm
MPF	Mode Participation Factor
MFR	Motion Fidelity Rating
OMCT	Objective Motion Cueing Test
PFG	Primary Flight Display
SP	Short Period
SRS	SIMONA Research Simulator
UGP	Upper Gimbal Point
WC	World Cup

Latin Symbols

$A_{\_}$	Absement [m·s]
A_r	Moving platform platform circle radius [m]
a	Acceleration [m/s^2]
B_r	Lower motion platform circle radius [m]
$C_{m_{\_}}$	Aircraft pitching moment related dimensional stability/control derivative [-]
$C_{X_{\_}}$	Aircraft dimensionless stability/control derivative in the x direction [-]

$C_{Z\_}$	Aircraft dimensionless stability/control derivative in the z direction [-]
D	Half-separation distance, base-frame gimbal pair [mm]
D_c	Dimensionless representation of a time derivative [-]
$\bar{c}$	Mean aerodynamic chord [m]
$\bar{c}$	UGP coordinates with respect to LGP [m]
F	Cumulative distribution function [-]
f_x	Surge specific force [m/s^2]
f_z	Heave specific force [m/s^2]
g	Gravitational acceleration [m/s^2]
h	Altitude [m]
I_{yy}	Mass moment of inertia [kg/m^2]
$K\_$	Filter gain [-]
K_{YY}	Dimensionless representation of a mass moment of inertia [-]
$L_{max,o}$	Motion actuator maximum operational length [mm]
$L_{min,o}$	Motion actuator minimum operational length [mm]
l_x	Horizontal cockpit moment arm [m]
l_z	Vertical cockpit moment arm [m]
$\bar{l}$	Motion actuator length [mm]
$M\_$	Aircraft pitching moment related dimensional stability/control derivative
m	Mass [kg]
q	Pitch rate [rad/s]
$\bar{q}$	Motion actuator absolute length [mm]
P	Half-separation distance,upper-frame gimbal pair [mm]
$\dot{q}$	Pitch rate acceleration [rad/s]
S	Surface Area [m^2]
$S\_$	Displacement [m]
$\bar{S}$	Upper motion platform joint coordinates in the inertial reference frame [m]
T_{bI}	Transformation matrix from the inertial reference plane to the body reference frame
T_{Eb}	Transformation matrix from the body reference plane to the Euler reference frame
T_{Ib}	Transformation matrix from the body reference plane to the inertial reference frame
t	Time [s]

u	Aircraft velocity along the x axis in the stability reference plane [m/s]
$\hat{u}$	Dimensionless aircraft velocity along the x axis in the stability reference plane [-]
$\bar{u}$	State-space system input vector [-]
V	Velocity [m/s^2]
V	Modal matrix [-]
w	Aircraft velocity along the z axis in the stability reference plane [m/s]
$X_{\_}$	Aircraft dimensional stability/control derivative in the x direction
$\bar{x}$	State-space system state vector [-]
$\bar{y}$	State-space system output vector [-]
$Z_{\_}$	Aircraft dimensional stability/control derivative in the z direction
$\bar{z}$	Modal state [-]

Greek Symbols

α	Angle of attack [rad]
α	Moving platform gimbal-pair angle [rad]
β	Base platform gimbal-pair angle [rad]
δ	State perturbation [-]
δ_e	Elevator deflection [rad]
δ_t	Thrust setting [-]
$\delta_{u_{e/t}}$	Pilot input for elevator/thrust setting [rad]
γ_b	Half-separation angle, base-frame gimbals [rad]
λ	Eigenvalue
μ	Object worth [-]
π	Worth parameter [-]
ϕ	Roll angle [rad]
ψ	Yaw angle [rad]
ρ	Density [kg/m^2]
θ	Pitch angle [rad]
ω	Frequency [rad]
σ	Standard deviation
τ	Time constant [-]

ζ	Damping coefficient [-]

Superscripts

b	Element in the body reference frame
c	Combined system dynamics
I	Element in the inertial reference frame
m	MCA related dynamics
mp	Element coupling the MCA related dynamics to the pilot related dynamics
p	Pilot related dynamics
s	Element in the stability reference frame

Subscripts

0	Initial condition
c	Element at the cockpit position
cg	Element at the center of gravity
lp	low pass filtered element
m	MCA dynamics related element
mod	Modal state related element
p	Pilot dynamics related element
ph	Phugoid related element
rot	Element resulting from the purely rotational channel of the MCA
sc	Scaled element
sp	Short period related element
TA	Element resulting from the tilt-align channel of the MCA
z	z axis element
x	x axis element

I

Graduation Paper

1

Paper

Eigenmode Distortion Analysis for Motion Cueing Evaluation in Fixed-Wing Aircraft Simulators

S. Stoev*

The Eigenmode Distortion (EMD) analysis is a novel method for objective evaluation of simulator motion cueing fidelity, developed at Delft University of Technology. It expresses the distortions of the perceived motion cues in terms of the dynamic modes of a linear model of the vehicle and has been applied to assess rotorcraft simulations. This paper presents the adaptation of EMD for fixed wing aircraft, including performing the analysis at the pilot station instead of the centre of gravity. The method is applied to a combined linear model of a Cessna Citation 500 aircraft and the Classical Washout Algorithm (CWA). EMD is compared to the current state-of-the-art objective method, the Objective Motion Cueing Test (OMCT), which does not consider the dynamics of the simulated vehicle in its analysis. The two methods show different results in their cueing fidelity assessment of four CWA configurations. An experiment with six pilots is performed in the SIMONA Research Simulator to test the capability of EMD and OMCT to predict the cueing fidelity as perceived by pilots. The subjects perform pairwise comparisons between the four CWA configurations by exciting the short period dynamics of the aircraft. Results indicate that preferences vary considerably between pilots, causing both EMD and OMCT to show poor, but similar, predictive capabilities.

I. Introduction

The motion cues provided by ground-based flight simulators can usually not fully match the cues present in the real vehicle. Motion Cueing Algorithms (MCAs) are employed to translate the cues calculated by the simulator's vehicle model into simulator motions that fit inside the simulator's motion space. In this process the cues are inevitably distorted, which might decrease the simulator's usefulness in representing reality for the pilot.

The design and tuning of the MCA must reconcile the two competing goals of providing realistic cues and limiting the simulator motion. The most widely used procedure for this process relies heavily on subjective evaluations by experienced pilots [1]. The relative lack of objective metrics to characterize "good" motion can lead to vastly different motion profiles between operational simulators.[2].

The undesirability of a purely subjective evaluation of motion cueing quality was already recognized in the 1970s, when Sinacori [3] proposed a simple gain and phase distortion test of the MCA at a frequency of 1 rad/s, together with boundaries for low, medium, and high fidelity. This was later refined and expanded into tuning procedures based on this test by Schroeder[4] and Gouverneur[5].

Since then further research [6–8] has resulted in the current state-of-the art objective evaluation method: the Objective Motion Cueing Test (OMCT) [9], which is now part of the latest ICAO criteria for qualification of flight simulation training devices [10]. In OMCT, a frequency response analysis of the MCA and motion hardware dynamics is performed for all six axes of motion in twelve frequency points between 0.1 rad/s to 15.97 rad/s thus giving a more complete representation of the motion system's charateristics than the Sinacori test at 1 rad/s.

However, at the time of writing, fidelity regions comparable to the ones proposed by Sinacori and Schroeder are based on the averaged response of ten simulators of various qualification levels and simulated aircraft types [9]. Alternative fidelity criteria based on pilot task performance during flight tasks are investigated [1]. Despite that no definitive fidelity criteria have yet been identified, OMCT has also been used for tuning of the MCA. An example is the study by De Ridder and Roza [11], where OMCT is used in an automatic optimization process of MCA parameters.

*MSc Student,Control and Simulation section, Faculty of Aerospace Engineering, P.O. Box 5058, 2600GB Delft, The Netherlands;s.stoev@student.tudelft.nl

One drawback shared between the method of Sinacori and OMCT is that both tests only evaluate the MCA itself, and in the case of OMCT, the combination with the motion hardware dynamics. The simulated vehicle dynamics are not included in either test, and it is assumed that the MCA response to motion cues provided by the vehicle model is sufficiently similar to the combined responses of the individual motion axis responses tested in the Sinacori test or OMCT. Recent work by Dalmeijer et al.[12] indicates that cross-couplings and other non-linearities in the MCA might interact with vehicle dynamics to further amplify or attenuate certain cues at certain frequencies in ways that are not apparent in an OMCT evaluation. In order to further study this problem, a new objective method for motion cueing fidelity analysis, named Eigenmode Distortion (EMD), is developed by Miletović et al. [13]. EMD evaluates the distortions of the perceived motion cues imposed by the MCA while taking the dynamics of the simulated vehicle into account. This is made possible by coupling the dynamics of the MCA and the vehicle into a single combined system, enabling the representation of the human perceived motion cues in terms of the *dynamic modes* of the vehicle. Originally EMD was developed for and applied in rotorcraft simulation [13].

The purpose of this study is to investigate the use of EMD in fixed-wing aircraft simulations. To this end EMD is applied to a linear model of a Cessna Citation 500 for symmetric flight and the Classical Washout Algorithm (CWA) [14] used as the MCA. In addition, EMD is compared to OMCT for four CWA configurations. The capability of both methods to predict the cueing fidelity as perceived by pilots is tested in a piloted experiment in the SIMONA Research Simulator (SRS) [15] at the Delft University of Technology.

This paper is structured as follows. The general principles of EMD and its adaptation for use in fixed-wing aircraft is examined in Section II, followed by the practical application of EMD and comparison to OMCT in Section III. Next, the experiment to evaluate EMD's capabilities is discussed in Section IV with the results being shown in Section V. The paper ends with a discussion in Section VI and in Section VII the conclusions are given.

II. EMD application in fixed-wing aircraft

A. Main principles of the methodology

The current state-of-the-art method for objective evaluation of the motion cueing fidelity − the Objective Motion Cueing Test (OMCT) − analyses the frequency response of the Motion Cueing System (MCS) to a set of sine-wave input signals for the human perceived motion cues − specific forces and angular rates along all six simulator axes. The same input signals are used irrespective of the aircraft type being simulated. While OMCT gives a very detailed picture on the combined performance of the Motion Cueing Algorithm (MCA) and the motion hardware dynamics, its input signals do not realistically represent motions experienced during simulations of different aircraft types [16]. In addition, the response to each signal is studied in isolation, while the motions of the aircraft, and consequently the cues sent to the MCA, are linked through the vehicle dynamics.

The Eigenmode Distortion (EMD) analysis aims to address these shortcomings. It approaches the evaluation of the motion cueing fidelity from a different perspective. While OMCT analysis is performed in the frequency domain, EMD investigates the distortion of the motion cues imposed by the MCA in terms of eigenvectors representing the dynamic modes of the simulated vehicle. In this paper a typical fixed-wing aircraft will be considered. In the EMD analysis, linear dynamic models for the aircraft and MCA are used. They are presented respectively in Eq. (1) for symmetric flight and Eq. (2) for longitudinal motions. Here the p superscript refers to the dynamics experienced by the pilot and the m superscript to the MCA dynamics. The δ notation indicates that the states and inputs are in fact perturbations relative to the initial condition. Furthermore, while on the one hand the aircraft state vector $\delta^p_{\bar{x}}$ is known from classical flight dynamics, the exact formulation of $\delta^m_{\bar{x}}$ depends on the used MCA. On the other hand, the MCA inputs $\delta^m_{\bar{u}}$ are universal and consist of the reference motion cues (or human perceived quantities):

$$\begin{aligned} \dot{\delta}^p_{\bar{x}} &= A^p \delta^p_{\bar{x}} + B^p \delta^p_{\bar{u}} \\ \delta^p_{\bar{x}} &= \begin{bmatrix} \delta_u & \delta_w & \delta_\theta & \delta_q \end{bmatrix}^T \\ \delta^p_{\bar{u}} &= \begin{bmatrix} \delta_{\delta_e} & \delta_{\delta_t} \end{bmatrix}^T \end{aligned} \tag{1}$$

$$
\begin{aligned}
\dot{\delta}^m_{\bar{x}} &= A^m \delta^m_{\bar{x}} + B^m \delta^m_{\bar{u}} \\
\delta^m_{\bar{u}} &= \begin{bmatrix} \delta_{f_{x_p}} & \delta_{f_{z_p}} & \delta_{q_p} \end{bmatrix}
\end{aligned}
\tag{2}
$$

The EMD analysis is made possible by effectively combining the linear dynamic systems of the aircraft and the MCA into a single system which is excited only by the pilot inputs $\delta^p_{\bar{u}}$, as seen in Eq. (3). This is achieved through adding the perturbed specific forces $\delta_{f_{x_p}}$ and $\delta_{f_{z_p}}$ to the aircraft state vector $\delta^p_{\bar{x}}$ which are in turn given as inputs to the MCA dynamics through the A^{mp} matrix. The end result is a new combined system matrix A^c with a corresponding state vector $\delta^c_{\bar{x}}$ [13].

$$
\begin{aligned}
\begin{pmatrix} \dot{\delta}^p_{\bar{x}} \\ \dot{\delta}^m_{\bar{x}} \end{pmatrix} &= \begin{bmatrix} A^p & 0 \\ A^{mp} & A^m \end{bmatrix} \begin{pmatrix} \delta^p_{\bar{x}} \\ \delta^m_{\bar{x}} \end{pmatrix} + \begin{bmatrix} B^p \\ 0 \end{bmatrix} \begin{pmatrix} \delta^p_{\bar{u}} \\ 0 \end{pmatrix} = A^c \delta^c_{\bar{x}} + B^c \delta \bar{u}^c \\
\begin{pmatrix} \delta^p_{\bar{y}} \\ \delta^m_{\bar{y}} \end{pmatrix} &= \bar{y}^c = C^c \delta^c_{\bar{x}} \\
\delta^p_{\bar{y}} &= \begin{bmatrix} \delta_{f_{x_p}} & \delta_{f_{z_p}} & \delta_{q_p} \end{bmatrix} \\
\delta^p_{\bar{y}} &= \begin{bmatrix} \delta_{f_{x_m}} & \delta_{f_{z_m}} & \delta_{q_m} \end{bmatrix}
\end{aligned}
\tag{3}
$$

As a result of this formulation of the combined system, the eigenmodes of the simulated vehicle that can be obtained from the A^p matrix are carried over to the combined system matrix A^c. Furthermore, by employing a modal coordinate transformation, as will be explained in Section II.C, the combined aircraft and simulator motion cues (defined in matrix A^c) can be expressed as (potentially complex) eigenvectors related to the original aircraft eigenmodes. This in turn enables a systematic analysis of the degree to which the simulator motion cue eigenvectors are distorted in magnitude and phase with respect to the aircraft motion cues. Through showing the eigenvectors in the complex plane one can investigate the distortions of all dynamics caused by the MCA.

It is important to clarify that the EMD analysis captures *only* the linear dynamics of the *perturbed* human perceived quantities. Therefore the analysis is valid only close to the given initial condition. If it is desired to evaluate a broader region of the flight envelope, EMD must be performed across multiple points which are subsequently connected by techniques such as gain scheduling. In order to simplify the notations for the remainder of the paper, the δ notation is dropped from the states, inputs and outputs.

B. Application to a linear aircraft model

In this paper, the application of EMD in symmetric flight conditions will be studied. They are described with the dimensional symmetric equations of motion, presented in Eq. (4), that originate from classical flight dynamics. There the influence of the aircraft dynamics can be seen through the stability and control derivatives. It must be stated that the aircraft model used in this study is defined in the stability reference frame, indicating that a transformation is required to express the perceived cues in the pilot-aligned body reference frame. The equations of motion can also be represented in a state-space form, which forms the basis for the A^p and B^p matrices in Eq. (1):

$$
\begin{aligned}
-W \cos\theta_0 \theta + X_u u + X_w w + X_q q + X_{\delta_e} \delta_e + X_{\delta_t} \delta_t &= m\dot{u} \\
-W \sin\theta_0 \theta + Z_u u + Z_w w + Z_{\dot{w}} \dot{w} + Z_q q + Z_{\delta_e} \delta_e + Z_{\delta_t} \delta_t &= m(\dot{w} - qV) \\
M_u u + M_w w + M_{\dot{w}} \dot{w} + M_{\delta_e} \delta_e + M_{\delta_t} \delta_t &= I_{yy} \dot{q} \\
\dot{\theta} &= q
\end{aligned}
\tag{4}
$$

As already stated, $\bar{x}^p$ must be further extended by the inclusion of the specific forces as states in order to enable the coupling of both systems. In turn, the A^p matrix is modified to include the necessary equations for the new states.

State representation of f_{x_p} and f_{z_p}

The specific force can be defined as the non-gravitationally induced acceleration [14]. Therefore, the gravity related components must be removed from the first two equations of motion in Eq. (4) to obtain expressions for the specific forces at the centre of gravity:

$$\begin{aligned} f^s_{x_{cg}} &= \frac{X_u}{m}u + \frac{X_w}{m}w + \frac{X_q}{m}q + \frac{X_{\delta_e}}{m}\delta_e + \frac{X_{\delta_t}}{m}\delta_t \\ f^s_{z_{cg}} &= \frac{Z_u}{m}u + \frac{Z_w}{m}w + \frac{Z_{\dot{w}}}{m}\dot{w} + \frac{Z_q}{m}q + \frac{Z_{\delta_e}}{m}\delta_e + \frac{Z_{\delta_t}}{m}\delta_t \end{aligned} \tag{5}$$

However, the MCA requires the specific forces to be defined in the body reference frame. Therefore $f^s_{x_{cg}}$ and $f^s_{z_{cg}}$ must be transformed from the stability frame to the body frame, as demonstrated in Eq. (6). Here α_0 denotes the initial condition for angle of attack in the body reference frame, since, by definition, the initial angle of attack in the stability reference frame is 0. The transformation is not needed if the used aircraft model is already defined in the body reference frame.

$$\begin{aligned} f^b_{x_{cg}} &= f^s_{x_{cg}} \cos\alpha_0 - f^s_{z_{cg}} \sin\alpha_0 \\ f^b_{z_{cg}} &= f^s_{z_{cg}} \cos\alpha_0 + f^s_{x_{cg}} \sin\alpha_0 \end{aligned} \tag{6}$$

The final step to arrive at the complete expressions is to move the specific forces to the pilot station. This is an important requirement for the EMD implementation for fixed-wing aircraft, and in contrast to the application of the method in rotorcraft, where the cues can typically be evaluated at the vehicle centre of gravity (CG) [13]. In fixed-wing aircraft the pilot is often located a large distance in front of the CG, which is quantified by the horizontal and vertical cockpit moment arms l_x and l_z, see Fig. 1. Together with the pitch rotation acceleration these arms can considerably affect the specific forces perceived by the pilot from the ones at the centre of gravity as shown in Fig. 1 and Eq. (7). The extent to which this happens depends on the evaluated aircraft type. For example this effect will be more pronounced on an airliner than on a business jet, since the former aircraft tend to have larger cockpit moment arms than the latter.

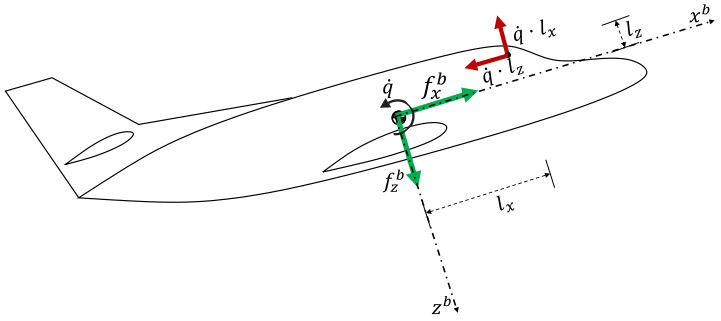

Fig. 1 Influence of the pitch acceleration on the specific forces at the pilot position

$$\begin{aligned} f_{x_p} &= f^b_{x_{cg}} - \dot{q}l_z \\ f_{z_p} &= f^b_{z_{cg}} - \dot{q}l_x \end{aligned} \tag{7}$$

To arrive at the state-space representation of f_{x_p} and f_{z_p}, their time derivative is found by differentiating their expressions obtained from combining Eqs. (5) to (7). In this process the time derivatives of the pilot inputs δ_e and δ_t are found by approximating their associated actuator dynamics as a first order lag filter as demonstrated in Eqs. (8) and (9). There $\delta_{u_{e/t}}$ stands for the pilot input for the elevator or thrust setting, while $\tau_{e/t}$ is the corresponding time constant. The

actuator dynamics approximation results in δ_e and δ_t being moved to the vehicle state vector and δ_{u_e} and δ_{u_t} form the new input vector.

$$H_{\delta_{e/t}} = \frac{1}{\tau_{e/t}s + 1} \tag{8}$$

$$\dot{\delta}_{e/t} = \delta_{u_{e/t}} - \frac{1}{\tau_{e/t}}\delta_{e/t} \tag{9}$$

It must be stated that the values of the time constants $\tau_{e/t}$ have no influence on the final eigenvector distortions of the motion cues. This behaviour is expected, since even though the actuator dynamics affect the aircraft motion cues, the latter are used only as the inputs in the MCA dynamics and therefore have no influence on them. However, in the specific case that the MCA also uses δ_e and δ_t as inputs, the values of $\tau_{e/t}$ must be selected to represent the simulated aircraft and flight condition. In the current analysis, the MCA does not rely on the pilot inputs and $\tau_{e/t} = 0.01$.

This concludes the derivation of the state-space representation of f_{x_p} and f_{z_p}. The resulting aircraft state and input vectors $\bar{x}^p$ and $\bar{u}^p$ are presented in Eq. (10) together with the total system output, vector $\delta^p_{\bar{y}}$.

$$\begin{aligned}
\bar{x}^p &= \begin{bmatrix} u & v & w & \theta & q & \delta_e & \delta_t & f_{x_p} & f_{z_p} & \dot{q} \end{bmatrix}^T \\
\bar{u}^p &= \begin{bmatrix} \delta_{u_e} & \delta_{u_t} \end{bmatrix}^T \\
\bar{y}^p &= \begin{bmatrix} q & f_{x_p} & f_{z_p} \end{bmatrix}^T
\end{aligned} \tag{10}$$

Linearization of the MCA

In this study, the used MCA is the Classical Washout Algorithm (CWA) [14], shown in Fig. 2. Since only the longitudinal motions will be analyzed, it is assumed that $\phi_m = \psi_m = 0°$. The algorithm is highly non-linear, and therefore has to be linearized so it can be used in the EMD analysis. It must be noted that the inputs to the CWA in fact represent the deviations from their initial conditions and the δ notation is omitted for simplification.

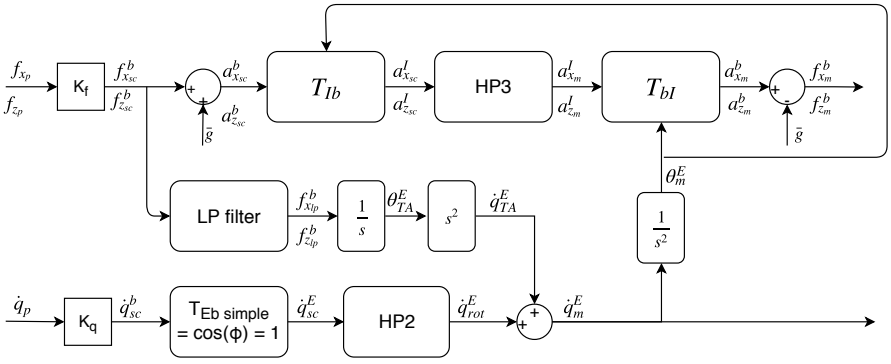

Fig. 2 The Classical Washout Algorithm adapted for longitudinal motions [14]

The different components of the CWA are presented from Eq. (11) to Eq. (15)

$$T_{Ib} = \begin{bmatrix} \cos\theta_m & \sin\theta_m \\ -\sin\theta_m & \cos\theta_m \end{bmatrix}; \quad T_{bI} = \begin{bmatrix} \cos\theta_m & -\sin\theta_m \\ \sin\theta_m & \cos\theta_m \end{bmatrix} \tag{11}$$

$$\bar{g} = \begin{bmatrix} -g\sin\theta_m \\ g\cos\theta_m \end{bmatrix} \approx \begin{bmatrix} -g\theta_m \\ g \end{bmatrix} \tag{12}$$

$$HP3 = \frac{s^2}{s^2 + 2\zeta_{hp}\omega_{n_{hp}}s + \omega_{n_{hp}}^2}\frac{s}{s+\omega_b} = \frac{s^3}{s^3 + A_{hp_3}s^2 + B_{hp_3}s + C_{hp_3}} \tag{13}$$
$$A_{hp_3} = 2\zeta_{hp}\omega_{n_{hp}} + \omega_b \qquad B_{hp_3} = \omega_{n_{hp}}^2 + 2\zeta_{hp}\omega_{n_{hp}}\omega_b \qquad C_{hp_3} = \omega_{n_{hp}}^2\omega_b$$

$$HP2 = \frac{s^2}{s^2 + 2\zeta_{hp}\omega_{n_{hp}}s + \omega_{n_{hp}}^2} = \frac{s^2}{s^2 + A_{hp_2}s + B_{hp_2}} \tag{14}$$
$$A_{hp_2} = 2\zeta_{hp}\omega_{n_{hp}} \qquad B_{hp_2} = \omega_{n_{hp}}^2$$

$$LP = \frac{\omega_{n_{lp}}^2}{s^2 + 2\zeta_{lp}\omega_{n_{lp}}s + \omega_{n_{lp}}^2} = \frac{B_{lp}}{s^2 + A_{lp}s + B_{lp}} \tag{15}$$
$$A_{lp} = 2\zeta_l p\omega_{n_{lp}} \qquad B_{lp} = \omega_{n_{lp}}^2$$

The transformation matrices (T_{Ib},T_{bI}) and the gravity component vector $\bar{g}$ introduce the non-linearities in the system. A small angle approximation can be made in $\bar{g}$, as indicated in Eq. (12). The linearization of the equations resulting from T_{Ib} and T_{bI} are shown in Eq. (16) and Eq. (17) respectively. One must bear in mind that the initial conditions for $a^b_{x_{sc(aled)}}$, $a^b_{z_{sc(aled)}}$, $a^I_{x_m}$ and $a^I_{z_m}$ used in the linearization are equal to zero, since these are not the true states, but rather the deviations from the true initial conditions.

$$\begin{aligned} a^I_{x_{sc}} &= \quad a^b_{x_{sc}}\cos\theta_m + a^b_{z_{sc}}\sin\theta_m \quad \approx a^b_{x_{sc}} \\ a^I_{z_{sc}} &= -a^b_{x_{sc}}\sin\theta_m + a^b_{z_{sc}}\cos\theta_m \quad \approx a^b_{z_{sc}} \end{aligned} \tag{16}$$

$$\begin{aligned} a^b_{x_m} &= a^I_{x_m}\cos\theta_m - a^I_{z_m}\sin\theta_m \quad \approx a^I_{x_m} \\ a^b_{z_m} &= a^I_{x_m}\sin\theta_m + a^I_{z_m}\cos\theta_m \quad \approx a^I_{z_m} \end{aligned} \tag{17}$$

After the linearization has been completed, the high-pass and low-pass filters can be transformed from their Laplace domain transfer function form to a state-space form. This results in formulating the state-space model of the complete linearised CWA model, shown in Eq. (18) and Eq. (19), with the matrix definitions presented in Eq. (22) and Eq. (23). The state and input vectors ($\delta^m_{\bar{x}}$,$\delta^m_{\bar{u}}$) are defined in Eq. (20) and Eq. (21), where A^I_{x/z_m}, S^I_{x/z_m}, V^I_{x/z_m} are the inertial simulator absement (integrated displacement), displacement and velocity in the surge and heave axes. The inputs are the aircraft surge and heave specific forces at the cockpit (f_{x_c}, f_{z_c}) and the aircraft pitch acceleration $\dot{q}$.

$$\dot{\delta}^m_{\bar{x}} = A^m\delta^m_{\bar{x}} + B^m\delta^m_{\bar{u}} \tag{18}$$

$$y = \begin{bmatrix} q_m \\ f^b_{x_m} \\ f^b_{z_m} \end{bmatrix} = C^m\delta^m_{\bar{x}} + D^m\delta^m_{\bar{u}} \tag{19}$$

$$\delta^m_{\bar{x}} = \begin{bmatrix} A^I_{x_m} & S^I_{x_m} & V^I_{x_m} & A^I_{z_m} & S^I_{z_m} & V^I_{z_m} & \theta_{rot} & q_{rot} & \theta_{TA} & q_{TA} & \theta_m & q_m \end{bmatrix}^T \tag{20}$$

$$\delta^m_{\bar{u}} = \begin{bmatrix} f_{x_c} & f_{z_c} & \dot{q} \end{bmatrix}^T \tag{21}$$

$$A^m = \begin{bmatrix} 0 & 1 & 0 & 0 & 0 & 0 & 0 & 0 & 0 & 0 & 0 & 0 \\ 0 & 0 & 1 & 0 & 0 & 0 & 0 & 0 & 0 & 0 & 0 & 0 \\ -C_{hp_x} & -B_{hp_x} & -A_{hp_x} & 0 & 0 & 0 & 0 & 0 & 0 & 0 & -g & 0 \\ 0 & 0 & 0 & 0 & 1 & 0 & 0 & 0 & 0 & 0 & 0 & 0 \\ 0 & 0 & 0 & 0 & 0 & 1 & 0 & 0 & 0 & 0 & 0 & 0 \\ 0 & 0 & 0 & -C_{hp_z} & -B_{hp_z} & -A_{hp_z} & 0 & 0 & 0 & 0 & 0 & 0 \\ 0 & 0 & 0 & 0 & 0 & 0 & 0 & 1 & 0 & 0 & 0 & 0 \\ 0 & 0 & 0 & 0 & 0 & 0 & -B_{hp_q} & -A_{hp_q} & 0 & 0 & 0 & 0 \\ 0 & 0 & 0 & 0 & 0 & 0 & 0 & 0 & 0 & 1 & 0 & 0 \\ 0 & 0 & 0 & 0 & 0 & 0 & 0 & 0 & -B_{lp} & -A_{lp} & 0 & 0 \\ 0 & 0 & 0 & 0 & 0 & 0 & 0 & 0 & 0 & 0 & 0 & 1 \\ 0 & 0 & 0 & 0 & 0 & 0 & -B_{hp_q} & -A_{hp_q} & -B_{lp} & -A_{lp} & 0 & 0 \end{bmatrix} \tag{22}$$

$$C^m = \begin{bmatrix} 0 & 0 & 0 & 0 & 0 & 0 & 0 & 0 & 0 & 0 & 0 & 1 \\ -C_{hp_x} & -B_{hp_x} & -A_{hp_x} & 0 & 0 & 0 & 0 & 0 & 0 & 0 & 0 & 0 \\ 0 & 0 & 0 & -C_{hp_z} & -B_{hp_z} & -A_{hp_z} & 0 & 0 & 0 & 0 & 0 & 0 \end{bmatrix}$$

$$B^m = \begin{bmatrix} 0 & 0 & 0 \\ 0 & 0 & 0 \\ K_x & 0 & 0 \\ 0 & 0 & 0 \\ 0 & 0 & 0 \\ 0 & K_z & 0 \\ 0 & 0 & 0 \\ 0 & 0 & K_q \\ 0 & 0 & 0 \\ K_x \frac{B_{lp}}{g} & 0 & 0 \\ 0 & 0 & 0 \\ K_x \frac{B_{lp}}{g} & 0 & K_q \end{bmatrix} \qquad D^m = \begin{bmatrix} 0 & 0 & 0 \\ K_x & 0 & 0 \\ 0 & K_z & 0 \end{bmatrix} \tag{23}$$

Coupling of the two systems

The coupling of the aircraft and MCA linear systems is done through the A^{mp} matrix as was previously stated. Because the aircraft motion cues are present in its state vector, the A^{mp} can be directly constructed from the simulator input matrix B^m. The same process is repeated for the construction of the coupled system output matrix C^c, where C^{mp} effectively binds the MCA outputs to the aircraft dynamics, as seen in Eq. (24). The definitions for A^{mp} and C^{mp} are in turn shown in Eq. (25), in which D^m represents the MCA feedthrough matrix.

$$C^c = \begin{bmatrix} C^p & 0 \\ C^{mp} & C^m \end{bmatrix} \tag{24}$$

$$A^{mp} = [0 \quad B^m] \qquad C^{mp} = [0 \quad D^m] \tag{25}$$

C. Distorted eigenvector analysis

The final component of the EMD methodology is finding the extent of the distortion of the aircraft motion cues by the MCA dynamics. The combined system formulation presented in Eq. (3) enables the representation of the perceived

motion cues as components of the eigenvectors of the A^c matrix, which also describe the vehicle dynamic modes. In Eq. (10) it can be observed that the aircraft motion cues f_{x_p}, f_{z_p}, and q are already part of $\bar{x}^p$ and are thus represented in the eigenvectors of A^c. The same, however, is not valid for the motion cues in the simulator f_{x_m}, f_{z_m}, and q_m. As a result of the system coupling, these are expressed as a combination of aircraft and simulator states, which is observed in Eqs. (3), (24) and (25). Thus, in order to relate the simulator motion cues to the vehicle dynamic modes a *modal coordinate transformation* needs to be performed [17].

The modal coordinate transformation is in principle a change of basis of the system defined by A^c,B^c,C^c and D^c matrices. This is done with the help of the modal matrix V, defined in Eq. (26), where V contains the right eigenvectors of A^c corresponding to the eigenvalues λ_c [17]:

$$A^c V = \lambda_c V \tag{26}$$

In general it is assumed that there are n distinct eigenvalues, thus making V invertible. This assumption is valid for the current formulation of A^c. The modal matrix is used to define a new state vector − the modal state $\bar{z}$ and corresponding matrices, presented in Eqs. (27) to (30):

$$\bar{z} = V^{-1}\bar{x}^c \tag{27}$$

$$\dot{\bar{z}} = (V^{-1}A^c V)\bar{z} + (V^{-1}B^c)\bar{u}^c \tag{28}$$

$$\bar{y}^c = (C^c V)\bar{z} = C_{mod}\bar{z} \tag{29}$$

$$C_{mod} = \begin{bmatrix} f_{x_{p_{mod}}} & f_{z_{p_{mod}}} & q_{mod} & f_{x_{m_{mod}}} & f_{z_{m_{mod}}} & q_{m_{mod}} \end{bmatrix}^T \tag{30}$$

The new modal output matrix C_{mod} contains the motion cue components of all eigenvectors of A^c expressed in terms of the modal state $\bar{z}$ as shown in Eq. (29). The simulator-related entries in C_{mod} are therefore connected to the dynamic modes of the aircraft through $\bar{z}$. For the aircraft-related motion cues the rows in C_{mod} are equivalent to rows in V, which correspond to f_{x_p}, f_{z_p} and q. The end result is that it is possible to do a direct comparison between the motion of the aircraft and the motion cues produced by the simulator, all expressed as eigenvectors of the combined system. The comparison is then visualized by plotting all motion cue eigenvectors in the complex plane.

An example visualization of the distorted eigenvectors is presented in Fig. 3, where the used MCA is taken from [18] and is applied on a Cessna Citation 500 linear model. The solid and dashed lines represent the motion cue eigenvector components of, respectively, the aircraft and the simulator. The eigenvectors in Fig. 3a and Fig. 3b in turn correspond to the eigenvalues of the short period and phugoid eigenmodes. The aircraft related eigenvectors have different magnitude and phase relations to one another that originate from the aircraft model. Therefore they remain fixed and do not change with the MCA parameters. The relations between the MCA related eigenvectors change when altering the MCA parameters.

It is important to note that the comparison of eigenvector magnitudes can only be made for the same motion cues due to their different dimensions. For example in Fig. 3 it can be seen that f_{z_p} has a much higher amplitude than q_p for both eigenmodes. However, it would be wrong to conclude that f_{z_p} is a more dominant motion cue than q_p in these eigenmodes.

The magnitude distortion of an eigenvector can be defined as the ratio of the magnitudes of the simulator eigenvector with respect to the aircraft eigenvectors. For example, in Fig. 3a it is observed that $|f_z|_{sp} = \frac{|f_{z_m}|_{sp}}{|f_{z_p}|_{sp}} = 0.73$. Similarly, the phase distortion is characterized by the angle between the aircraft and simulator eigenvector. If the eigenvectors corresponding to the positive conjugate eigenvalues are visualized, counter-clockwise and clockwise phase distortions indicate, respectively, phase lead and phase lag. For example in Fig. 3a f_{z_m} has a phase distortion of 87 degrees counter-clockwise ($\angle(f_z)_{sp} = 87°$ lead), while q_m has a 13 degree clockwise distortion in phase ($\angle(q)_{sp} = 13°$ lag). The magnitude distortion for q_m is pronounced with $|q|_{sp} = 0.43$, while f_{x_m} has a good level of magnitude and phase distortions: $|f_x|_{sp} = 0.77$, and $\angle(f_x)_{sp} = 33°$ lead.

The eigenvector distortions can also be seen in the time domain. Consider that a system is excited with eigenmode i, which is described by a pair of complex conjugate eigenvectors v_i and v_i^*. This is visualized in the time domain through the zero-input response of the system to an initial condition of $2Re(v_i)$. The distortions related to the short period are

presented in Fig. 4a. Here it can be observed that f_{x_m} is slightly leading f_{x_p} while having a slightly lower amplitude, corresponding with the eigenvector distortions. Similar observations that correlate to Fig. 3a can be made for f_z and q.

The EMD analysis for the phugoid is presented in Fig. 3b. Immediately it is noticeable that the pitch and heave motion cues in the simulator are almost non-existent: $\angle(f_z)_{phug} = 108°$ lag, $|f_z|_{phug} = 5.65 \cdot 10^{-4}$ and $\angle(q)_{phug} = 101°$ lag, $|q|_{phug} = 0.097$. The surge cues are less distorted: $\angle(f_x)_{phug} = 16°$ lag, $|f_x|_{phug} = 0.71$. The time domain representation of the phugoid distortions is shown in Fig. 4b, where f_{z_m} and q_m are essentially zero.

Finally, the modal coordinate transformation results in a parameter presenting the modal response of the system in the time domain. This is the absolute value of the complex modal state $\bar{z}$ that gives information on the participation of each mode in the system response [13]. This measure is called a *Mode Participation Factor* (MPF) and its integrated value over a given time gives an indication of the relative contribution of each mode in a particular maneuver.

D. Proposed criteria for filter tuning

The currently proposed tuning approach used with EMD aims to preserve the aircraft motion cues in the simulator for one eigenmode of choice while using as much as possible from the available motion space. This is achieved by tuning with the following criteria shown in their order of importance:

1) Minimize the phase distortions of all motion cues.
2) Maintain the relative phases between the motion cues. This effectively translates to all motion cues having phase lag or phase lead distortions of similar proportions.
3) Minimize the magnitude distortions of all motion cues.
4) Attempt to maintain a similar magnitude distortion level for all motion cues.

After the tuning process is completed, it needs to be checked whether motion platform exceeds the available motion space for a desired task or manoeuvre. If the space is exceeded, the tuning process is repeated until the actuator length limits are no longer reached.

Finally, it must be stated that these criteria used for tuning are not necessarily optimal and are based on the current interpretation of EMD. Future research might prove that better approaches exist.

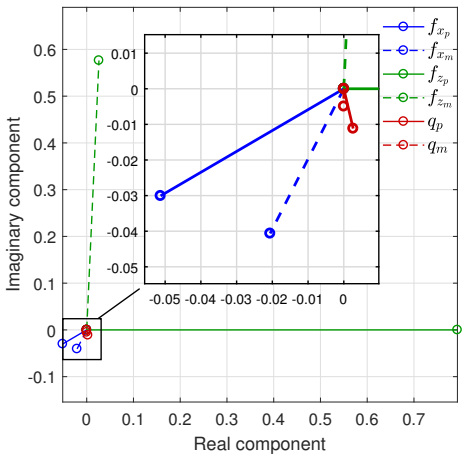

(a) Short Period, $\lambda_{sp} = -2.0362 \pm 3.0513i$

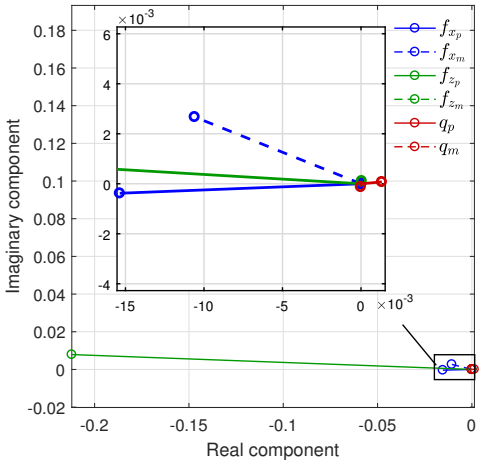

(b) Phugoid, $\lambda_{ph} = -0.0124 \pm 0.1149i$

Fig. 3 Example for eigenvector distortion plots

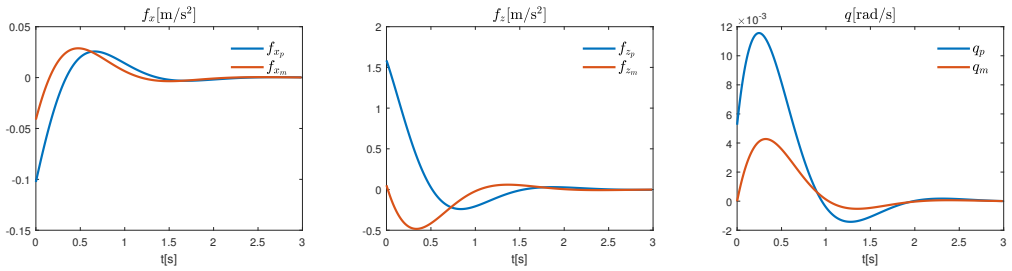

(a) Short period eigenmode

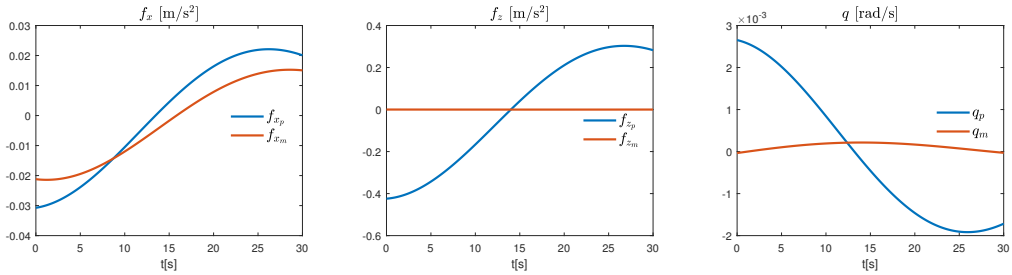

(b) Phugoid eigenmode

Fig. 4 Time histories of separately exciting the two eigenmodes of the aircraft

III. Practical application of EMD and comparison to OMCT

In this study the EMD analysis is applied to a linear model of the Cessna Citation 500 in cruise configuration, which is presented in Table 1. The goal is to arrive at configurations which accurately simulate one of the two eigenmodes.

Table 1 The Cessna Citation I (dimensionless) linear model parameters

C_{X_0}	= -0.0277	C_{Z_0}	= -0.216	C_{m_0}	= 0.213	m	= 5207 [kg]
C_{X_u}	= -0.0698	C_{Z_u}	= -0.4702	C_{m_u}	= 0.0561	S	= 24.2 [m^2]
C_{X_α}	= 0.0744	C_{Z_α}	= -5.6149	C_{m_α}	= -0.4982	$\bar{c}$	= 2.022 [m]
$C_{X_{\dot{\alpha}}}$	= 0.0259	$C_{Z_{\dot{\alpha}}}$	= -0.2039	$C_{m_{\dot{\alpha}}}$	= 0.1689	V	= 160.03 [m/s]
C_{X_q}	= -0.4179	C_{Z_q}	= -5.8339	C_{m_q}	= -10.152	h	= 5000 [m]
$C_{X_{\delta e}}$	= -0.0131	$C_{Z_{\delta e}}$	= -0.5814	$C_{m_{\delta e}}$	= -1.2269	ρ	= 0.7361 [kg/m^3]
$C_{X_{\delta_t}}$	= 0	$C_{Z_{\delta_t}}$	= 0	$C_{m_{\delta_t}}$	= 0	K_{YY}	= 1.114 [-]

The short period eigenmode is selected for tuning of the configurations. It is preferred to the phugoid since motion simulators are better suited to emulating high-frequency accelerations than ones of low-frequency due to the limited motion space [14]. Furthermore, magnitude and phase distortions become more prominent during precision control tasks and do not influence the fidelity of large amplitude manoeuvres [19]. The short period eigenmode is a better representative of the former. Moreover, in order for the phugoid to be the dominant eigenmode in a manoeuvre a large deviation from the initial trim condition is needed. This can lead to leaving the validity region of the EMD method, which analyses the linear dynamics of the system state and input *perturbations*. Finally, the distortions related to the short period exhibit noticeable variations with changing CWA parameter configurations, while the distortions for the phugoid remain similar to the behaviour observed in Fig. 3b with severely attenuated heave and pitch motion cues.

In total four CWA configurations, presented in Tables 2 and 3, were analyzed. The baseline configuration B is tuned based on established rules of thumb and previous experience from motion tuning experiments on the SRS. Furthermore, it is ensured that this configuration complies to the current OMCT criteria set in ICAO 9625 [10]. The next two configurations $E_{ph(ase)}$ and $E_{m(agnitude)}$ are tuned according to the EMD analysis approach. The difference between the two is that E_{ph} has the smallest phase distortion for f_x and q, while E_m has the smallest overall magnitude distortion summed over all motion cues. The final configuration O is tuned to pass the current OMCT tests while exhibiting unsatisfactory behaviour in the EMD analysis. For all configurations, a pull-up push-over manoeuvre of $\pm 5^\circ$ pitch angle capture was simulated to ensure that the available motion space was not exceeded. The result from these simulations is that all configurations were set with the same heave parameters, as the heave cue is largely uncoupled from the other degrees of freedom, and the most motion space is used up in replicating the heave movements. Furthermore, all subsequent performance differences are resulting from the settings for the coupled pitch and surge axes. Therefore from now on when magnitude and phase distortions are discussed, this is done for f_x and q unless specifically stated otherwise.

Table 2 Labels and description of the four used configurations of the Classical Washout Algorithm

Label	Description
B	Baseline configuration, complying with the OMCT criteria.
O	OMCT tuned configuration with bad performance in EMD, complying with the OMCT criteria.
E_{ph}	Configuration with smallest phase distortion, not complying with the OMCT criteria.
E_m	Configuration with the smallest magnitude distortion, not complying with the OMCT criteria.

Table 3 Classical Washout Algorithm filter parameters for all configurations used in the experiment

	K_x [-]	ω_{n_x} [rad/s]	ω_{b_x} [rad/s]	$\omega_{n_{lpx}}$ [rad/s]	ζ_x [-]	K_z [-]	ω_{n_z} [rad/s]	ω_{b_z} [rad/s]	ζ_z [-]	K_q [-]	ω_{n_q} [rad/s]	ζ_q [-]
B	0.7	0.8	0	2.5	1	0.5	2.5	0.2	1	0.7	0.8	1
O	0.7	2	0	4	1	0.5	2.5	0.2	1	0.7	1	1
E_{ph}	0.8	1	0	1	1	0.5	2.5	0.2	1	0.7	0.7	1
E_m	0.8	1.5	0	1	1	0.5	2.5	0.2	1	0.7	1	1

The eigenvector distortion plots for all configurations are shown in Fig. 5 with their distortions quantified in Table 4. By inspecting them it can be observed that configurations E_{ph} and E_m maintain fairly low phase distortions while attempting to keep the relative phase between f_x and q as inherent in the aircraft dynamics. The baseline configuration B exhibits reasonable phase and magnitude distortions. However, the relative phase is not preserved, as q is exhibiting phase lag, while f_x shows a phase lead distortion. A similar behaviour is observed in configuration O, where the phase distortion in f_x and magnitude distortion in q are prominent.

These trends are also evident in the time-domain representation of the distortions, presented in Fig. 6. For instance, note how f_{x_m} is out of phase with respect to f_{x_p} at $t = 0$ for configuration O, see Fig. 6b. This corresponds to its phase distortion of $\angle(f_x)_{sp} = 152.1^\circ$ lead. In the same figure, it is clearly visible that q_m has a higher amplitude than q_p and is lagging behind it, which is again in accordance with the eigenvector distortion results.

The excitation of the eigenmodes also aids in the understanding of how the MPFs behave. In Fig. 7a it can be observed that when the initial condition is the short period eigenvector, the SP MPF component starts from one and quickly reduces to zero. The opposite is seen in Fig. 7b, when the phugoid eigenvector is the initial condition, where the phugoid MPF gradually decreases while the aircraft is returning to its trimmed state. For both conditions, the MPF of the eigenmode that is not excited is verified to have a value zero throughout the entire evaluation. This behaviour is directed by the short period and phugoid eigenvalues (λ_{sp} and λ_{ph}), presented in Eq. (31), which govern the frequency and damping of both eigenmodes:

$$\lambda_{sp} = -2.0362 \pm 3.0513i \qquad \lambda_{ph} = -0.0124 \pm 0.1149i \tag{31}$$

While methods such as EMD and OMCT are usually used for evaluation of the motion cueing fidelity they can also be employed for tuning of the MCA. For example De Ridder and Roza [11] investigated an automatic tuning method using OMCT. The four CWA configurations used in the current study enable the presentation of both tuning and evaluation using EMD. For the former, configurations E_{ph} and E_m are tuned to produce motion cues at *least* as good as the baseline B, in terms of subjective pilot opinion. It is hypothesized that this statement is valid, since configurations E_{ph} and E_m have similar or lower phase and magnitude distortions than the baseline B, as seen in Table 4.

For the evaluation, a ranking can be made based on interpreting the outcome of the EMD analysis with respect to the tuning criteria and their relative importance, that are set in Section II.D. This ranking for the presented configurations is $E_{ph} > E_m > B > O$. Configuration E_{ph} has the lowest phase distortion for surge and pitch, while simultaneously maintaining reasonably low magnitude distortions. E_m has on average better magnitude distortions, but a slightly worse phase distortions which ranks it on second place. The baseline configuration B has worse phase distortions and magnitude than E_{ph} and E_m. Furthermore it fails to preserve the relative phase between f_{x_p} and q_p, since f_{x_m} has a phase lead distortion, while q_m has a phase lag distortion. Configuration O has the same problem, which is even more pronounced due to the large phase lead distortion of f_{x_m}. This, combined with it having the largest magnitude distortion for q_m, gives it the last place in the EMD based ranking.

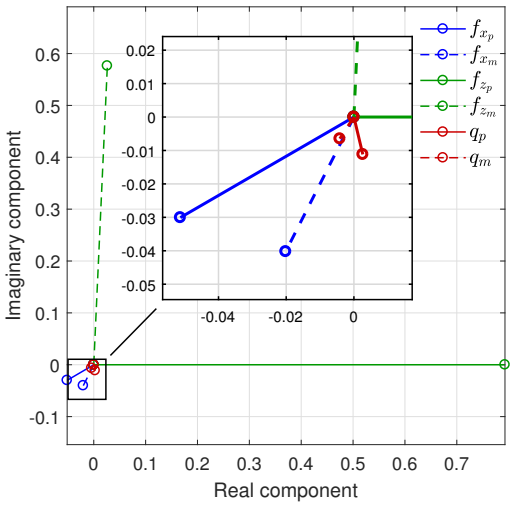

(a) Configuration B

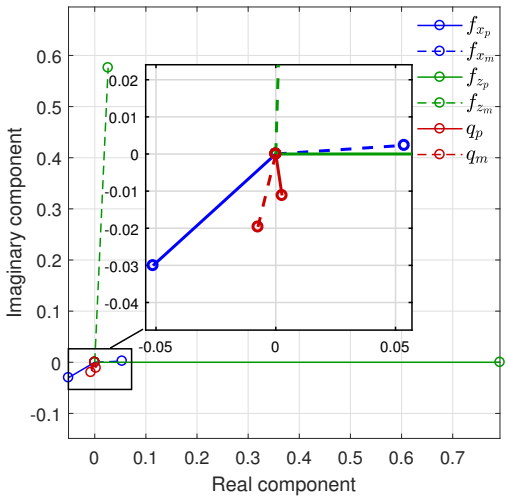

(b) Configuration O

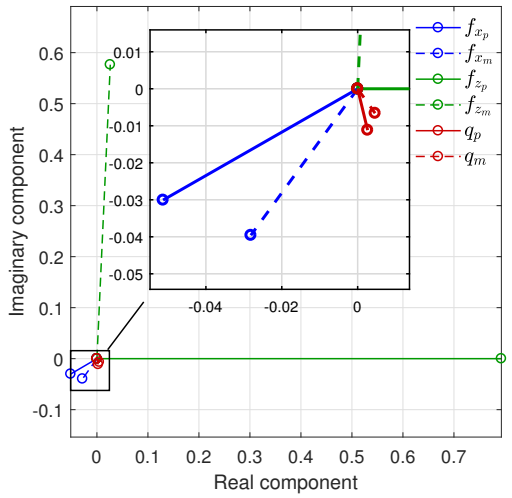

(c) Configuration E_{ph}

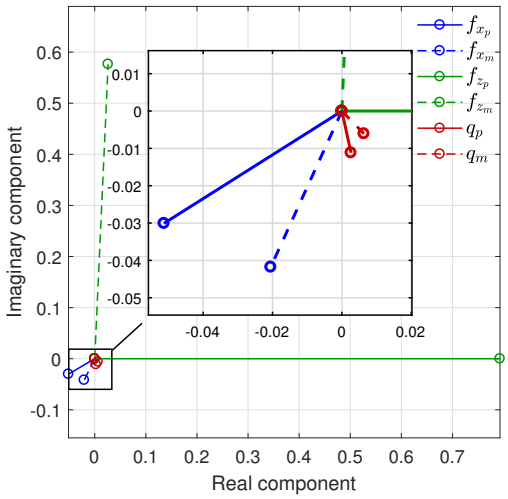

(d) Configuration E_m

Fig. 5 Short period eigenvector distortion plots for all CWA configurations

Table 4 Short period eigenvector magnitude and phase distortions for all CWA configurations

	$\lvert f_x \rvert_{sp}$	$\angle(f_x)_{sp}[^\circ]$	$\lvert f_z \rvert_{sp}$	$\angle(f_z)_{sp}[^\circ]$	$\lvert q \rvert_{sp}$	$\angle(q)_{sp}[^\circ]$
B	0.76	33.0 lead	0.73	87.4 lead	0.67	45.9 lag
O	0.90	152.1 lead	0.73	87.4 lead	1.83	34.0 lag
E_{ph}	0.82	24.2 lead	0.73	87.4 lead	0.70	21.6 lead
E_m	0.78	33.5 lead	0.73	87.4 lead	0.76	33.1 lead

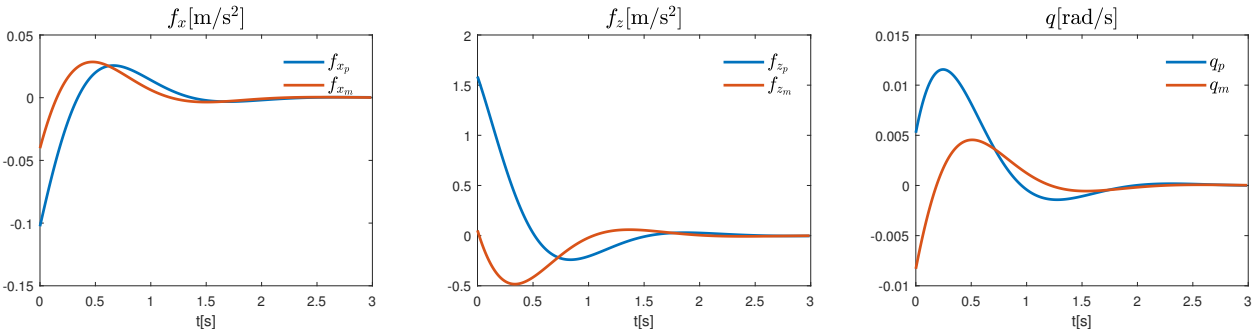

(a) B

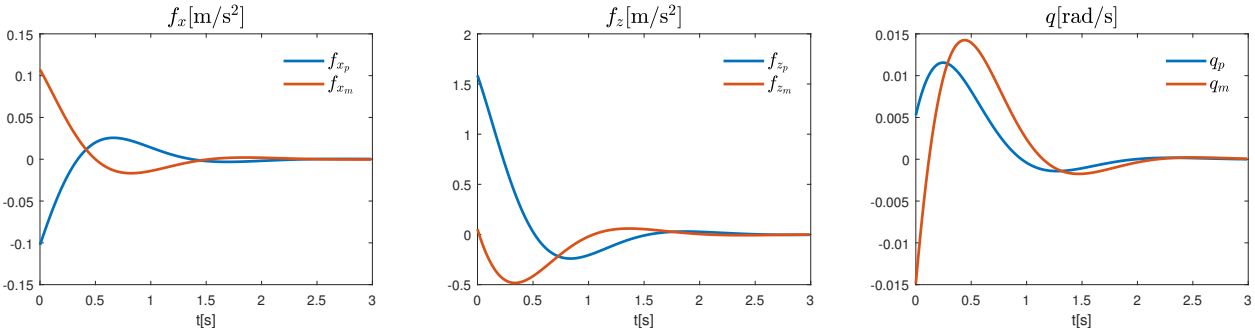

(b) O

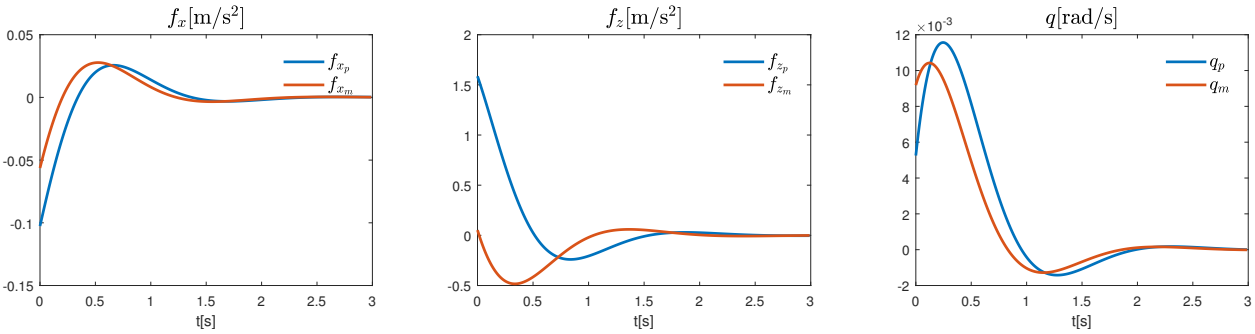

(c) E_{ph}

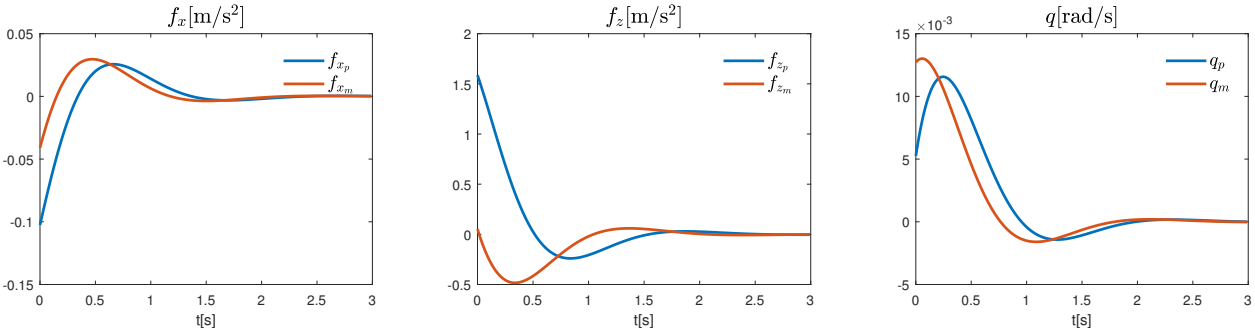

(d) E_m

Fig. 6 System response to the short period eigenmode excitation

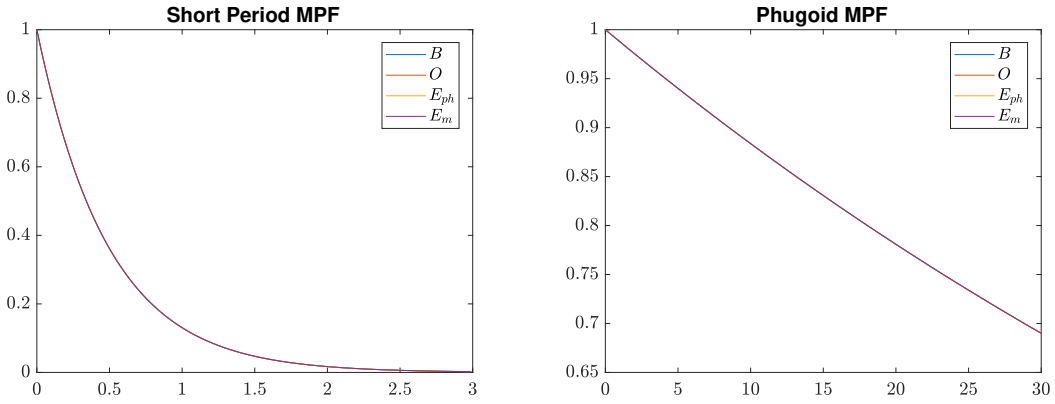

(a) Short Period initial condition **(b) Phugoid initial condition**

Fig. 7 MPF evolution for the system response to both eigenvector initial conditions

The four CWA configurations are also subjected to offline OMCT tests excluding the dynamics of the motion platform [18]. Their results are presented in Fig. 8 where the fidelity boundaries are the ones defined in ICAO 9625 [10]. As previously stated, configurations B and O manage to comply to the OMCT conditions. It is also observed that B manages to stay within the boundaries a bit better than O, since for the latter in surge test 6 the magnitude at $\omega = 1.585$rad/s lies just outside the lower boundary.

The frequency response of the EMD tuned configurations E_{ph} and E_m lies outside these boundaries for almost the entire tested frequency range for pitch test 1 and for its lower half for surge test 6 as observed in Fig. 8a. Furthermore, E_m lies further away from the fidelity boundaries than E_{ph} for both the pitch and surge tests. Therefore, a ranking based on the OMCT results can also be devised: $B > O > E_{ph} > E_m$.

Even though the two rankings overlap in the sense that in both $B > O$ and $E_{ph} > E_m$, they exhibit enough differences for the used configurations. The validity of both rankings can be tested in a piloted experiment.

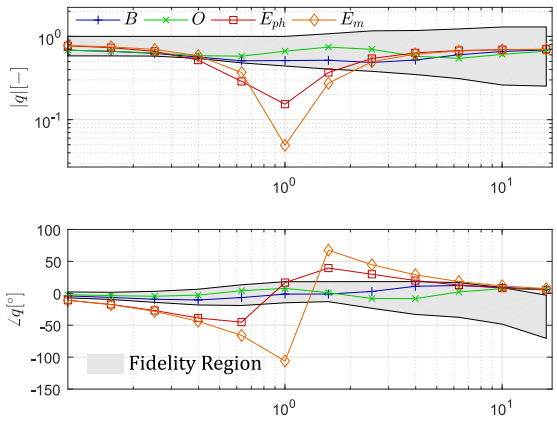

(a) Pitch due to pitch (test 1)

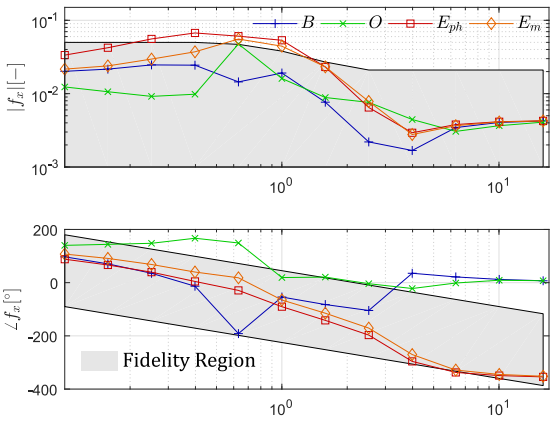

(b) Surge due to pitch (test 2)

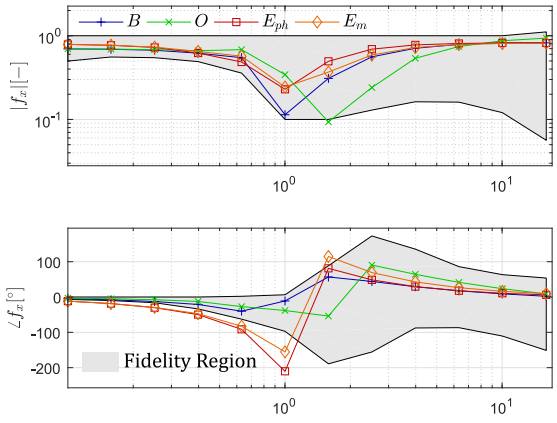

(c) Surge due to surge (test 6)

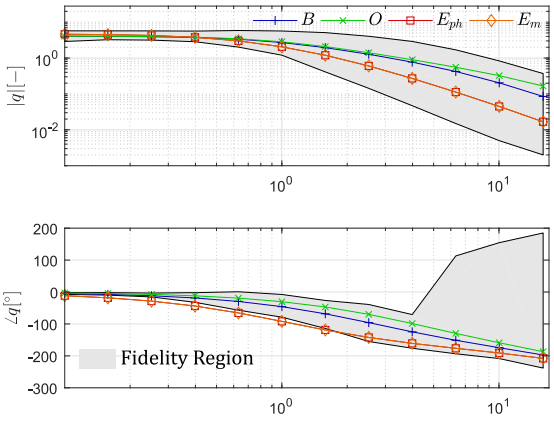

(d) Pitch due to surge (test 7)

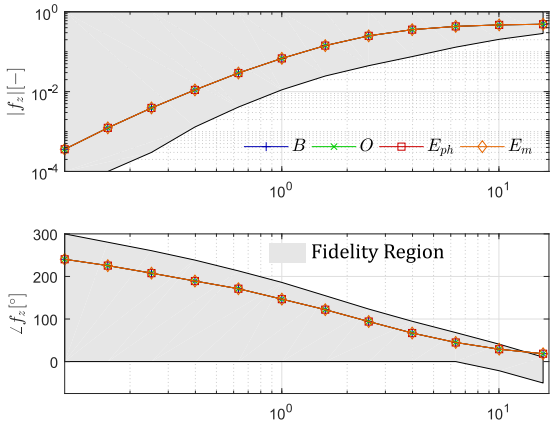

(e) Heave due to heave (test 10)

Fig. 8 OMCT results for all configurations

IV. Experiment set up

In order to investigate the predictive capabilities of the EMD methodology and to validate its inherent assumptions, a pilot-in-the loop experiment is performed in the SIMONA Research Simulator (SRS). The used MCA configurations are the ones presented in Table 2, while the simulated aircraft is a non-linear high-fidelity model of the Cessna Citation 500 business jet. The initial trim condition is at an altitude of 5000m and Mach number of 0.5 with the corresponding velocities V_{TAS} = 160 m/s and V_{IAS} = 245 kts. Six pilots of different background performed double-blind pairwise comparisons between all four CWA configurations by exciting the aircraft short period dynamics. This section will present the a-priori hypothesis, followed by a discussion of the task flown by the pilots, the experimental structure, and a brief description of the participants.

A. Hypothesis

The main experiment hypothesis is that EMD is a better predictor of the subjective motion cueing fidelity given by pilots for motions exciting the aircraft short period oscillation dynamics than OMCT. An alternative formulation is that the EMD-based ranking will better correspond to the winners of the pairwise comparisons than the OMCT-based ranking.

B. Experiment Task

The task of the evaluation pilots is to excite the aircraft and subsequently the simulator motion system in a way allowing them to confidently state a preference for the most realistic condition in the evaluated pair. Pilots are instructed to excite the aircraft short period dynamics as they wish, on the condition that they obey the following boundaries:

- The airspeed must not deviate more than ±10 knots from the trim airspeed.
- Any pitch captures that are performed must not exceed ±5°.
- No full deflections of the side stick are allowed.
- Different strategies for exciting the short period can be tried during training, but only a single strategy can be used during the evaluation runs.

There are several reasons for these limitations. First, the aircraft must not deviate too much from the trimmed condition, since the motion filters are specifically tuned for it. Second, large pitch inputs must be avoided since it is easy to overstress the simulated aircraft and quickly run out of available motion space due to excessive heave. An additional measure to prevent this is the implementation of a force curve on the side stick identical to the one used in the Airbus A320 in a cruise configuration. The strategy must remain consistent to ensure that any perceived differences in the simulator motion are resulting only from the evaluated CWA configurations. To ensure that this condition is met, a plot of the pilot inputs and the excited MPFs is drawn in real time in the simulator control room (see Fig. 9). This enables the instructor to inform the pilot should he deviate too much from his initial control strategy.

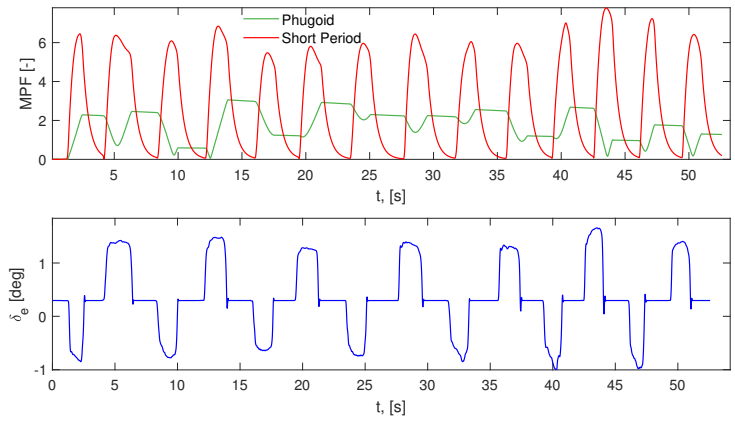

Fig. 9 Visualization of the MPFs (top) and the inputs (bottom) as seen by the instructor during the experiment. The current plot is from Subject 6 flying with configuration *B*.

C. Experiment Structure

Simulator setup

- Visuals - A full outside visual is provided at all times. In the cockpit, a basic instrument panel, as the one shown in Fig. 10, is displayed in front of the pilot.
- Sound - Engine noise is played while the pilots are performing the task in order to mask any noise coming from the hydraulic motion actuators.
- Control devices - A sidestick is used for controlling the aircraft in pitch. All roll and yaw controls are disabled.
- Aircraft configuration - The aircraft is in a cruise configuration:
  - Flaps: UP
  - Gear: UP
  - Thrust: 94.8% Fan RPM
  - δ_{e_0}: 0.3 degrees

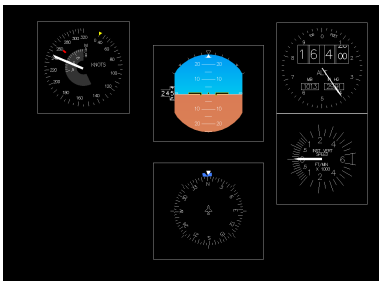

Fig. 10 Instrument panel used during the piloted experiment

Dependent measures

The main recorded variable is the preferred CWA configuration from each paired comparison. Pilots are briefed to select the 'winner' as the configuration which presents the most realistic motion cues. For validation purposes, time histories of the pilot inputs, aircraft states and specific forces, and the simulation motion cues are recorded.

Training

Each pilot is subjected to approximately 20 minutes of training. In this phase, the pilots fly all four CWA configurations two times in a randomized order. Every training run lasts for one minute, during which a pilot can explore different control strategies that enable him to make an evaluation of the motion cueing fidelity. All pilots are instructed to choose a single strategy by the end of the training and keep using it in the evaluation phase.

There are two additional training runs in the form of a standard pair comparison that are done immediately after a short break.

Evaluation phase

The evaluation phase begins after the training has concluded. The pilots first perform all six paired comparisons once. After a break, the paired comparisons are repeated with the CWA configurations presented in the opposite order. The Latin square matrix of all configurations is presented in Table 5.

Table 5 Latin Square matrix of the experiment conditions for all pilots

Subject	Conditions											
1	$B-O$	$B-E_{ph}$	E_m-E_{ph}	$B-E_m$	E_m-O	$O-E_{ph}$	$E_{ph}-O$	$O-E_m$	E_m-B	$E_{ph}-E_m$	$E_{ph}-B$	$O-B$
2	$B-E_{ph}$	$B-E_m$	$B-O$	$O-E_{ph}$	E_m-E_{ph}	$O-E_m$	E_m-O	$E_{ph}-E_m$	$E_{ph}-O$	$O-B$	E_m-B	$E_{ph}-B$
3	$B-E_m$	$O-E_{ph}$	$B-E_{ph}$	$O-E_m$	$B-O$	$E_{ph}-E_m$	E_m-E_{ph}	$O-B$	E_m-O	$E_{ph}-B$	$E_{ph}-O$	E_m-B
4	$O-E_{ph}$	$O-E_m$	$B-E_m$	$E_{ph}-E_m$	$B-E_{ph}$	$O-B$	$B-O$	$E_{ph}-B$	E_m-E_{ph}	E_m-B	E_m-O	$E_{ph}-O$
5	$O-E_m$	$E_{ph}-E_m$	$O-E_{ph}$	$O-B$	$B-E_m$	$E_{ph}-B$	$B-E_{ph}$	E_m-B	$B-O$	$E_{ph}-O$	E_m-E_{ph}	E_m-O
6	$E_{ph}-E_m$	$O-B$	$O-E_m$	$E_{ph}-B$	$O-E_{ph}$	E_m-B	$B-E_m$	$E_{ph}-O$	$B-E_{ph}$	E_m-O	$B-O$	E_m-E_{ph}

For every pair, one evaluation run of maximum one minute is performed for each CWA configuration. The pilots can stop the run once they feel that they sufficiently know the motion signature of the condition.

'World Cup' phase

After the evaluation phase has ended, the pilots perform three more pairwise comparisons as a part of the *'World Cup'* phase. Its purpose is to have pilots arrive at a *'best'* condition through a process of direct elimination (similar to how the World Cup finals are conducted). The first two pairwise comparisons act as the *'semifinals'*, the winners from which are subsequently compared in the *'final'*. The configurations present in the two semifinal pairs are the same for every subject. They are selected at random prior to the start of the experiment process, due to its double-blind nature. After the experiment results are analyzed, the World Cup *'champion'* is compared to the most preferred configuration for each subject as another means of evaluating pilot consistency. It must be noted that the results from the World Cup evaluations are not used during the testing the main experiment hypothesis.

Test subjects

Six pilots with a varying degree of experience participated in the piloted experiment. All of them gave their informed consent prior to starting the experiment. Their background is summarized below:

- *Subject 1* - Retired military test pilot with experience in motion simulation experiments.
- *Subject 2* - Active general aviation pilot.
- *Subject 3* - Active aerobatic glider pilot experienced in motion cueing evaluation of Level-D Full Flight Simulators (FFS).
- *Subject 4* - Active Cessna Citation 550 research pilot with experience in motion simulation experiments.
- *Subject 5* - Active test pilot of commercial airliners with experience in motion simulation experiments.
- *Subject 6* - Active airline pilot and Cessna Citation 550 research pilot with experience in motion simulation experiments.

V. Results

The results for all pairwise comparisons grouped for all subjects is presented in Fig. 11. The height of bars represents the total number of times this configuration has been preferred in this current pair. The different colours correspond to the evaluations given by each subject. It must be noted that there is one missing data point for the pair $B-E_m$ as Subject 1 was unable to give a confident preference in one of his evaluations.

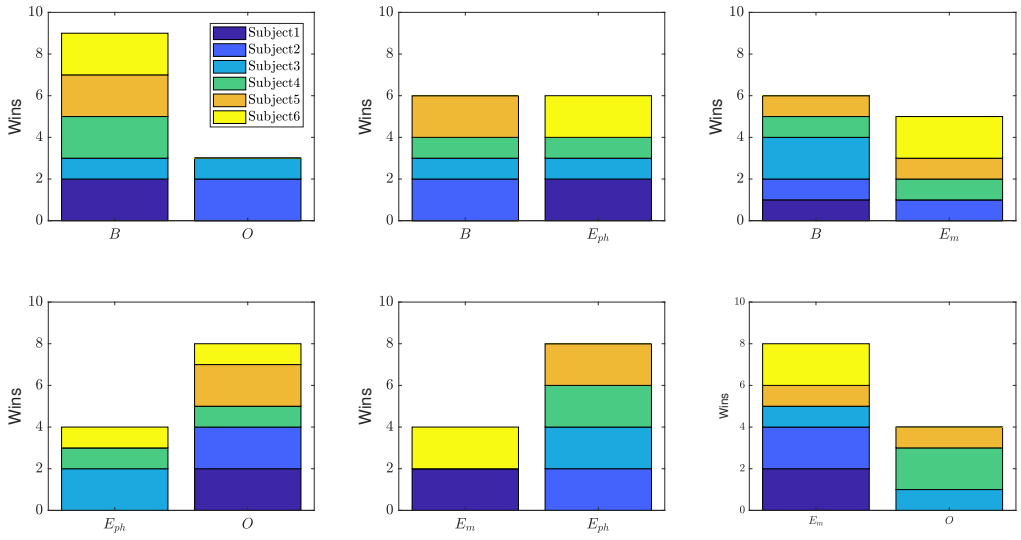

Fig. 11 Results of the pairwise comparisons for all pairs evaluated by all pilots

In Fig. 11 it can be observed that the subjects express two types of consistency. The first is the *within-pair* consistency which is satisfied when the same configuration is preferred in both evaluations of a given pair, visualized by a full bar in Fig. 11. It is seen that for the pair $E_{ph} - E_m$ all subjects are within-pair consistent. The second consistency type is related to the *transitivity* of the evaluations from the different pairs. An example of a perfectly transitive evaluation is when $B > O$, $O > E_{ph}$, $E_{ph} > E_m$, and $O > E_m$. When the data for all pilots are analyzed, it can be concluded that it is intransitive, since a circular triad is present: $O > E_{ph}$, $E_{ph} > E_m$, but $E_m > O$. This prevents the formulation of a clear and intuitive ranking based on the absolute results from all pilots for every pair.

However, it is possible to use statistical modelling techniques in order to arrive at an estimation of a data-based ranking. Many methods exist for statistical analysis of paired comparisons data which is likely to have high degree of dependence [20], as is the case with the evaluations of a repeated measures experiment. One approach is to fit the data to a Bradley-Terry pattern model with the *R* package **`prefmod`** [21]. The model assumes that the evaluations made by a single pilot are dependent, while the evaluations of the different pilots are independent. The resulting ranking is $B > E_{ph} > E_m > O$ with corresponding worth parameters $\left\{\pi_B, \pi_{E_{ph}}, \pi_{E_m}, \pi_O\right\} = \left\{0.348, 0.335, 0.174, 0.143\right\}$. There are other methods that can provide more accurate models which are better tailored to the specific data [20]. Their implementation is unfortunately not straightforward [20] and considerable time would have to be spend on it.

From further analysis of Fig. 11 it is seen that the subjects can be divided in three groups based on their consistency. The first group, formed by Subjects 1 and 2, is within-pair consistent (5 out of 6 pairs) but not transitivity consistent. The second group, represented by Subjects 3 and 4, is the worst with respect to within-pair consistency (3 out of 6 pairs) but is transitively consistent when discarding the inconsistently rated pairs. The third group of Subjects 5 and 6 is both within-pair consistent (with respectively 4/6 and 5/6 pairs) and transitively consistent.

As stated in Section IV.C the *'World Cup'* (WC) experiment phase is also used for checking the pilot consistency. This is done by comparing the WC winner against the most preferred configuration from the evaluation phase, i.e. the configuration wins the most pairwise comparisons. The results of the WC phase are summarized in Table 6. There it is seen that the WC winner is different from the most preferred configuration for all pilots. It can be thus concluded that the WC format is not suitable for testing the subject consistency.

Table 6 Results from the World Cup finals compared to the CWA configuration that was preferred most times in the evaluation phase.

Subject	WC final	WC winner	Most preferred configuration
1	$E_{ph} - B$	B	E_m
2	$E_m - B$	E_m	O
3	$O - E_m$	O	E_{ph}
4	$O - E_{ph}$	O	B/E_{ph}
5	$O - E_{ph}$	E_{ph}	B
6	$E_m - B$	B	E_m

The experiment hypothesis is tested by comparing the ratio of correct paired comparison outcome predictions to the EMD-based ranking and the OMCT-based ranking. Since the two predictors have a degree of similarity - both state that $B > O$ and $E_{ph} > E_m$, the analysis is done for all outcomes as well as the truly discriminatory outcomes (from pairs $B - E_{ph}$, $B - E_m$, $O - E_{ph}$, $O - E_m$), which are indicated as EMD* and OMCT*. These ratios are visualized through box plots in Fig. 12. The data points for each test subject are shown as circles and overlaid on top of the box plots in order to provide a good representation of the data distribution. The colours used for the data points representing the subjects correspond to the legend in Fig. 11. It is interesting to note that while Subjects 5 and 6 are the most consistent overall, they have completely opposite preferences. Subject 6 picks a winner according to the EMD ranking for 9 out of 12 evaluations, while Subject 5 is consistent with the OMCT ranking for 10 of the total 12 evaluations.

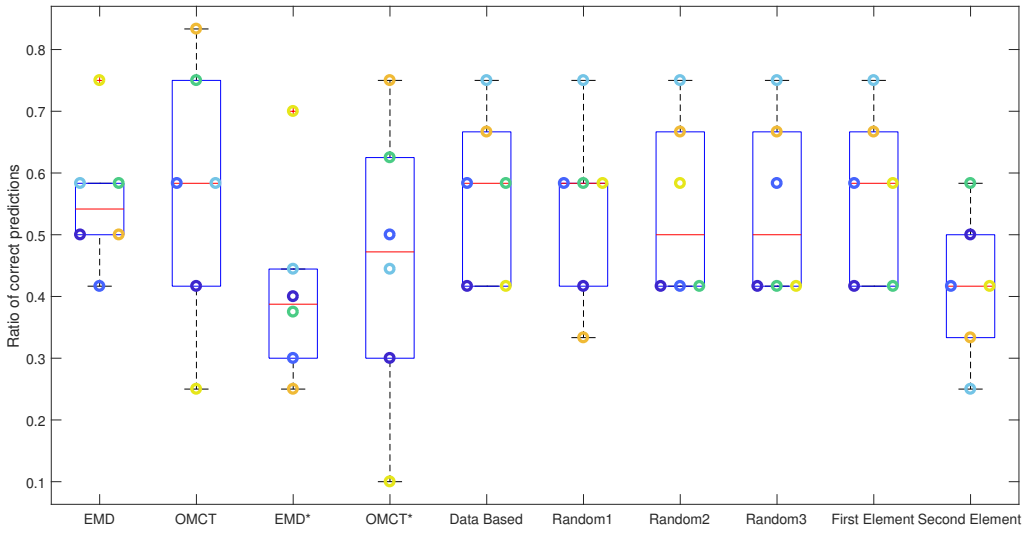

Fig. 12 Box plots of the ratio of correct predictions

By observing Fig. 12 it can be concluded that the main hypothesis is rejected as the medians of the complete and discriminatory OMCT ratios are higher than the medians of the corresponding EMD ratios. Furthermore, the difference between the two methods is not expected to be significant. This is confirmed with a statistical analysis. A non-parametric Friedmann ANOVA test is used for this, since the data does not satisfy the homogeneity of variance assumption. The results are $\chi^2(1) = 0.2, p = 0.65$ for both the complete ratios and the discriminatory pairs, indicating that for both of them the difference is indeed not significant.

Several other "predictors" are tested as well. They are not subjected to a statistical analysis, but serve as a baseline for the predictive performance of EMD. The first one is based on the ranking derived from the data with the Bradley-Terry

model. Additionally, three random predictors are initialized with the following seeds:

1) The experiment date (e.g. *20180818*)
2) The subject number after the experiment date (e.g *201808183*)
3) The subject number before the experiment date (e.g *320180818*)

The random predictors are used as an unbiased measure to gauge the predictive capabilities of EMD and OMCT for pilot subjective cueing fidelity. It can clearly be seen in Fig. 12 that both methods do not seem to perform better than the random predictors. Finally, the ratio of wins for the first and second presented filter in the pair is compared in order to see if an order effect is present. Their corresponding box plots show a more noticeable difference in favour of the first element of the pair being preferred, which may potentially be significant. The result from the statistical test for the order effect is $\chi^2(3) = 0.964, p = 0.81$, meaning that it is not significant when taken over all pilots.

VI. Discussion

The main goal of this paper is to present the application of EMD to fixed-wing aircraft and investigate its capability to predict the subjective motion cueing fidelity perceived by pilots. In order to test this, six pilots compare four MCA configurations in pairs of two, by exciting the short period dynamics of a Cessna Citation 500 aircraft.

After completing the experiment all pilots reported they had difficulties in consistently giving evaluations of a high confidence, since according to them all four configurations had a similar feel. The test subjects gave a positive feedback on the pairwise comparison format of the experiment however, as it better enabled them to differentiate between the different configurations. Another opinion shared between the majority of the participants is that high frequency pitch oscillations, aiming to excite the short period dynamics for longer periods of time, were not beneficial for distinguishing differences between the configurations. On the contrary, slower movements resulting from manoeuvres such as pitch angle intercepts enabled the pilots to better observe deficiencies in the motion. Therefore it is recommended that in future experiments a specifically defined task is used.

In addition, the pilot feedback indicates that the currently used EMD tuning approach can be improved upon by considering simultaneous tuning for the short period and phugoid. Since both eigenmodes are excited during longitudinal motions, a weighted tuning approach based on their relative MPFs for a set of manoeuvres can be investigated.

From the experiment results, it can be concluded that there are no significant differences between the predictive capabilities of EMD and OMCT. Both methods exhibit a performance similar to a random predictor, indicating that they are not the most reliable tools for predicting subjective cueing fidelity for MCA configurations which appear to be very similar, such as the ones used in this experiment.

Additionally, the accuracy of the ratios of correct predictions for EMD and OMCT can be argued, since some pilots tended to report varying levels of confidence when giving their evaluations. However, this was not done in a systematic manner for all pilots and was therefore not addressed in the statistical analysis. Should a similar experiment be attempted in future studies, it is recommended to add the confidence level of each evaluation to the dependent metrics. It can subsequently be used to improve the statistical modelling performed with the Bradley-Terry pattern model or another more complex method.

Furthermore, the subjective evaluation method of MCA configurations is not an inherently consistent and consequently reliable metric for measuring the predictive performance of EMD and OMCT. The evaluation criteria employed by different pilots can vary even when measures, such as providing universal instructions and briefing, are taken to minimize this. For instance, one pilot stated during the experiment that sometimes he might prefer a configuration that is not necessarily the most representative of the real aircraft, but more beneficial for training. Therefore it is recommended for future studies to investigate other more objective methods of quantifying and evaluating the performance of objective metrics such as EMD and OMCT.

Another observation based on the experiment results is that the currently used fidelity boundaries for OMCT need to be further refined, as there is a clearly expressed difference in the preference given to the two configurations conforming to OMCT, which is visible in the results for pair $B - O$. Studies have already been performed that analyze the fidelity boundaries based on pilot performance [1]. Similar research can be done with respect to different aircraft types and flight conditions.

Finally, the results of the pair $E_{ph} - E_m$ are unexpected, since these two conditions were hypothesized to be the most similar to one another and hence that pilots would find a little difference between them. The experiment showed that, on the contrary, this is the only pair where all pilots had consistent evaluations and on average E_{ph} is preferred to E_m. This is another indication for potential deficiencies in the currently used set of EMD based tuning criteria. Therefore further research into the methodology is needed.

VII. Conclusions

This paper presented the application of a novel method for objective motion cueing fidelity evaluation, Eigenmode Distortion, to fixed-wing aircraft. It was shown how this method can assess MCA settings for a specific aircraft model and flight condition, and how it can generate a ranking between MCA settings which sometimes conflicts with state-of-the-art OMCT assessments.

Validation through pilot opinion of both these ranking methods was hampered by inconsistencies between and within pilots. A reliable and objective "gold standard" to calibrate cueing assessment techniques that minimizes the influence of individual preferences and variability would strongly benefit a confident demonstration of EMD's value in the future. It is questionable if such a standard can (or should) be constructed without reference to expert pilot opinion.

In general EMD provides an alternative perspective on the tuning and assessment of motion cueing algorithms. It has the potential to identify issues with MCA configurations for a given flight condition that are not noticeable with the current objective criteria. Since the methodology is applicable to any aircraft throughout its flight envelope, it can be used as a stepping stone to understanding aircraft and flight condition specific motion cueing and for enhancing the currently used methods.

References

[1] Zaal, P. M. T., Schroeder, J. A., and Chung, W. W. Y., "Objective Motion Cueing Criteria Investigation Based on Three Flight Tasks," *Proceedings of the RAeS Flight Simulation Conference, 9-10 June 2015, London, UK*, Royal Aeronautical Society, 2015.

[2] Hosman, R. J. A. W., Advani, S. K., and Takats, J., "Status of the ICAO Objective Motion Cueing Test," *Autumn Flight Simulation Conference: Flight Simulation Research - New Frontiers*, Royal Aeronautical Society, Royal Aeronautical Society, 2012.

[3] Sinacori, J. B., "The Determination of Some Requirements for a Helicopter Research Simulation Facility," Tech. Rep. NASA-CR-152066, Systems Technology Inc., Sep. 1977.

[4] Schroeder, J. A., "Helicopter Flight Simulation Motion Platform Requirements," Tech. Rep. NASA-TP-1999-208766, National Aeronautics and Space Administration, Jul. 1999.

[5] Gouverneur, B., Mulder, J. A., van Paassen, M. M., Stroosma, O., and Field, E. J., "Optimisation of the SIMONA Research Simulator's Motion Filter Settings for Handling Qualities Experiments," *Proceedings of the AIAA Modeling and Simulation Technologies Conference and Exhibit, Austin, Texas, Aug. 11-14, 2003*, American Institute of Aeronautics and Astronautics, 2003.

[6] Hosman, R. J. A. W., "Are Criteria for Motion Cueing and Time Delays Possible?" *Proceedings of the AIAA Modelling and Simulation Technologies Conference and Exhibit, Portland (OR)*, American Institute of Aeronautics and Astronautics, 1999. doi:10.2514/6.1999-4028.

[7] Advani, S. K., and Hosman, R. J. A. W., "Revising Civil Simulator Standards – An Opportunity for Technological Pull," *Proceedings of the AIAA Modeling and Simulation Technologies Conference and Exhibit, Keystone (CO)*, American Institute of Aeronautics and Astronautics, 2006.

[8] Hosman, R. J. A. W., and Advani, S. K., "Are Criteria for Motion Cueing and Time Delays Possible? Part 2." *Proceedings of the AIAA Modeling and Simulation Technologies Conference, Boston (MA)*, American Institute of Aeronautics and Astronautics, 2013.

[9] Hosman, R. J. A. W., and Advani, S. K., "Design and Evaluation of the Objective Motion Cueing Test and Criterion," *The Aeronautical Journal*, Vol. 120, No. 1227, 2016, pp. 873–891. doi:10.1017/aer.2016.35.

[10] Anonymous, "Manual of Criteria for the Qualification of Flight Simulation Training Devices. Volume 1 – Airplanes," ICAO Doc 9625, International Civil Aviation Organization, 2015. Fourth edition.

[11] De Ridder, K., and Roza, M., "Automatic Optimization of Motion Drive Algorithms using OMCT," *AIAA Modeling and Simulation Technologies Conference, Kissimmee, FL*, American Institute of Aeronautics and Astronautics, 2015, p. 1139.

[12] Dalmeijer, W., Miletović, I., Stroosma, O., and Pavel, M. D., *Extending the Objective Motion Cueing Test to Measure Rotorcraft Simulator Motion Characteristics*, 2017, pp. 1876–1891.

[13] Miletović, I., Pavel, M. D., Stroosma, O., Pool, D. M., van Paassen, M. M., Wentink, M., and Mulder, M., "Motion Cueing Fidelity in Flight Simulation: A Novel Perspective," 2018. To be submitted.

[14] Reid, L. D., and Nahon, M. A., "Flight Simulation Motion-Base Drive Algorithms. Part 1: Developing and Testing the Equations," Tech. Rep. UTIAS 296, University of Toronto, Institute for Aerospace Studies, Dec. 1985.

[15] Stroosma, O., van Paassen, M. M., and Mulder, M., "Using the SIMONA Research Simulator for Human-machine Interaction Research," *Proceedings of the AIAA Modeling and Simulation Technologies Conference and Exhibit, Austin, Texas, Aug. 11-14, 2003*, American Institute of Aeronautics and Astronautics, 2003, pp. 1–8.

[16] Seehof, C., Durak, U., and Duda, H., "Objective Motion Cueing Test - Experiences of a New User," *AIAA Modeling and Simulation Technologies Conference, Atlanta, Georgia, US*, , No. AIAA 2014-2205, 2014, pp. 1–14. doi:10.2514/6.2014-2205.

[17] Oppenheim, A. V., and Verghese, G. C., *Signals, systems and inference*, 1st ed., Pearson, Hoboken, NJ, 2015, Chap. 5.

[18] Stroosma, O., van Paassen, M. M., Mulder, M., Hosman, R. J. A. W., and Advani, S. K., "Applying the Objective Motion Cueing Test to a Classical Washout Algorithm," *Proceedings of the AIAA Modeling and Simulation Technologies Conference, Boston (MA)*, American Institute of Aeronautics and Astronautics, 2013.

[19] Zaichik, L. E., Yashin, Y. P., and Desyatnik, P., "Peculiarities of Motion Cueing for Precision Control Tasks and Maneuvers," *ICAS. Nice, France. ICAS Paper*, Vol. 602, 2010.

[20] Cattelan, M., "Models for Paired Comparison Data: A Review with Emphasis on Dependent Data," *Statistical Science*, 2012, pp. 412–433.

[21] Hatzinger, R., and Dittrich, R., "Prefmod: An R Package for Modelling Preferences Based on Paired Comparisons, Rankings, or Ratings," *Journal of Statistical Software*, Vol. 48, No. 10, 2012, pp. 1–31.

II

Appendices

A

Decomposition of the Extended Aircraft State-Space System

This appendix contains the definition of every element in all matrices (A^p,B^p,C^p,D^p) in the extended aircraft state-space system. For simplicity, the matrix coefficients of the state space form of the dimensional equations of motion (shown in Eq. (A.1)) are presented first and are subsequently used in the definitions of the state equations for f_{x_p} and f_{z_p}.

The state-space form of the symmetric aircraft equations of motion is presented in Eqs. (A.2) and (A.3) and the definition of every component in its A,C, and B,D matrices is presented in Tables A.1 and A.2.

$$\begin{aligned} -W\cos\theta_0\theta + X_u u + X_w w + X_q q + X_{\delta_e}\delta_e + X_{\delta_t}\delta_t &= m\dot{u} \\ -W\sin\theta_0\theta + Z_u u + Z_w w + Z_{\dot{w}}\dot{w} + Z_q q + Z_{\delta_e}\delta_e + Z_{\delta_t}\delta_t &= m(\dot{w} - qV) \\ M_u u + M_w w + M_{\dot{w}}\dot{w} + M_{\delta_e}\delta_e + M_{\delta_t}\delta_t &= I_{yy}\dot{q} \\ \dot{\theta} &= q \end{aligned} \tag{A.1}$$

$$\dot{\delta}_{\bar{x}_p} = A\delta_{\bar{x}_p} + B\delta_{\bar{u}_p}$$

$$\begin{bmatrix} \dot{u} \\ \dot{w} \\ \dot{\theta} \\ \dot{q} \end{bmatrix} = \begin{bmatrix} A_{uu} & A_{uw} & A_{u\theta} & A_{uq} \\ A_{wu} & A_{ww} & A_{w\theta} & A_{wq} \\ 0 & 0 & 0 & 1 \\ A_{qu} & A_{qw} & A_{q\theta} & A_{qq} \end{bmatrix} \begin{bmatrix} u \\ w \\ \theta \\ q \end{bmatrix} + \begin{bmatrix} B_{u\delta_e} & B_{u\delta_t} \\ B_{w\delta_e} & B_{w\delta_t} \\ 0 & 0 \\ B_{q\delta_e} & B_{q\delta_t} \end{bmatrix} \begin{bmatrix} \delta_e \\ \delta_t \end{bmatrix} \tag{A.2}$$

$$y = C\delta_{\bar{x}_p} + D\delta_{\bar{u}_p}$$

$$\begin{bmatrix} f_{x_p} \\ f_{z_p} \end{bmatrix} = \begin{bmatrix} C_{xu} & C_{xw} & C_{x\theta} & C_{xq} \\ C_{zu} & C_{zw} & C_{z\theta} & C_{zq} \end{bmatrix} \begin{bmatrix} u \\ w \\ \theta \\ q \end{bmatrix} + \begin{bmatrix} D_{x\delta_e} & D_{x\delta_t} \\ D_{z\delta_e} & D_{z\delta_t} \end{bmatrix} \begin{bmatrix} \delta_e \\ \delta_t \end{bmatrix} \tag{A.3}$$

	$A_{u...}$	$A_{w...}$	$A_{q...}$
u	$\frac{X_u}{m}$	$-\frac{Z_u}{Z_{\dot{w}}-m}$	$\frac{1}{I_{yy}}(M_u - Z_u\frac{M_{\dot{w}}}{Z_{\dot{w}}-m})$
w	$\frac{X_w}{m}$	$-\frac{Z_w}{Z_{\dot{w}}-m}$	$\frac{1}{I_{yy}}(M_w - Z_w\frac{M_{\dot{w}}}{Z_{\dot{w}}-m})$
θ	$-g\cos\theta_0$	$-\frac{W\sin\theta_0}{Z_{\dot{w}}-m}$	$\frac{1}{I_{yy}}\frac{M_{\dot{w}}}{Z_{\dot{w}}-m}W\sin\theta_0$
q	$\frac{X_q}{m}$	$-\frac{Z_q+mV}{Z_{\dot{w}}-m}$	$\frac{1}{I_{yy}}(M_q + \frac{M_{\dot{w}}}{Z_{\dot{w}}-m})(Z_q+mV)$
	$C_{x...}$		$C_{z...}$
u	$\cos\alpha_0\frac{X_u}{m} - \alpha_0(\frac{Z_u}{m} + \frac{Z_{\dot{w}}}{m}A_{wu}) - l_z A_{qu}$		$\frac{Z_u}{m} + \frac{Z_{\dot{w}}}{m}A_{wu} + \alpha_0\frac{X_u}{m} - l_x A_{qu}$
w	$\cos\alpha_0\frac{X_w}{m} - \alpha_0(\frac{Z_w}{m} + \frac{Z_{\dot{w}}}{m}A_{ww}) - l_z A_{qw}$		$\frac{Z_w}{m} + \frac{Z_{\dot{w}}}{m}A_{ww} + \alpha_0\frac{X_w}{m} - l_x A_{qw}$
θ	$-\alpha_0(\frac{Z_{\dot{w}}}{mA_{w\theta}}) - l_z A_{q\theta}$		$\frac{Z_{\dot{w}}}{m}A_{w\theta} - l_x A_{q\theta}$
q	$\cos\alpha_0\frac{X_q}{m} - \alpha_0(\frac{Z_q}{m} + \frac{Z_{\dot{w}}}{m}A_{wq}) - l_z A_{qq}$		$\frac{Z_q}{m} + \frac{Z_{\dot{w}}}{m}A_{wq} + \alpha_0\frac{X_q}{m} - l_x A_{qq}$

Table A.1: Dimensional EOM A and C matrix coefficients

	δ_e	δ_t
$B_{u...}$	$\frac{X_{\delta_e}}{m}$	$\frac{X_{\delta_t}}{m}$
$B_{w...}$	$-\frac{Z_{\delta_e}}{Z_{\dot{w}}-m}$	$-\frac{Z_{\delta_t}}{Z_{\dot{w}}-m}$
$B_{q...}$	$\frac{1}{I_{yy}}(M_{\delta_e} - Z_{\delta_e}\frac{M_{\dot{w}}}{Z_{\dot{w}}-m})$	$\frac{1}{I_{yy}}(M_{\delta_t} - Z_{\delta_t}\frac{M_{\dot{w}}}{Z_{\dot{w}}-m})$
$D_{x...}$	$\cos\alpha_0\frac{X_{\delta_e}}{m} - \alpha_0(\frac{Z_{\delta_e}}{m} + \frac{Z_{\dot{w}}}{m}B_{w\delta_e}) - l_z B_{q\delta_e}$	$\cos\alpha_0\frac{X_{\delta_t}}{m} - \alpha_0(\frac{Z_{\delta_t}}{m} + \frac{Z_{\dot{w}}}{m}B_{w\delta_t}) - l_z B_{q\delta_t}$
$D_{z...}$	$\frac{Z_{\delta_e}}{m} + \frac{Z_{\dot{w}}}{m}B_{w\delta_e} + \alpha_0\frac{X_{\delta_e}}{m} - l_x B_{q\delta_e}$	$\frac{Z_{\delta_t}}{m} + \frac{Z_{\dot{w}}}{m}B_{w\delta_t} + \alpha_0\frac{X_{\delta_t}}{m} - l_x B_{q\delta_t}$

Table A.2: Dimensional EOM B and D matrix coefficients

In Chapter 1 it is explained that the specific forces perceived by the pilot (f_{x_p}, and f_{z_p}) must be expressed as states and added to the aircraft state-space system, so that it can be combined with the linearized CWA system into the final coupled system, which forms the basis of the EMD analysis. The resulting extended aircraft state space system is presented in Eqs. (A.4) and (A.5) and the state coefficients for f_{x_p} and f_{z_p} are shown in Table A.3.

$$\dot{\delta}_{\bar{x}_p} = A^p \delta_{x_p} + B^p \delta_{\bar{u}_p}$$

$$\begin{bmatrix} \dot{u} \\ \dot{w} \\ \dot{\theta} \\ \dot{q} \\ \dot{\delta}_e \\ \dot{\delta}_t \\ \dot{f}_{x_p} \\ \dot{f}_{z_p} \\ \ddot{q} \end{bmatrix} = \begin{bmatrix} A_{uu} & A_{uw} & A_{u\theta} & A_{uq} & B_{u\delta_e} & B_{u\delta_t} & 0 & 0 & 0 \\ A_{wu} & A_{ww} & A_{w\theta} & A_{wq} & B_{w\delta_e} & B_{w\delta_t} & 0 & 0 & 0 \\ 0 & 0 & 0 & 1 & 0 & 0 & 0 & 0 & 0 \\ A_{qu} & A_{qw} & A_{q\theta} & A_{qq} & B_{q\delta_e} & B_{q\delta_t} & 0 & 0 & 0 \\ 0 & 0 & 0 & 0 & 0 & -\frac{1}{\tau_e} & 0 & 0 & 0 \\ 0 & 0 & 0 & 0 & 0 & 0 & -\frac{1}{\tau_t} & 0 & 0 \\ A_{f_x u} & A_{f_x w} & A_{f_x \theta} & A_{f_x q} & A_{f_x \delta_e} & A_{f_x \delta_t} & 0 & 0 & 0 \\ A_{f_z u} & A_{f_z w} & A_{f_z \theta} & A_{f_z q} & A_{f_z \delta_e} & A_{f_z \delta_t} & 0 & 0 & 0 \\ A_{\dot{q}u} & A_{\dot{q}w} & A_{\dot{q}\theta} & A_{\dot{q}q} & A_{\dot{q}\delta_e} & A_{\dot{q}\delta_t} & 0 & 0 & 0 \end{bmatrix} \begin{bmatrix} u \\ w \\ \theta \\ q \\ \delta_e \\ \delta_t \\ f_{x_p} \\ f_{z_p} \\ \dot{q} \end{bmatrix} + \begin{bmatrix} 0 & 0 \\ 0 & 0 \\ 0 & 0 \\ 0 & 0 \\ \frac{1}{\tau_e} & 0 \\ 0 & \frac{1}{\tau_t} \\ \frac{D_{x\delta_e}}{\tau_e} & \frac{D_{x\delta_t}}{\tau_t} \\ \frac{D_{z\delta_e}}{\tau_e} & \frac{D_{z\delta_t}}{\tau_t} \\ \frac{1}{\tau_e} & \frac{1}{\tau_t} \end{bmatrix} \begin{bmatrix} \delta_{u_e} \\ \delta_{u_t} \end{bmatrix} \tag{A.4}$$

$$\begin{aligned} \delta_{\bar{y}}^{p} &= \begin{bmatrix} q \\ f_{x_c} \\ f_{z_c} \end{bmatrix} = C^{p}\delta_{\bar{x}}^{p} + D^{p}\delta_{\bar{u}}^{p} \\ \delta_{\bar{y}}^{p} &= \begin{bmatrix} 0 & 0 & 0 & 1 & 0 & 0 & 0 & 0 & 0 \\ 0 & 0 & 0 & 0 & 0 & 0 & 1 & 0 & 0 \\ 0 & 0 & 0 & 0 & 0 & 0 & 0 & 1 & 0 \end{bmatrix} \delta_{\bar{x}}^{p} + [0]\delta_{\bar{u}}^{p} \end{aligned} \tag{A.5}$$

	$A_{f_x...}$	$A_{f_z...}$	$A_{\dot{q}...}$
u	$C_{xu}A_{uu} + C_{xw}A_{wu} + C_{xq}A_{qu}$	$C_{zu}A_{uu} + C_{zw}A_{wu} + C_{zq}A_{qu}$	$A_{qu}A_{uu} + A_{qw}A_{wu}$
w	$C_{xu}A_{uw} + C_{xw}A_{ww} + C_{xq}A_{qw}$	$C_{zu}A_{uw} + C_{zw}A_{ww} + C_{zq}A_{qw}$	$A_{qu}A_{uw} + A_{qw}A_{ww}$
θ	$C_{xu}A_{u\theta} + C_{xw}A_{w\theta} + C_{xq}A_{q\theta}$	$C_{zu}A_{u\theta} + C_{zw}A_{w\theta} + C_{zq}A_{q\theta}$	$A_{qu}A_{u\theta} + A_{qw}A_{w\theta}$
q	$C_{xu}A_{uq} + C_{xw}A_{wq} + C_{xq}A_{qq} + C_{x\theta}$	$C_{zu}A_{uq} + C_{zw}A_{wq} + C_{zq}A_{qq} + C_{z\theta}$	$A_{qu}A_{uq} + A_{qw}A_{wq} + A_{q\theta}$
δ_e	$C_{xu}B_{u\delta_e} + C_{xw}B_{w\delta_e} + C_{xq}B_{q\delta_e} - \frac{D_{x\delta_e}}{\tau_e}$	$C_{zu}B_{u\delta_e} + C_{zw}B_{w\delta_e} + C_{zq}B_{q\delta_e} - \frac{D_{z\delta_e}}{\tau_e}$	$A_{qu}B_{u\delta_e} + A_{qw}B_{w\delta_e} - \frac{B_{q\delta_e}}{\tau_e}$
δ_t	$C_{xu}B_{u\delta_t} + C_{xw}B_{w\delta_t} + C_{xq}B_{q\delta_t} - \frac{D_{x\delta_t}}{\tau_t}$	$C_{zu}B_{u\delta_t} + C_{zw}B_{w\delta_t} + C_{zq}B_{q\delta_t} - \frac{D_{z\delta_t}}{\tau_t}$	$A_{qu}B_{u\delta_t} + A_{qw}B_{w\delta_t} - \frac{B_{q\delta_t}}{\tau_e}$

Table A.3: Coefficients for the f_x and f_z states

B

Phugoid related EMD results

This appendix contains the phugoid eigenvector distortion plots for all four CWA configurations. They are displayed in Fig. B.1, with the corresponding magnitude and phase distortion values given in Table B.1. The system response to the excitation of the phugoid eigenmode only is shown in Fig. B.2. As previously stated in Sec. II C in the paper, this is a means of visualizing the eigenvector distortions in the time domain.

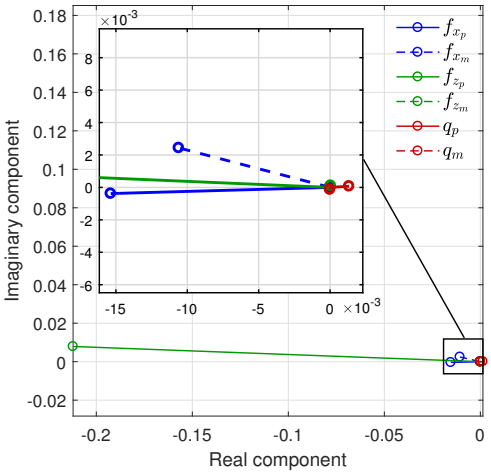

(a) Configuration B

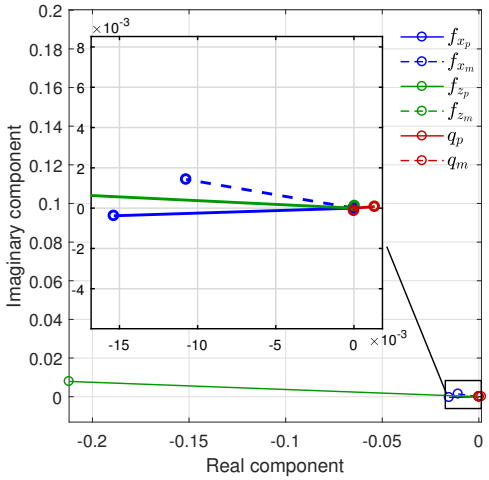

(b) Configuration O

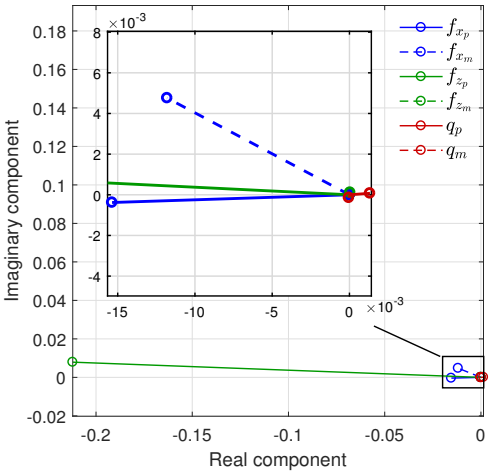

(c) Configuration E_{ph}

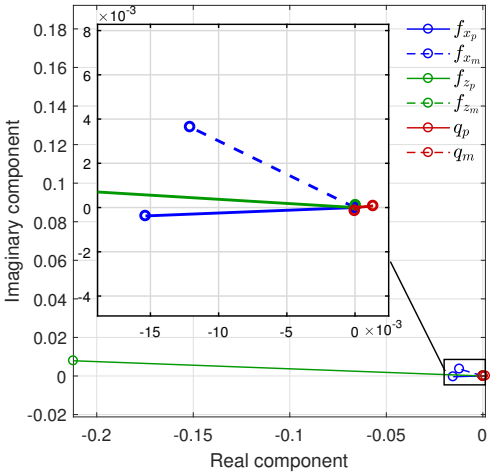

(d) Configuration E_m

Figure B.1: Phugoid eigenvector distortion plots for all CWA configurations

	$\|f_x\|_{ph}$	$\angle(f_x)_{ph}[°]$	$\|f_z\|_{ph}$	$\angle(f_z)_{ph}[°]$	$\|q\|_{ph}$	$\angle(q)_{ph}[°]$
B	0.71	14.4 lead	$5.65{\cdot}10^{-5}$	108.3 lead	0.1	99.7 lag
O	0.70	9.0 lead	$5.65{\cdot}10^{-5}$	108.3 lead	0.1	94.6 lag
E_{ph}	0.83	23.4 lead	$5.65{\cdot}10^{-5}$	108.3 lead	0.11	108.7 lag
E_m	0.82	18.2 lead	$5.65{\cdot}10^{-5}$	108.3 lead	0.11	103.7 lag

Table B.1: Phugoid period eigenvector magnitude and phase distortions for all CWA configurations

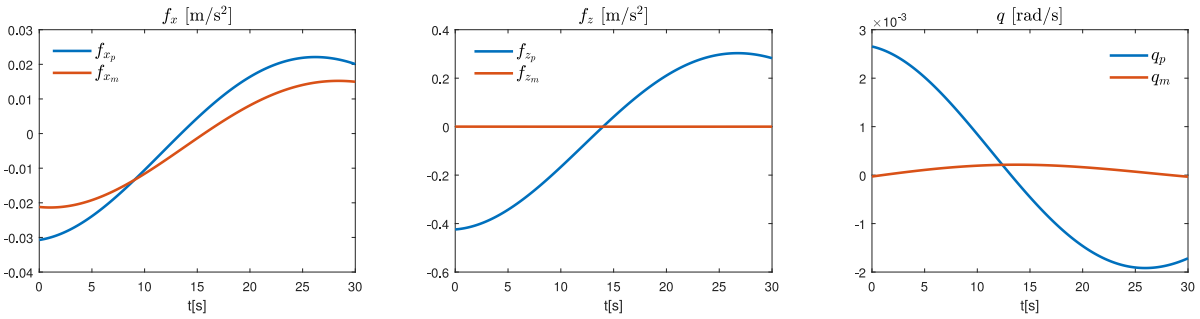

(a) B

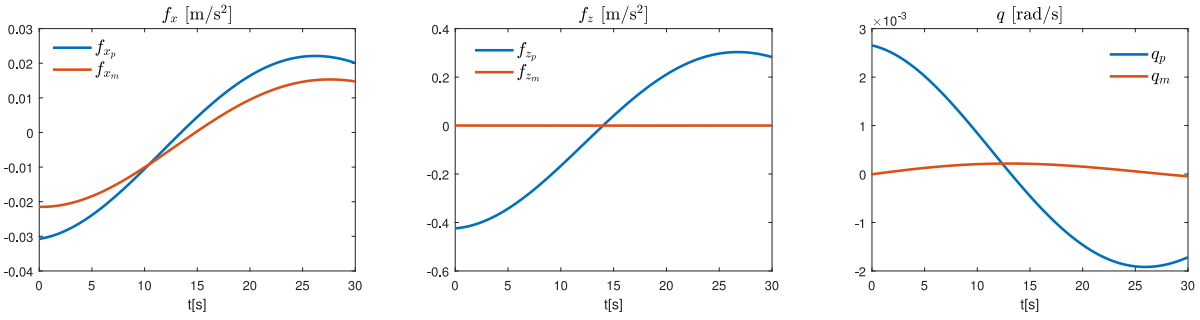

(b) O

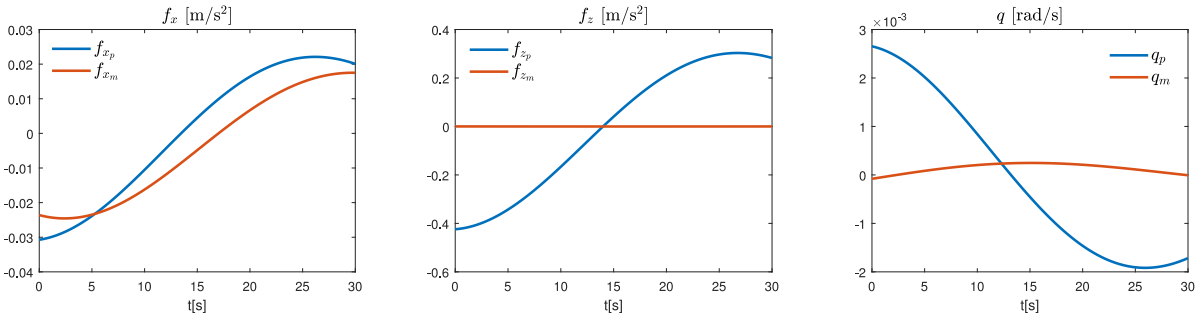

(c) E_{ph}

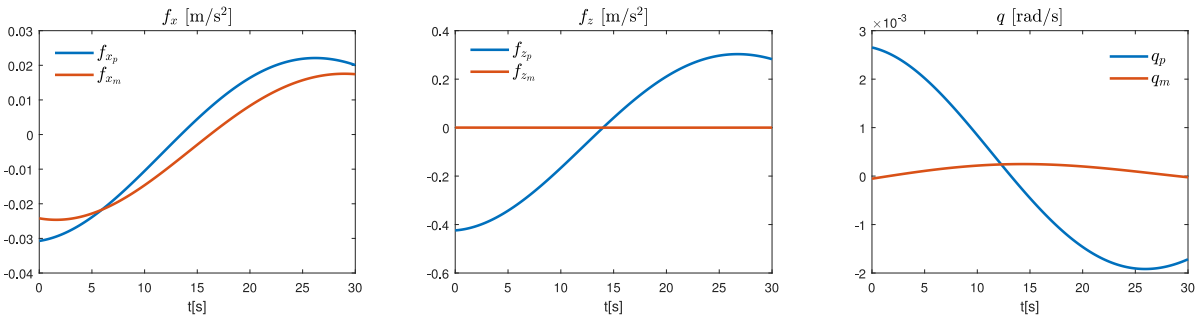

(d) E_m

Figure B.2: System response to the phugoid eigenmode excitation

C

Verification and Validation

Verification and validation are an inseparable part of any design and development processes that are performed to ensure the correct implementation and the validity of the design or methodology. During the development of EMD for use in fixed-wing aircraft simulations, verification and validation were continuously performed. The verification and validation results are presented in Appendices C.1 and C.2, respectively.

C.1. Verification

C.1.1. Dimensional Aircraft System

The EMD analysis method uses the dimensional equations of motion (presented in Eq. (A.1)) as the basis for the aircraft state-space system. It is often the case, however, that the aircraft stability and control derivatives are expressed in a dimensionless form. This facilitates an easier and more intuitive comparison between the flight dynamics properties of different aircraft.

To arrive at the dimensionless form of the stability and control derivatives, the first two equations in Eq. (A.1) are divided by a $\frac{1}{2}\rho V^2 S$ term, since they are force equations. Similarly, the third equation is divided by $\frac{1}{2}\rho V^2 S\bar{c}$ due to it being a moment equation. The result is the dimensionless equations of motion. They are presented in Eq. (C.1), with the new dimensionless definitions for the states and other coefficients given in Table C.1. The resulting relation between the dimensional and dimensionless stability and control derivatives is shown in Table C.2. The verification plots for the aircraft states are presented in Fig. C.1, which show the system response to an elevator pulse input of $\delta_e = -1.5°$. This input is also used in all subsequent simulations presented in this section. As expected, the dimensionless and dimensional equations of motion are identical in their response.

$$\begin{aligned}
C_{Z_0}\theta + C_{X_u}\hat{u} + C_{X_\alpha}\alpha + C_{X_q}D_c\theta + C_{X_{\delta_e}}\delta_e + C_{X_{\delta_t}}\delta_t &= 2\mu_c D_c\hat{u} \\
-C_{X_0}\theta + C_{Z_u}\hat{u} + C_{Z_\alpha}\alpha + C_{Z_{\dot{\alpha}}}D_c\alpha + C_{Z_q}D_c\theta + C_{Z_{\delta_e}}\delta_e + C_{Z_{\delta_t}}\delta_t &= 2\mu_c\left(D_c\alpha - D_c\theta\right) \\
C_{m_u}\hat{u} + C_{m_\alpha}\alpha + C_{m_{\dot{\alpha}}}D_c\alpha + C_{m_q}D_c\theta + C_{m_{\delta_e}}\delta_e + C_{m_{\delta_t}}\delta_t &= 2\mu_c K_{YY}D_c\frac{q\bar{c}}{V} \\
D_c\theta\frac{\bar{c}}{V} &= \frac{q\bar{c}}{V}
\end{aligned} \tag{C.1}$$

$\hat{u} = \frac{u}{V}$	$\alpha = \frac{w}{V}$	$D_c = \dot{t}/\frac{V}{\bar{c}}$	$\mu_c = \frac{m}{\rho S\bar{c}}$

Table C.1: Definition of the dimensionless states and coefficients

$X_0 = C_{X_0} \frac{1}{2} \rho V^2 S$	$Z_0 = C_{Z_0} \frac{1}{2} \rho V^2 S$	$I_{YY} = K_{YY} m \bar{c}^2$
$X_u = C_{X_u} \frac{1}{2} \rho V S$	$Z_u = C_{Z_u} \frac{1}{2} \rho V S$	$M_u = C_{m_u} \frac{1}{2} \rho V S \bar{c}$
$X_w = C_{X_\alpha} \frac{1}{2} \rho V S$	$Z_w = C_{Z_\alpha} \frac{1}{2} \rho V S$	$M_w = C_{m_\alpha} \frac{1}{2} \rho V S \bar{c}$
$X_q = C_{X_q} \frac{1}{2} \rho V S \bar{c}$	$Z_{\dot{w}} = C_{Z_{\dot{\alpha}}} \frac{1}{2} \rho V S \bar{c}$	$M_{\dot{w}} = C_{m_{\dot{\alpha}}} \frac{1}{2} \rho V S \bar{c}^2$
$X_{\delta_e} = C_{X_{\delta_e}} \frac{1}{2} \rho V^2 S$	$Z_q = C_{Z_q} \frac{1}{2} \rho V S \bar{c}$	$M_q = C_{m_q} \frac{1}{2} \rho V S \bar{c}^2$
$X_{\delta_t} = C_{X_{\delta_t}} \frac{1}{2} \rho V^2 S$	$Z_{\delta_e} = C_{Z_{\delta_e}} \frac{1}{2} \rho V^2 S$	$M_{\delta_e} = C_{m_{\delta_e}} \frac{1}{2} \rho V^2 S \bar{c}$
	$Z_{\delta_t} = C_{Z_{\delta_t}} \frac{1}{2} \rho V^2 S$	$M_{\delta_t} = C_{m_{\delta_t}} \frac{1}{2} \rho V^2 S \bar{c}$

Table C.2: Definition of the dimensional stability and control derivatives [10]

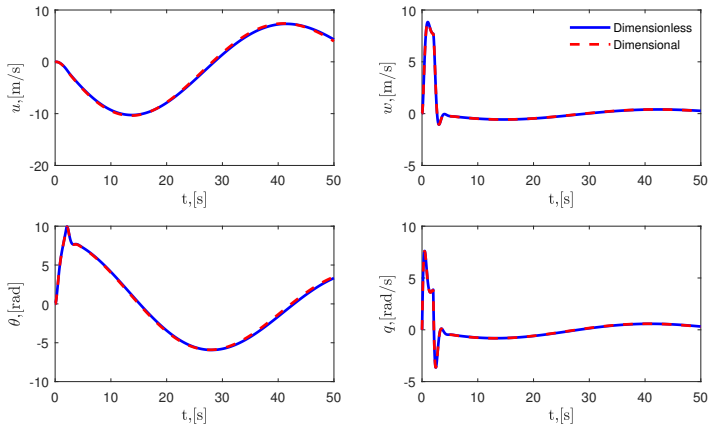

Figure C.1: Verification of the motion cues in the simulated aircraft

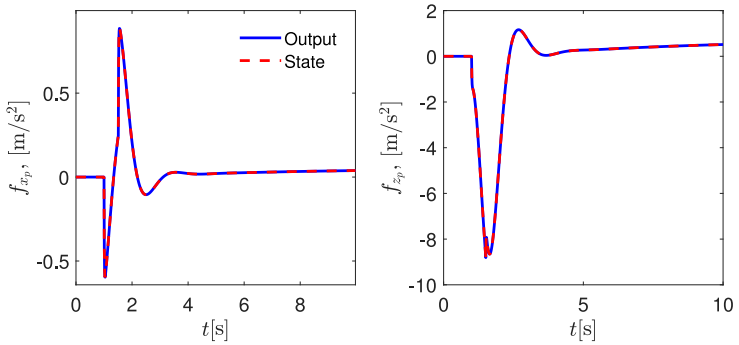

Figure C.2: Verification of the state representation of f_{x_p} and f_{z_p}

C.1.2. State representation of f_{x_p} and f_{z_p}

The state representation of the aircraft specific forces is a key part in the formulation of the combined state-space system. Therefore it is important to verify that its derivation is done correctly. This is done by comparing the time histories of the direct output formulation for f_{x_p} and f_{z_p}, presented in Eq. (A.3), and their state

formulations. The results are visualized in Fig. C.2, where it can be observed that the two time histories are identical. Therefore the state representation is correctly derived.

C.1.3. Linear CWA model

The linearized CWA model that is part of the combined system, used in the EMD method, is verified with a Simulink model of the CWA algorithm, which is shown in Fig. C.3. The specific forces and the pitch rotation acceleration resulting from the aircraft response shown in Fig. C.1 are used as the input signals that are visualized in Fig. C.4a. The verification outputs are presented in Fig. C.4b, where it can be observed that the linear model has the same response as the Simulink model. It must be noted that, for the verification of the pitch CWA channel, the simulator pitch angle θ_m is used instead of the pitch rate q_m. This is due to the Simulink model not being able to produce the output for the tilt-align pitch rate and consequently the simulator pitch rate. Nevertheless, since the resulting pitch angle responses are identical, the pitch rates are verified too.

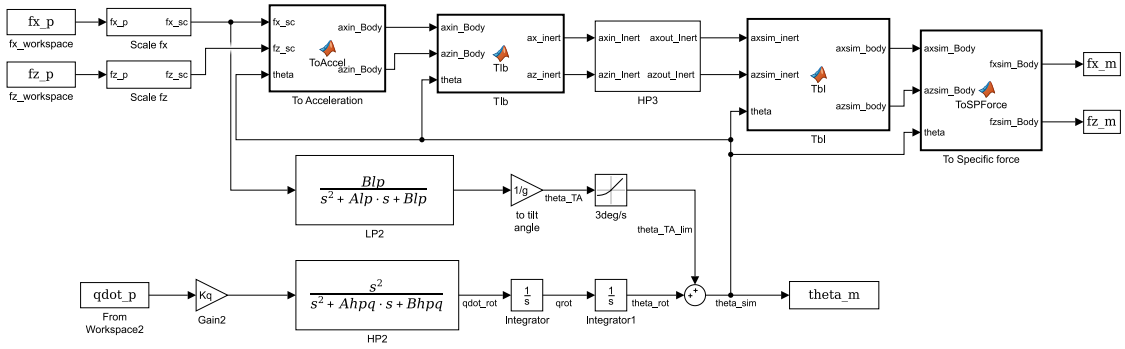

Figure C.3: Non-linear Simulink model of the Classical Washout Algorithm

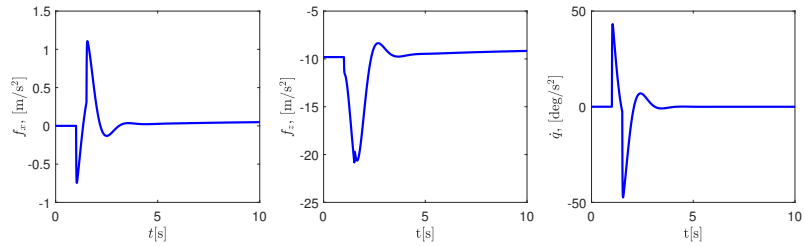

(a) Verification inputs

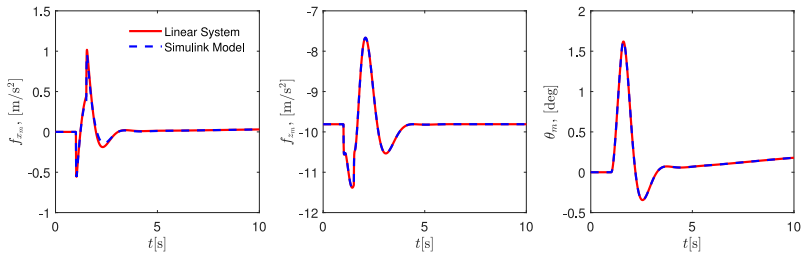

(b) Verification outputs (with CWA configuration E_m)

Figure C.4: Verification of the linear CWA model

C.1.4. Combined system

The verification of the combined state-space system used for the EMD analysis is performed by comparing the simulator related outputs – f_{x_m}, f_{z_m}, q_m – of the combined system and the linear CWA model, using the aircraft motion cues from the combined system as inputs. The verification plots for the three motion cues

are presented in Fig. C.5. There it can be seen that the outputs of the combined system perfectly match the outputs of the linear CWA model, meaning that the coupled system is correctly defined.

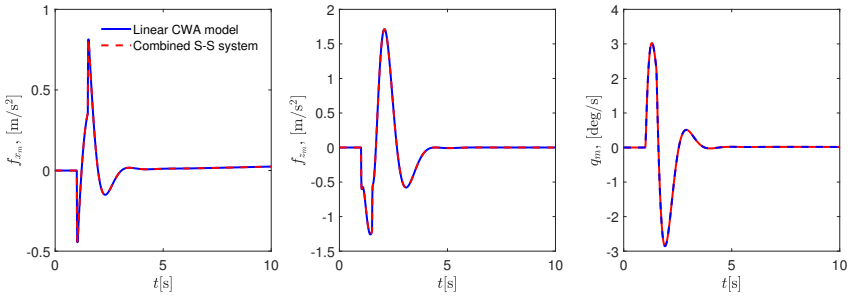

Figure C.5: Verification of the combined state-space system

C.2. Validation

C.2.1. Flight Test Data

After the extended aircraft state-space system is defined, it is validated using flight test data [1] obtained as part of the course 'AE3212-II: Simulation, Verification, and Validation', part of the curriculum of the BSc Aerospace Engineering program of TU Delft. The flight test for the used data was performed on 15.03.2018 at 10:30AM. This specific flight is chosen since it is in almost perfect trim condition just prior to the initialization short period approximation maneuver. The used aircraft is a Cessna Citation 550. Therefore, the linear model used for the piloted experiment in the SRS could not be used for this validation and the model provided in the course is used instead [9]. It is shown in Table C.3.

C_{X_0}	-0.0277	C_{Z_0}	-0.2160	C_{m_0}	0.0297	m	5950 [kg]
C_{X_u}	-0.0279	C_{Z_u}	-0.3762	C_{m_u}	0.0699	S	30 [m^2]
C_{X_α}	-0.4797	C_{Z_α}	-5.7434	C_{m_α}	-0.5626	$\bar{c}$	2.057 [m]
$C_{X_{\dot{\alpha}}}$	0.0833	$C_{Z_{\dot{\alpha}}}$	-0.0035	$C_{m_{\dot{\alpha}}}$	0.1780	V	102.93 [m/s]
C_{X_q}	-0.2817	C_{Z_q}	-5.6629	C_{m_q}	-8.7941	h	3055 [m]
$C_{X_{\delta_e}}$	-0.0373	$C_{Z_{\delta_e}}$	-0.6961	$C_{m_{\delta_e}}$	-1.1642	ρ	0.8415 [kg/m^3]
$C_{X_{\delta_t}}$	0	$C_{Z_{\delta_t}}$	0	$C_{m_{\delta_t}}$	0	K_{YY}	1.3925

Table C.3: Aircraft Data used for the validation of the extended aircraft system [9]

The validation plots of the aircraft states and the specific forces for the short period eigenmode are presented in Figs. C.6 and C.7 respectively. During the validation of the expressions for f_{x_p}, it was observed that the output from the combined system has a vastly different behavior than its flight test counterpart - it is heavily attenuated throughout the entire maneuver. This behavior is unexpected, especially given the fact that f_{z_p} is very similar to the flight test data. Upon further inspection it was found that the used aircraft model has a wrong sign for the C_{X_α} stability derivative. The sign of C_{X_α} in the model is negative, while C_{X_α} is usually positive [10]. After correcting this error, the response f_{x_p} is similar to the flight test data. In Figs. C.6 and C.7 the response of the system using the negative C_{X_α} is shown in green, while the one of the positive C_{X_α} is

[1] The flight test data can be downloaded from `http://dueca.tudelft.nl/testflight/data_2018/`

presented in red. It can be clearly observed that the change of sign does not have a big influence on the response of the aircraft states and the remaining motion cues which makes it difficult to spot the model error. Furthermore, from Fig. C.7 it can be concluded that the angle of attack has an important contribution to f_x in the short period eigenmode.

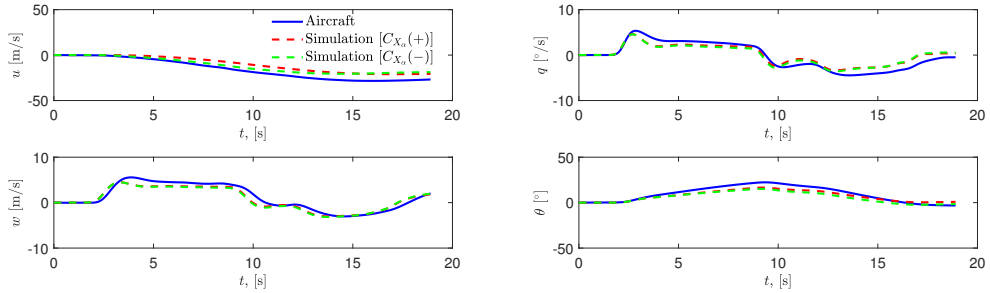

Figure C.6: Validation of the motion cues experienced in the simulator

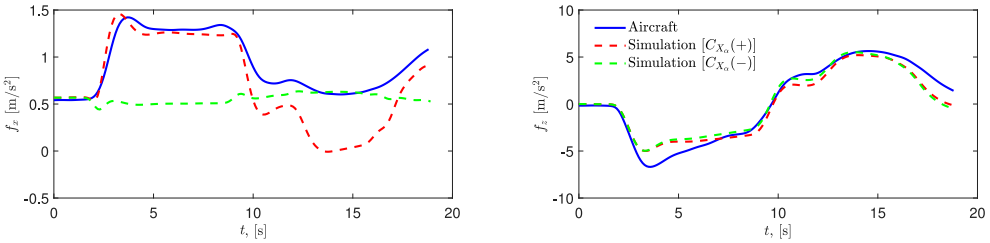

Figure C.7: Validation of the motion cues in the simulated aircraft

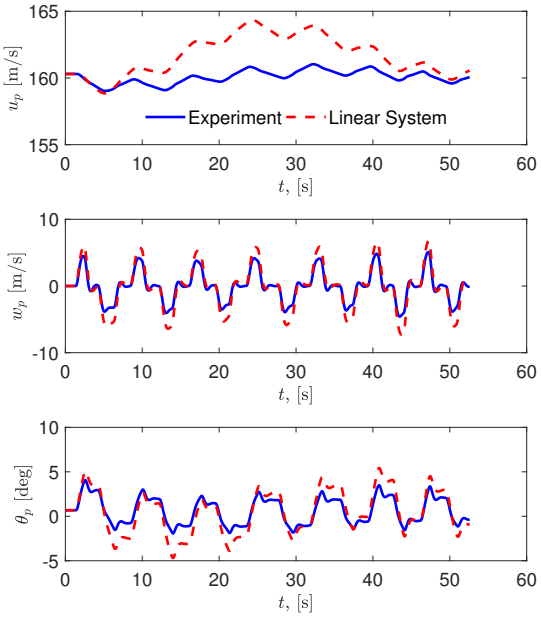

Figure C.8: Validation of the aircraft states with experiment data

C.2.2. Experiment Data

The validation of the coupled system used for the EMD analysis is carried out using experiment data taken from the run of Subject 6, flying CWA configuration B, part of the pair $E_m - B$. The validations of the aircraft states together with the aircraft and simulator motion cues are presented in Figs. C.8, C.9a and C.9b. It is observed that the linear system manages to approximate the aircraft states very well, with only the body velocity u_p exhibiting a slight deviation from the experiment data. Its consequent effect on the motion cues, particularly f_{x_p}, is however negligible. The results of the validation of the simulator motion cues are similar. The outputs of the linear system closely resemble the experiment data, with only f_{x_m} having slight deviations. Therefore, it can be concluded that, for the purposes of the EMD analysis, the combined linear system gives an accurate enough representation of the non-linear aircraft model and MCA dynamics.

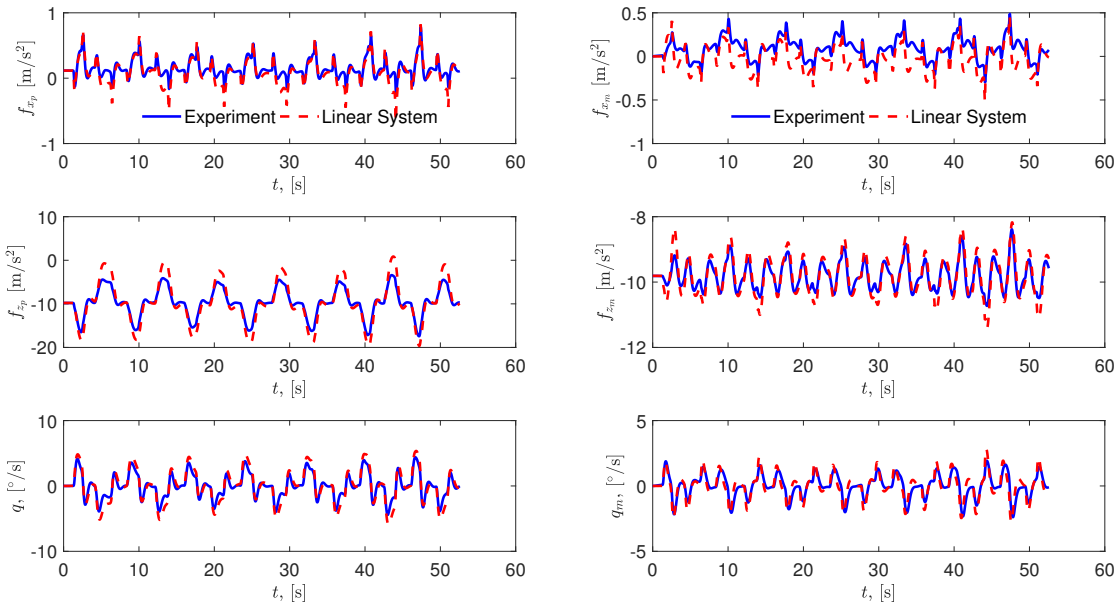

(a) Simulated aircraft cues

(b) Simulator cues

Figure C.9: Validation of the motion cues with experiment data

D

GUI Tool for tuning with EMD

D.1. Benefits of using a GUI tool

While it is possible to perform the EMD tuning of the CWA filters by doing all steps in the process through programme code, the use of a GUI tool specifically designed for this purpose significantly reduces the time it takes to do that. This is due to several reasons:

- The magnitude and phase distortion values are directly printed below the eigenvector plots. This makes it easier to make comparisons between different CWA configurations more quickly, since their EMD performance can be directly juxtaposed.
- The filter parameters are always displayed and can be quickly adjusted. This allows for a more agile development of configurations, as the effect of the filter parameter changes can be observed immediately.
- The functionality of the tool is tailored to the currently used tuning methodology, which enables the quick execution of all successive steps. However, this also implies that the tool would have to be adapted if a different tuning methodology is to be used.

D.2. Breakdown of the tool functionality

The main window of the EMD GUI tool is shown in Fig. D.1. The CWA filter parameters are set in the upper left corner. They can be saved in a configuration by pressing the *'Save Filter'* button. Similarly, a saved configuration can be loaded with the *'Load Filter'* button. The *'Analyse'* button must be pressed in order to calculate and plot the eigenvector distortions. Furthermore, once the configuration has been analyzed, the linear CWA response to the approximation maneuver inputs can be observed in the tabs `'PitchCapture SimOut'` and `'AltitudeCapture SimOut'`. The tab names correspond to the approximation maneuvers for each eigenmode. For the short period this is a pitch capture of $\pm 5^{\circ}$ (also known as a pull-up, push-over maneuver) , and for the phugoid eigenmode – an altitude capture of +200ft → -200ft → 0ft from the initial condition. An example for the pitch capture responses is seen in Fig. D.2. In the right side of the GUI tool window there is a switch enabling zooming and panning for all figures, since these controls are not available by default in the *App Designer* environment in MATLAB. The *'Reset'* button located beneath the switch can be pressed for returning to the initial view of the figures.

The next step is to evaluate whether the simulator motion space is exceeded with the selected configuration. The non-linear Simulink CWA model, shown in Fig. C.3, is used for this purpose in order to obtain more accurate estimates of the motion platform position. The simulation is started by pressing the *'Check Actuator Limits'* button. Before the simulation is started, a red light is present, which turns yellow while the simulation is running, and becomes green when the simulation has finished. The platform displacement is visualized in

one of the tabs on the top of the window. This is shown in Fig. D.3. Notice that the motion space is exceeded in the heave axis, and that there is a message warning about this in the lower left corner of the tool's window. The extensions of the individual actuators can also be visualized, as seen in Fig. D.4. Their lengths are calculated by using the inverse platform kinematics, which are described by Eq. (D.1) [1]. The absolute actuator lengths $\bar{q} = ||\bar{l}||$ are subsequently used for checking whether the actuator limits have been exceeded.

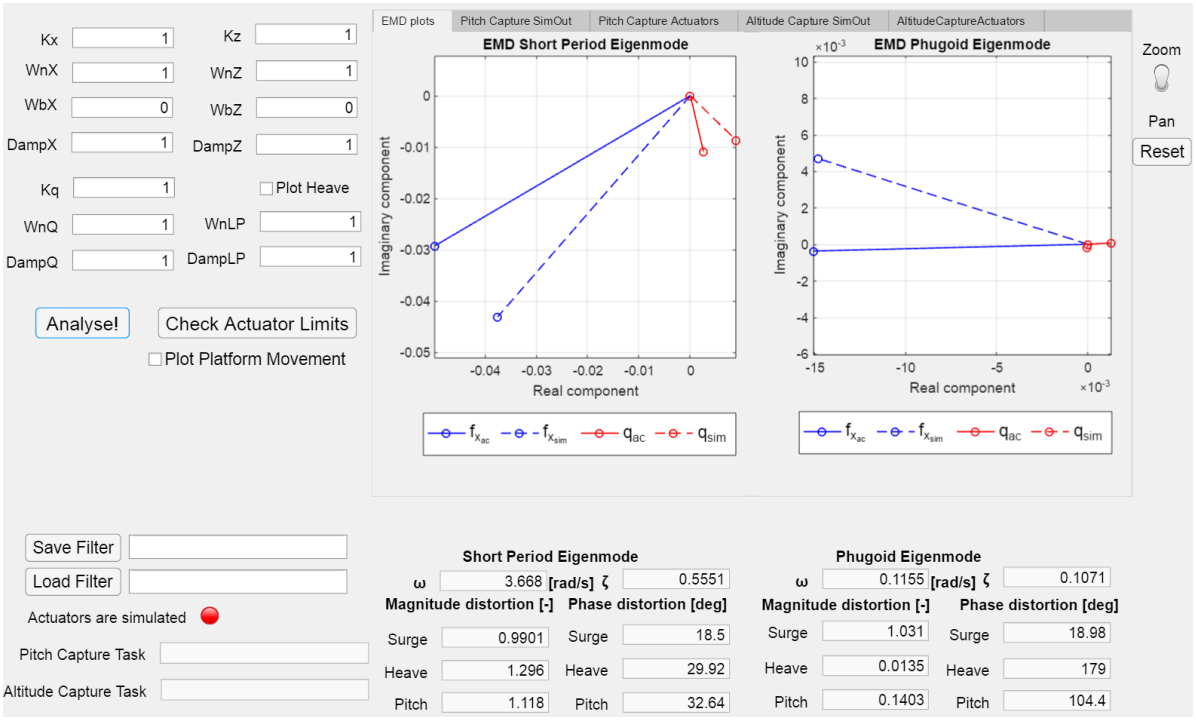

Figure D.1: The main window of the EMD GUI tuning tool

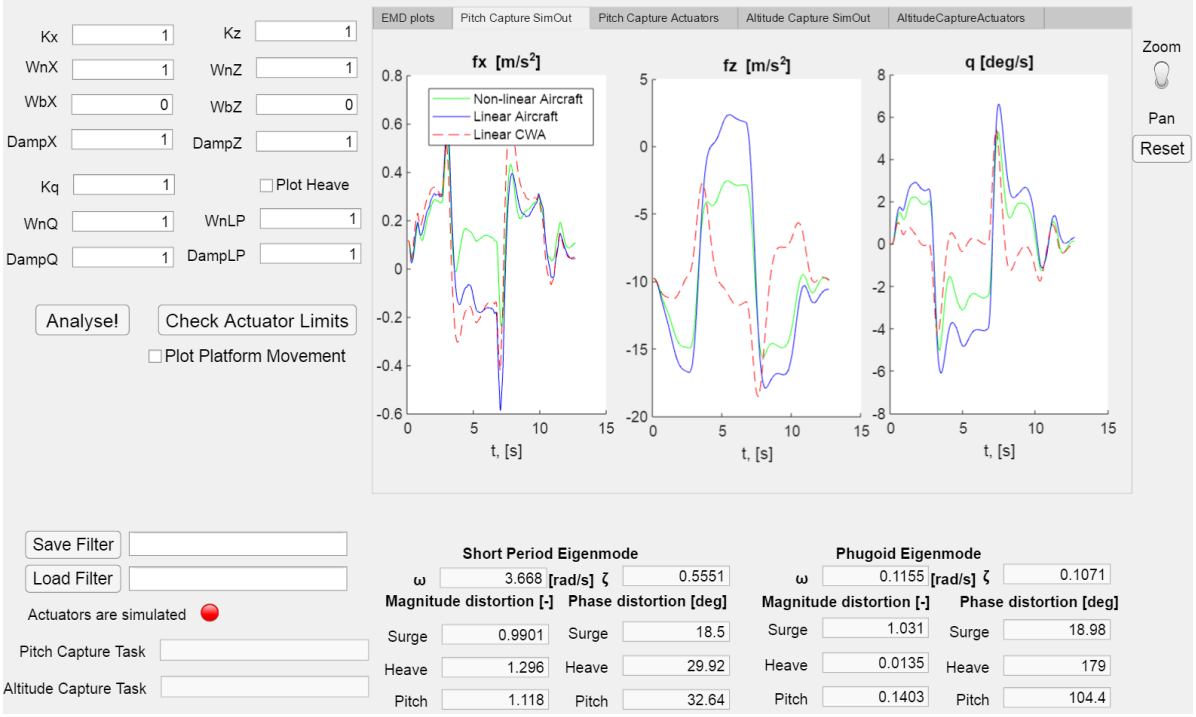

Figure D.2: The time histories of the simulator motion cues for the short period approximation maneuver

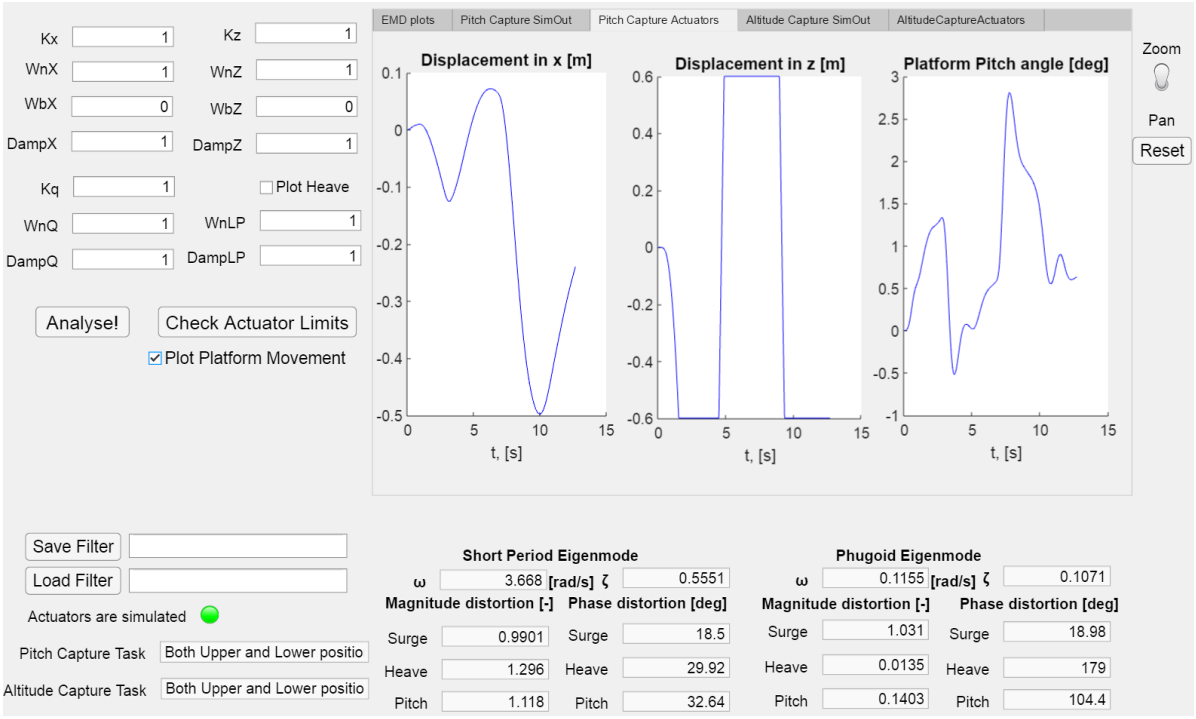

Figure D.3: The time histories of the platform displacement

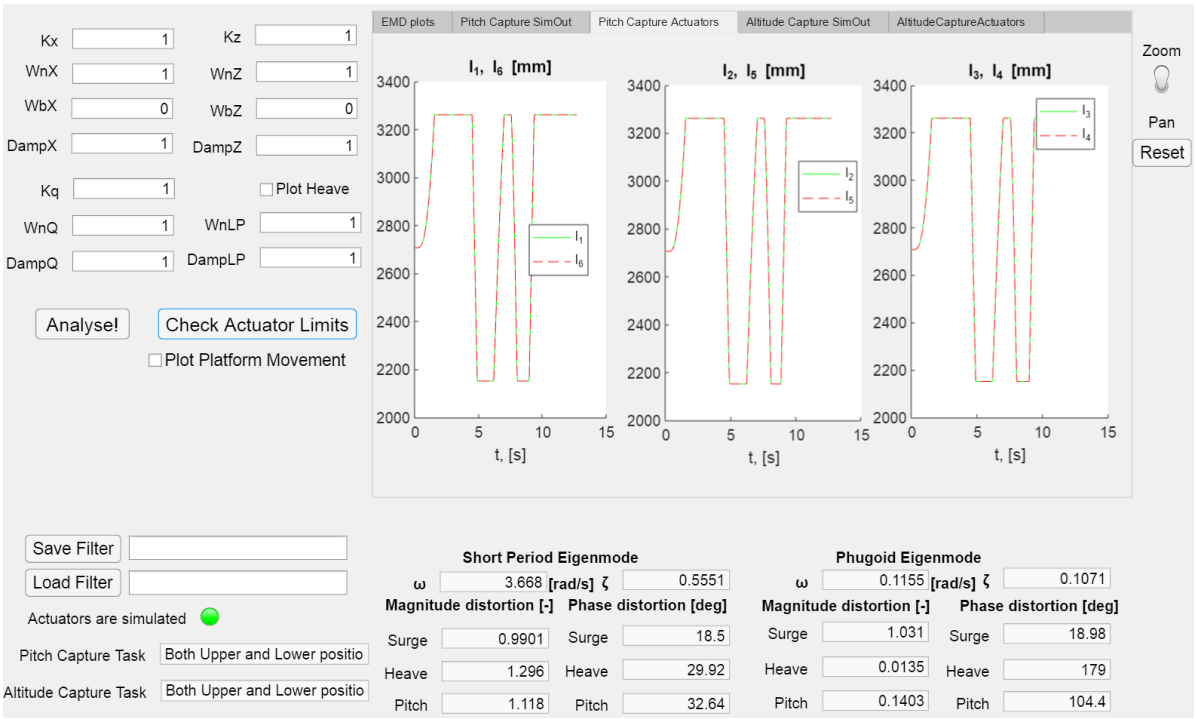

Figure D.4: The time histories of the actuator extensions

$$\bar{l} = \bar{S} + \bar{c} - \bar{B} \tag{D.1}$$

Here $\bar{l}$ denotes the vector containing the length of all actuators and $\bar{c}$ is the vector coordinates of the location

of the UGP with respect to the LGP, as shown in Fig. D.6. The $\bar{c}$ vector is represented by the displacement commands given to the motion platform by the MCA added to the coordinates of the neutral platform position ($\bar{x} = [0, 0, -2.39m]$ [1]). $\bar{B}$ contains the Cartesian coordinates of the lower platform joints. The coordinates of the upper platform joints in the inertial reference frame are represented by $\bar{S}$. They are obtained by transforming the coordinates in the body frame $\bar{A}$, as shown in Eq. (D.2). The transformation matrix T_{Ib} is simplified by assuming that $\phi = \psi = 0°$, since only longitudinal motions are studied. It is presented in Eq. (D.4). The definition of the lower and upper joint coordinate matrices is presented in Eq. (D.3), with the relevant platform geometries shown in Figs. D.5a and D.5b and quantified in Table D.1. It must be noted that the actuator minimum and maximum operational lengths, $L_{min,o}$ and $L_{max,o}$, are correspondingly increased and decreased with 20mm. This is done in order to provide an additional movement buffer which ensures a smoother stopping of actuators when their limits are reached, thus reducing the wearing out of the motion hardware.

$$\bar{S} = T_{Ib}\bar{A} \tag{D.2}$$

$$\begin{aligned} \bar{A} &= \begin{bmatrix} A_1 & A_2 & A_3 & A_4 & A_5 & A_6 \end{bmatrix} \\ \bar{B} &= \begin{bmatrix} B_1 & B_2 & B_3 & B_4 & B_5 & B_6 \end{bmatrix} \end{aligned} \tag{D.3}$$

$$T_{Ib} = \begin{bmatrix} \cos\theta_m & 0 & \sin\theta_m \\ 0 & 1 & 0 \\ -\sin\theta_m & 0 & \cos\theta_m \end{bmatrix} \tag{D.4}$$

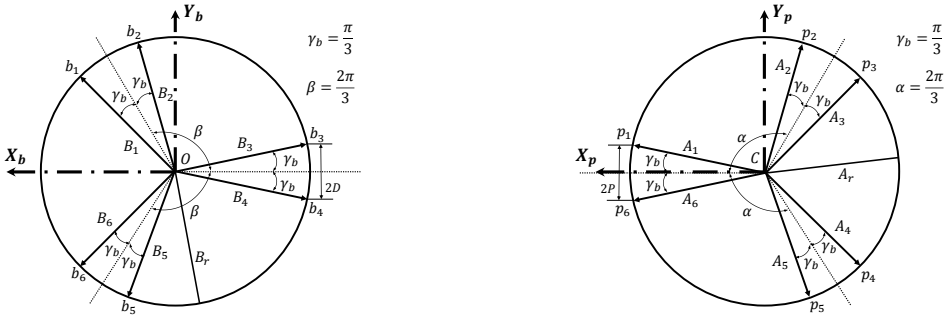

(a) Lower (base) platform geometry

(b) Upper (moving) platform geometry

Figure D.5: Geometry of the lower and upper motion platforms

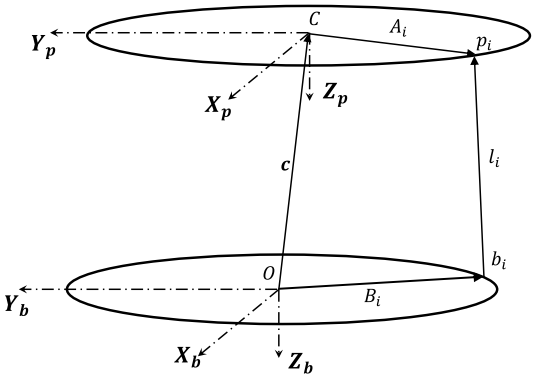

Figure D.6: Relation between the SIMONA motion platforms

Platform Property	**Notation**	**Value [mm]**
Upper Circle Radius	A_r	1600
Lower Circle Radius	B_r	1650
Upper Gimbal Spacing	$2P$	200
Lower Gimbal Spacing	$2D$	600
Actuator Maximum Operational Length	$L_{max,o}$	3281
Actuator Minimum Operational Length	$L_{min,o}$	2131

Table D.1: Relevant parameters of the SIMONA motion platform and actuators [1]

E

Experiment Documentation

E.1. Pilot Briefing

Briefing: Fidelity Comparison Between Differently Tuned Motion Cueing Algorithms

A novel method for objective motion cueing evaluation is currently being developed in the Control & Simulation group of the Faculty of Aerospace Engineering in TU Delft. This method specifically targets a realistic cueing of the short period oscillation dynamics.

In the experiment taking place today, you will perform a series of pair-wise comparisons between a total of four configurations of the Classical Washout MCA in the SIMONA Research Simulator (SRS). Besides motion cueing, you will be provided with a full outside visual and basic aircraft instrumentation, shown in Figure 1. The aircraft you will be flying is a Cessna Citation 500 in a cruise configuration, which you will control with a sidestick. You will wear a set of noise cancelling headphones playing an engine noise sound, which will mask the false auditory cues coming from the hydraulic motion actuators.

Your goal during the experiment is to compare pairs of MCA configurations and to select a 'winner' for each pair. The winner is the configuration which more resembles real flight. For each configuration you have one minute to fly the aircraft. In this time you need to excite its dynamics in a way that allows you to get a good feel for the motion cueing. First, you will perform a short training, where you will fly each configuration twice in a random order. During the training you are free to explore strategies on how to excite the aircraft, so you can get a better feel for the motion cueing. Some example manoeuvres that you can use include the following:

- A pull-up push-over manoeuvre consisting of a sequence of pitch angle captures of +5° → 0° →-5° → 0°.
- Elevator pulse input followed by observing the aircraft response.
- Series of elevator pulse inputs.

After the training has concluded, you have to choose a single evaluation strategy and stick to it during the evaluation runs. Furthermore, you must stick to the following experiment boundaries:

- Do not perform pitch captures of more than ±5°.
- Do not exceed deviation of +-10kts from your trimmed airspeed.
- Do not apply full stick deflections.

In addition to the normal evaluation runs, there will be a 'World Cup' stage, where you will compare two sets of pairs in 'semi-finals' and the winners of which will face off in the 'final'. In this stage you must again stick to the strategy you used in the previous evaluations.

The structure of the experiment is as follows:

1. Training runs (±15 minutes)
2. Evaluation runs (±30 minutes)
3. Break (±20 minutes)
4. Evaluation runs (±30 minutes)
5. World Cup (±15 minutes)
6. (Optional) Semi-blind World Cup

The experiment will take approximately 2 hours including the break. Note that your participation in the experiment is voluntary and you can terminate it at every time.

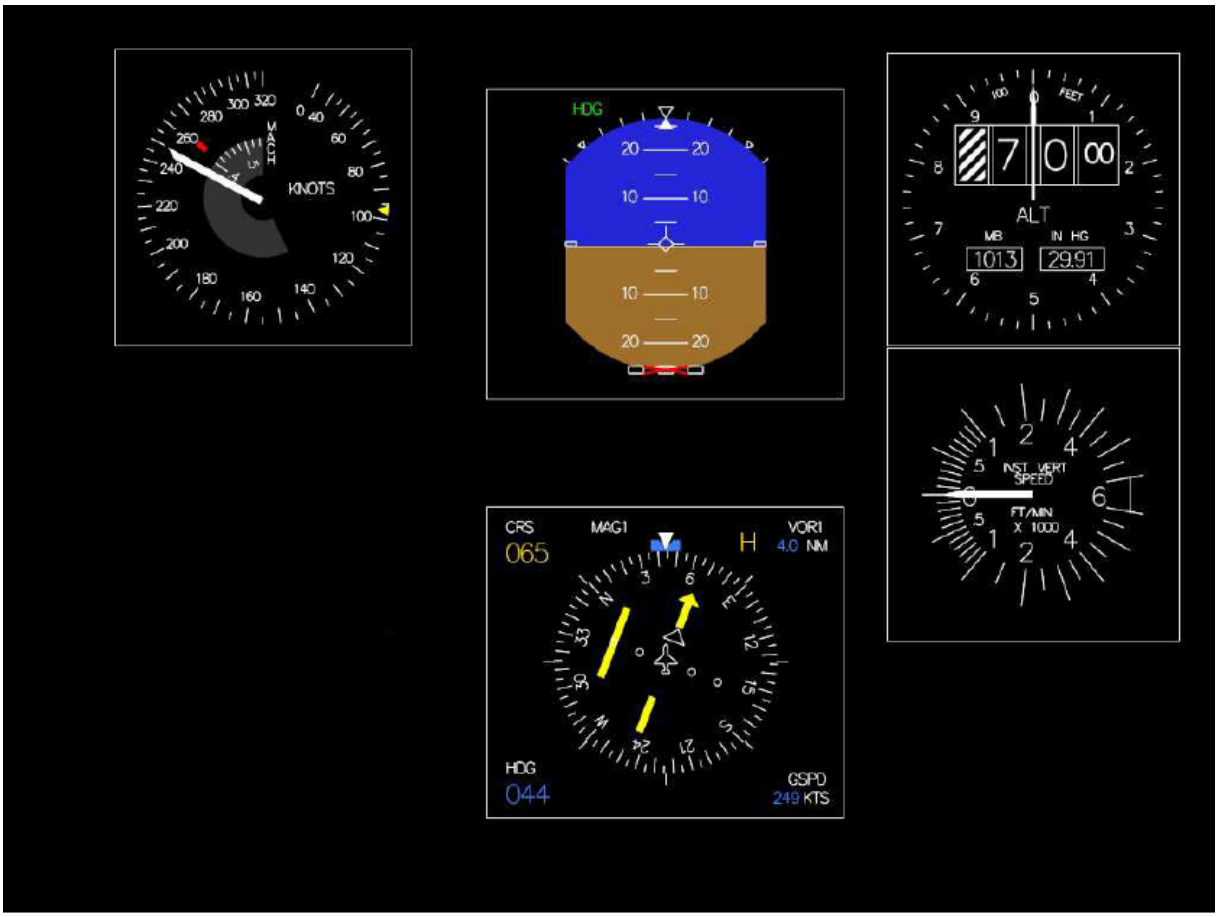

Figure 1 **The Instrument Panel**

E.2. Subject Consent Form

Experiment Consent Form

Fidelity comparison between differently tuned Motion Cueing Algorithms

I hereby confirm that:

1. I volunteer to participate in the experiment conducted by the researcher (**Stanimir Stoev**) under Supervision of **ir. Olaf Stroosma** from the Faculty of Aerospace Engineering of TU Delft. I understand that my participation in this experiment is voluntary and that I may withdraw and discontinue participation at any time, for any reason.
2. I have read the experiment briefing. Also, I affirm that I understand the experiment instructions and have had all remaining questions answered to my satisfaction.
3. I understand that my participation involves performing evaluation of different Motion Cueing Algorithms in a moving base simulator. Also, I understand the researcher will request subjective assessments from me throughout the experiment.
4. I consent to my voice being recorded during the experiment and that it will be used during the analysis of the experiment results. Furthermore, I understand that the recordings will be deleted after all relative information has been written down.
5. I confirm that the researcher has provided me with detailed safety and operational instructions for the hardware (simulator setup, sidestick) used in the experiment.
6. I understand that the researcher will not identify me by name in any reports or publications that will result from this experiment, and that my confidentiality as a participant in this study will remain secure. Also, I understand that any comments I make during the experiment can appear in the said reports and publications
7. I have been given a copy of this consent form.

My Signature	Date
My Printed Name	Signature of researcher

Contact information researcher:	Contact information research supervisor
Stanimir Stoev	Ir. OlafStroosma
S.Stoev@student.tudelft.nl	O.Stroosma@tudelft.nl
+31 6 26239068	+31 6 45244293

E.3. Latin-Square Matrices

E.3.1. Training

Subject	Conditions							
1	B	O	E_m	E_{ph}	E_m	B	E_{ph}	O
2	O	E_{ph}	B	E_m	E_{ph}	E_m	O	B
3	E_{ph}	E_m	O	B	O	E_{ph}	B	E_m
4	E_m	B	E_{ph}	O	B	O	E_m	E_{ph}
5	O	E_{ph}	B	E_m	E_{ph}	E_m	O	B
6	E_m	B	E_{ph}	O	B	O	E_m	E_{ph}

Table E.1: Latin square matrix for the training runs for all subjects

E.3.2. Evaluation

Subject	Conditions										
1	$B-O$	$B-E_{ph}$	E_m-E_{ph}	$B-E_m$	E_m-O	$O-E_{ph}$	$E_{ph}-O$	$O-E_m$	E_m-B	$E_{ph}-E_m$	$E_{ph}-B$	$O-B$
2	$B-E_{ph}$	$B-E_m$	$B-O$	$O-E_{ph}$	E_m-E_{ph}	$O-E_m$	E_m-O	$E_{ph}-E_m$	$E_{ph}-O$	$O-B$	E_m-B	$E_{ph}-B$
3	$B-E_m$	$O-E_{ph}$	$B-E_{ph}$	$O-E_m$	$B-O$	$E_{ph}-E_m$	E_m-E_{ph}	$O-B$	E_m-O	$E_{ph}-B$	$E_{ph}-O$	E_m-B
4	$O-E_{ph}$	$O-E_m$	$B-E_m$	$E_{ph}-E_m$	$B-E_{ph}$	$O-B$	$B-O$	$E_{ph}-B$	E_m-E_{ph}	E_m-B	E_m-O	$E_{ph}-O$
5	$O-E_m$	$E_{ph}-E_m$	$O-E_{ph}$	$O-B$	$B-E_m$	$E_{ph}-B$	$B-E_{ph}$	E_m-B	$B-O$	$E_{ph}-O$	E_m-E_{ph}	E_m-O
6	$E_{ph}-E_m$	$O-B$	$O-E_m$	$E_{ph}-B$	$O-E_{ph}$	E_m-B	$B-E_m$	$E_{ph}-O$	$B-E_{ph}$	E_m-O	$B-O$	E_m-E_{ph}

Table E.2: Latin Square matrix of the experiment conditions for all pilots

F

Reflections on the experiment results

The goal of this appendix is to present the feedback given by the pilots and provide a more detailed description of their performance. Based on parts of the pilot feedback, further recommendations are given for similar experiments involving subjective evaluation of motion cueing fidelity.

The structure of the appendix is as follows. In Appendix F.1 the feedback given by all pilots is summarized. A discussion on some of the time-specific pilot comments is presented in Appendix F.2. Finally, the recommendations for future experiments are given in Appendix F.3.

F.1. Summary of the pilot feedback

During the evaluation phase of the experiment all pilots provided some varying amount of feedback after evaluating each pair of CWA configurations. These comments are summarized in tables for every test subject, that also show the winner of each evaluation. The winner is colored in green. The outcomes and comments of the World Cup stage are also summarized. It must be noted that the subjects were offered to perform an additional, single blind World Cup round. This enables the subjects to be shown during the debrief which condition became the latest World Cup winner. These results are also not used for testing the experiment hypothesis. Any additional information about the subject's performance during the experiment, as well as a discussion on their results, is also presented.

F.1.1. Subject 1

Subject 1 belongs to the group of the most *within-pair* consistent pilots with 5/6 consistent pairs. On average, this pilot managed to maintain a consistent input profile between the different experiment runs. Subject 1 also gave detailed comments during the debriefing:

"During the test I found out that I could only rate 3 things. First, if you could find any objectionable behavior on the change of the movement in the reversal in the short period. Second, if you could see lag. During the test, especially in the large slow movements, you could feel the washout, the reversal. I think what was most difficult between one run and the second run that both had that objectionable reversal feeling during the large movements, but it was slightly more or slightly less. That's where I tried to rate, that's what determined the rating in most cases - the washout quality. In the very first runs I was not focused on the washout quality, but initially I was more focused on the short period. So it is better to do the larger changes - from $+5^\circ$ *to* -5°*, because there are larger changes there. The high frequency movements feel very similar."*

In the slow movements I felt the amount of washout. I was judging on the washout quality in the large movements.[...] Basically if you have a slower washout it felt less objectionable.[...] The objectionable thing from a

pilot's point of view is where you feel a motion where it isn't any."

Pair	Repetition			Subject Comments
$B-O$	B	-	O	*In the second condition there was some delay or floating, it felt less natural*
	O	-	B	*The hesitation on the high velocity was less pronounced in the second condition than in the first one. That is why I opt for the second.*
$B-E_{ph}$	B	-	E_{ph}	*Both felt quite reasonable, a small favour for the second condition.*
	E_{ph}	-	B	*There is a ripple in the large movements. I vote for the first condition because the second condition felt less natural at the high amplitudes, at the amplitude changes: going up → going down → going up*
$B-E_m$	B	-	E_m	*Both of them felt more or less alike. Both were comfortable, with no objections, more or less equal. I am in no position to choose.*
	E_m	-	B	*I would vote for the second condition. What I am trying to distinguish now between the slow down in the movements in the larger amplitude motions. During the second condition the slow down was less noticeable, but still noticeable.*
$E_{ph}-O$	E_{ph}	-	O	*Slight favor for the second condition. The quick movement seems to be a little bit better, but on both I notice that slowing down on the fast rate. The impression is more pronounced on the first one.*
	O	-	E_{ph}	*On the slow movements there is a hesitation when you go at the maximum speed. It is like the bleed-off but I think it was more pronounced for the second condition, so I would go for the first.*
$E_{ph}-E_m$	E_{ph}	-	E_m	*I vote for the second condition. Both had the hesitation, but the first one had something in the reversal from going up to going down (in pitch angle) that was kind of a ripple or floating over in the reversal.*
	E_m	-	E_{ph}	*The second condition has the ripple on the fast movement, you feel a change of speed when you are going down with the same rate. It is not in sync with the visual when feeling the ripple.*
E_m-O	E_m	-	O	*It felt if the bleed-off of the motion was so quick that you could feel it.You feel the acceleration, but you could feel it bleed-off while you were still moving off. This was less pronounced in the first condition, so that is why I opt for it.*
	O	-	E_m	*In the fast movements there was no difference, both had hesitations in the large movements and I thought on the first condition the hesitation was more, so the second one is slightly better. It is hard though.*

Table F.1: Subject 1 – pairwise evaluation outcomes (winner shown in green) and general comments

World Cup (Double Blind)				
Stage	Pair			Subject Comments
Semifinal 1	E_{ph}	-	E_m	*Both had a slowdown, but the second one felt a little bit different in the reversals.*
Semifinal 2	O	-	B	*I would go for the second one.*
Final	E_{ph}	-	B	*I opt for the last one. The slowdown on the large rate was slightly less. It remains difficult though.*
World Cup (Single Blind)				
Stage	Pair			Subject Comments
Semifinal 1	O	-	B	*It looks like the washout is slightly less objectionable in the second one. Minor difference.*
Semifinal 2	E_m	-	E_{ph}	*I would go for the second one, because on the first one there was an objection on the reversals.*
Final	B	-	E_{ph}	*You could feel the washout on both. On the second one I could feel it go up and also going down. On the first one it was more pronounced on the down than the up, so I would say that the first one was slightly better, but the differences are minute.*

Table F.2: Subject 1 – outcomes of both World Cup stages: double- and single-blind (winner shown in green)

F.1.2. Subject 2

Subject 2 is also part of the most *within-pair* consistent group of pilots, with 5 out of 6 consistent evaluations. Some of his comments reveal, however, that there is an element of chance in experiments using subjective evaluations. If the comments for the pair $E_{ph} - O$ are compared, it can be seen that Subject 2 used contradicting criteria in the different evaluations. He preferred the condition with less pitching moment in the first evaluation and the condition with more pitching moment in the second evaluation. Interestingly, in both evaluations the winner is configuration O even though the subject had contradicting descriptions of his perception of it. During the debriefing, Subject 2 gave the following comment regarding the experiment task:

"Overall. I am not a big fan of having experiments that do not have a specifically defined task. It makes it a little bit tricky to find what the instructors are looking for."

Pair	Repetition			Subject Comments
$B - O$	B	-	O	*The initial pitching moment is less pronounced in the second condition than in the first one. I prefer the less pronounced pitching moment onset. I would say that when you just start flying in the simulator you wouldn't notice the secondary wobble that much, while the initial pitching onset will be dominant.*
	O	-	B	*The second condition felt sluggish. It feels like when you put an input comes with a bit of a delay, like it is hitting a phase margin. It was the same magnitude of movement as the first condition, but it was delayed.*
$B - E_{ph}$	B	-	E_{ph}	*The first condition had a lot less secondary wobble. The first wobble and then the phase out. Doesn't feel there is a lot of difference, but I like the first one a little bit more. Feels like most of the subtlety is not in the initial response, but really in the latter part - if you give an input and the movement of the display stops - what comes after. The secondary response after you stop it again.*
	E_{ph}	-	B	*In the first condition it felt like there was a really high motion gain, with too much stuff going on. The second condition felt less intensive, more easy. I didn't really notice a wobble in the end, maybe I didn't excite it at the right frequency. But I really like that one.*
$B - E_m$	B	-	E_m	*It feels for the second condition that the intensity of the motion is a lot larger for the same input. For the small input it feels that there is a lot. I really feel that there is too much going on. It feels that the motion is a lot more like a 747 than for a Cessna. Honestly I don't know which degree of freedom is too much though. I think it was more pitching, but I'm not sure. I felt it in my back*
	E_m	-	B	*The second condition had a lot more wobble than the first one.*
$E_{ph} - O$	E_{ph}	-	O	*The first condition had more initial pitch feeling. In the second condition it is less pronounced and feels more realistic. I think if the pitching moment is too much, people start overreacting on that maybe (maybe it's because I think in terms of fly-by-wire)*
	O	-	E_{ph}	*The second condition had much less pitching moment but a lot more pronounced wobble*
$E_{ph} - E_m$	E_{ph}	-	E_m	*It feels the last condition is with a lot of pitching moment, with a lot of wobble in the end. The wobble is less in the first one, that's why I prefer it.*
	E_m	-	E_{ph}	*These two are feel very close; gut feeling tells me second condition feels better. Not sure why, but I think that the first one had a bit less initial pitching and there was wobble in the end. The second condition had more initial pitching moment and less wobble in the end. The changes are very subtle.*
$E_m - O$	E_m	-	O	*Especially in the first inputs which I did for the condition, the initial pitch response was slimmed down to nothing. And there was wobble in the end again.*
	O	-	E_m	*The first condition had more initial pitching than he second one. It felt again that the first condition was the heavy motion and you don't feel the secondary wobble any more. In the second condition the initial pitching was less pronounced with a bit more wobble. That's why I prefer the second condition.*

Table F.3: Subject 2 – pairwise evaluation outcomes (winner shown in green) and general comments

World Cup (Double Blind)				
Stage	Pair			Subject Comments
Semifinal 1	E_m	-	E_{ph}	*Here the second one again felt there was more gain, too much stuff going on. The first one felt less saturated, that's why I pick it.*
Semifinal 2	O	-	B	*Both of them were not too bad. The first one had more wobble compared to the second one.*
Final	E_m	-	B	*The magnitude for the initial pitching moment is the same for both of them, but the second one had more of the wobble in the end.*
World Cup (Single Blind)				
Stage	Pair			Subject Comments
Semifinal 1	E_m	-	E_{ph}	*Magnitudes about the same, but the second one had a bit less wobble at the end.*
Semifinal 2	B	-	O	*The second one there was more stuff going on, like the B747 comment before. So I like the first one more.*
Final	E_{ph}	-	B	*Less motion than the first one, where the motion felt too much. I like the second one better.*

Table F.4: Subject 2 – outcomes of both World Cup stages: double- and single-blind (winner shown in green)

F.1.3. Subject 3

Subject 3 is part of the least *within-pair* consistent group, with only 3/6 consistently evaluated pairs. Furthermore, he demonstrated the highest order effect with expressing preference for the first presented condition in the pair for a total of seven pairs. The subject did have some comments while exciting the aircraft dynamics, but they were not recorded due to a malfunction of the recording system, which was operational only when the instructor microphone was turned on. The subject had the following comments during the debriefing:

"I tried to pitch up to $+5° \rightarrow -5° \rightarrow 0°$ *and see how it actually feels and how the simulator would react. With some of the filters you could feel the washout. Then I tried short inputs to see how easy it is to control. With the filter I preferred it was easier to control. I didn't look at the visual. You could still hear the motion actuators even with the headset. I tried make this not have any effect with my results."*

Pair	Repetition			Subject Comments
$B-O$	B	-	O	*The first condition is slightly better. When I do the fast pitching movements there is hardly any difference between the two conditions, but when I do the bigger movements the first one is better.*
	O	-	B	*The first condition shows the picture in sure more smoothly. During the second condition the motion system is more lively and is moving too much.*
$B-E_{ph}$	B	-	E_{ph}	*I have a preference for the first condition, but the second one is not bad either.*
	E_{ph}	-	B	*The first condition is marginally better. It is very subtle to judge.*
$B-E_m$	B	-	E_m	*In the first condition I felt more surge in the movement up and the pitch was more pronounced. In the second condition the heave was more and was dominant over the other cues.*
	E_m	-	B	*I think the second condition is the same filter as the first one after the break. It is a definite winner over the first condition.*
$E_{ph}-O$	E_{ph}	-	O	*The second condition feels a bit funny. It does not feel right, but I cannot tell why.*
	O	-	E_{ph}	*The differences between the two conditions are very subtle. The second one is slightly better, but it is very marginal.*
$E_{ph}-E_m$	E_{ph}	-	E_m	*There is too much washout in the second condition, the first one is definitely better*
	E_m	-	E_{ph}	*The two conditions felt very similar, but the second one is still better.*
E_m-O	E_m	-	O	*The first conditions feels more smooth in a way and it is easier to control. In the second condition I would adjust a little bit more. Also in the second, after you stop pitching you would still feel something.*
	O	-	E_m	*In the second condition, you can feel as if you are braking when you pitch up.*

Table F.5: Subject 3 – pairwise evaluation outcomes (winner shown in green) and general comments

World Cup (Double Blind)				
Stage	Pair			Subject Comments
Semifinal 1	B	-	O	*Hard one to choose.*
Semifinal 2	E_m	-	E_{ph}	*The first condition felt more precise; hard to explain; wobbles less at the end; makes it easier to control feels more natural*
Final	O	-	E_m	*The first has more pitch than the second one and feels more natural*
World Cup (Single Blind)				
Stage	Pair			Subject Comments
Semifinal 1	E_{ph}	-	E_m	*It still hard to choose, but I'd say the second one is better.*
Semifinal 2	B	-	O	*Slightly better than the second one.*
Final	E_m	-	B	

Table F.6: Subject 3 – outcomes of both World Cup stages: double- and single-blind (winner shown in green)

F.1.4. Subject 4

Prior to starting with the experiment, Subject 4 noted that he slept little during the night, but that he was feeling fine. His judgment was that he could participate in the experiment, since he was in a condition to pilot an aircraft if it was necessary. Therefore it was decided to proceed with the experiment. Subject 4 is also a part of the least *within-pair* consistent pilot group. A probable reason for his inconsistency is that the subject performed most runs for a time much lower than the allotted minute, with some runs having a duration between 15 and 20 seconds. Additionally, Subject 4 managed to continuously excite the short period eigenmode, with its MPF being dominant for the better part of the evaluation runs. This pilot also had a different criteria for giving his preference, as he stated during the debriefing:

"I think for me the gain was more interesting than the phase. Obviously it didn't go out of phase, which I wouldn't notice. If you have someone more experienced on various aircraft, they would pay more attention to the relative phase.[...]I am not sensitive to heave, so this is interesting to bear in mind. Towards the end I had a feeling that I managed to recognize the different conditions."

Pair	Repetition			Subject Comments
$B-O$	B	-	O	*They are both pretty good, but I like the first condition better*
	O	-	B	*The second condition had more pitch than the first one. However, I cannot put a number on in, since on the last run I liked the condition with less pitch.*
$B-E_{ph}$	B	-	E_{ph}	*I liked the first condition better than the second one.*
	E_{ph}	-	B	*The first condition is more realistic. In the second one it felt that not much is going on, like a damped version of the motion.*
$B-E_m$	B	-	E_m	*I think that the second condition is a little better, but if you tell me they are the same I would believe you.*
	E_m	-	B	*Both conditions are not very nice, the second one is better than the first one.*
$E_{ph}-O$	E_{ph}	-	O	*The first condition feels pretty unresponsive, there is less pitch, and it is hard to describe. The second condition immediately felt better.*
	O	-	E_{ph}	*The two conditions were pretty close. Both of them had more pitch. The first condition had maybe too much pitch, while the second one felt more natural.*
$E_{ph}-E_m$	E_{ph}	-	E_m	*I did not like both conditions. The first one was a little better (i.e. less bad). It feels like both conditions are mostly heave. Therefore both did not feel realistic. If you make really hard excursions you feel some pitch coming in, but overall both felt unnatural*
	E_m	-	E_{ph}	*The first condition is not bad, but the second one is better. It had more pitch, and apparently I like more pitch.*
E_m-O	E_m	-	O	*The two conditions are close together, but I still like the second one more than the first. It is still difficult to judge, though.*
	O	-	E_m	*The first condition feels like it has more pitch than the second one. Because of that it feels more realistic. In the second condition it feels there is mostly heave. There is some pitch for sure, but not as much as the first one.*

Table F.7: Subject 4 – pairwise evaluation outcomes (winner shown in green) and general comments

World Cup (Double Blind)				
Stage	Pair			Subject Comments
Semifinal 1	O	-	B	*The first condition was better.*
Semifinal 2	E_m	-	E_{ph}	*Again they are quite close. I think I like the second condition better but it is a tough call.*
Final	O	-	E_{ph}	*Definitely the first one. I knew that it would be better also based on the conditions I flew in the second semifinal*
World Cup (Single Blind)				
Stage	Pair			Subject Comments
Semifinal 1	E_m	-	E_{ph}	*The first one is better, because it has more pitch and feels more realistic.*
Semifinal 2	B	-	O	*I didn't really like the first one. This one (the second condition) is better. I think I'm flying the winner now against the loser.*
Final	E_m	-	O	*The second one is the winner. This is the best of the four. It feels pretty clear.*

Table F.8: Subject 4 – outcomes of both World Cup stages: double- and single-blind (winner shown in green)

F.1.5. Subject 5

Subject 5 is one of the two most consistent pilots, by showing a good degree of both *within-pair* and *transitivity* consistency. He summarized his evaluation method after he finished evaluating the first condition: *"In the first half of the run I feel what I see and see what I feel. In the second part of the run I close my eyes and feel without looking. That is what I also do when I tune motions."* It must also be noted that during the first three evaluation runs, Subject 5 thought that the first condition was always the same, despite reading the briefing. This introduces a potential confound for his results. Furthermore, his evaluation criteria would not always conform to the requirements set in the briefing (i.e. the most realistic condition). Prior to starting evaluation number 8, the subject stated:

"When I choose I choose the one I prefer in the simulator. This is not always the same with what the aircraft is doing. For example for training, in some aircraft it is difficult to feel the onset of an engine failure and you use special tricks to augment that effect a little bit. There you would prefer to have a better simulation than the reference aircraft."

This introduces even further uncertainty in the validity of his results. It is interesting to note that Subject 5 has the most evaluations (10 out of 12) conforming to the OMCT based configuration ranking ($B \rightarrow O \rightarrow E_{ph} \rightarrow E_m$). A potential explanation for this result is the subject's preference to conditions that would be more beneficial for simulator training, but which might not necessarily be the most realistic. However, this statement cannot be supported with any specific evidence and is therefore not used to affect the treatment of the results of Subject 6 in the final data analysis.

Pair	Repetition			Subject Comments
$B-O$	B	-	O	*Again, this is a difficult evaluation and I am not in a position to choose. If I have to choose, it would be the first condition with very low confidence.*
	O	-	B	*This is a difficult evaluation. To be honest I would not know the difference. Perhaps the second condition is a bit better, but I say this with very low confidence.*
$B-E_{ph}$	B	-	E_{ph}	*In the second condition, when the motion of the aircraft has stopped and the PFD is still, I can still feel the motion working.*
	E_{ph}	-	B	*In the second condition the pitch rate was closer and matches better what I see than in the first condition.*
$B-E_m$	B	-	E_m	*It is difficult to say. The second condition has more heave than the first one.*
	E_m	-	B	*I have the impression that the second condition was too sensitive to motion. If I have to quantify it, with the same stick inputs I had more motion in the second condition, which I didn't like.*
$E_{ph}-O$	E_{ph}	-	O	*The second condition is simply closer to an aircraft, I have a very natural feeling for it.*
	O	-	E_{ph}	*It is difficult to say. The overshoot in the second condition is more than in the first one. The PFD in the simulator stops, but I can still feel the motion in the simulator.*
$E_{ph}-E_m$	E_{ph}	-	E_m	*The second condition feels too sloppy. I can be more violent and use bigger inputs to feel the same motion effect.*
	E_m	-	E_{ph}	*I like this one better, but it is difficult to quantify.*
E_m-O	E_m	-	O	*What I feel in the second condition is that the motion still continues after the visual has already stopped.*
	O	-	E_m	*The amplitude in the pitch axis is much lower in the second one than in the first one.*

Table F.9: Subject 5 – pairwise evaluation outcomes (winner shown in green) and general comments

World Cup (Double Blind)				
Stage	Pair			Subject Comments
Semifinal 1	O	-	B	*The reactions of the motion are closer to what I see in the first condition than in the second one.*
Semifinal 2	E_{ph}	-	E_m	*I like the first one better.*
Final	O	-	E_{ph}	*The second condition is closer to what I see. General comment for the simulation: I'm missing heave, but then again I'm used to flying bigger aircraft.*
World Cup (Single Blind)				
Stage	Pair			Subject Comments
Semifinal 1	E_m	-	E_{ph}	*The first condition is very close to the 2nd one. The difference is small. I have felt better filters*
Semifinal 2	O	-	B	
Final	E_m	-	B	

Table F.10: Subject 5 – outcomes of both World Cup stages: double- and single-blind (winner shown in green)

F.1.6. Subject 6

Subject 6 is the most consistent pilot overall, by having 5/6 consistently evaluated pairs, and has a completely transitive preference order when the only inconsistent pair is not considered. Furthermore, the subject managed to maintain a very consistent input profile between the evaluation runs and actively corrected any deviations from it. Subject 6 also often give his feedback while flying the simulated airplane, which enabled the correlation of his comments to the motion cues time history of his flying. During the feedback, Subject 6 gave the following comment:

"It was very difficult to distinguish between the different conditions. I have the feeling that I might give different results if I do the experiment again."

Pair	Repetition			Subject Comments
$B-O$	B	-	O	*The first condition feels pretty good, there are no really annoying artifacts. In the second one the washout takes a bit too long. I feel a pronounced movement for almost maybe a second after the motion has stopped; you can feel something going on.*
	O	-	B	*I prefer the second condition, since in the first one it looked that there were more heave cues than rotational cues.*
$B-E_{ph}$	B	-	E_{ph}	*In the first condition there is a very noticeable washout, and the onset could be a little bit quicker. The focus of the motion seems to lie in the second part of the pitch up moment. Initially you do o't feel very much, then it starts ramping up, and after you release it continues for half a second. It's not too bad, but it's not perfect. The second condition looked to be a little bit out of phase in the beginning of the run. I would chose the second condition, but I do not know exactly why.*
	E_{ph}	-	B	*I prefer the first condition, because the second one continues to move (with rotational input) after the aircraft is stable.*
$B-E_m$	B	-	E_m	*The first condition feels a bit laggy. The motion comes after the aircraft movement. The second condition feels fairly balanced and pretty quick to respond. It looks like it is ramping up the motion – the initial part is maybe a little bit too soft, but it picks up during the motion and stops when it should stop. I prefer the second condition.*
	E_m	-	B	*I prefer the first condition, because it looked like the second one was not instantaneous in its onset.*
$E_{ph}-O$	E_{ph}	-	O	*In the first condition, there is a very pronounced feeling of washing out. It continues for almost a second after the motion. The onset is pretty good, but the washout is really noticeable. The second condition feels pretty good and has no obvious flaws.*
	O	-	E_{ph}	*I prefer the first condition, because in the second one the motion is not strong enough. The difference is subtle, however.*
$E_{ph}-E_m$	E_{ph}	-	E_m	*The first condition has some annoying after feel. You are flying level and you still feel your head tumbling. The second condition has benign motion cues. It has not false cues, but it is slower to react. I prefer the second condition.*
	E_m	-	E_{ph}	*In the first condition there is a lot going on in pitch. It has pretty pronounced washout, but it is not disturbing. In the second condition it seems that the initiation of motion is pretty slow. Initially it doesn't do a lot and then it picks up. The second condition feels less natural than the first one.*
E_m-O	E_m	-	O	*In the first condition it takes pretty long before you feel something. I also think there is a little bit of a delay in the motion. In the second condition you feel a lot of turning in your head after the motion has finished, which is pretty annoying. Therefore I prefer the first condition, even though it is a little bit slow.*
	O	-	E_m	*I prefer the second condition because it is quicker to respond. With the first condition I made a motion with the plane and it took less than half a second for the motion to kick in.*

Table F.11: Subject 6 – pairwise evaluation outcomes (winner shown in green) and general comments

World Cup (Double Blind)		
Stage	Pair	Subject Comments
Semifinal 1	E_m - E_{ph}	*The first condition has a quick response, but noticeable washout, which is not really bothering me. I like the quick response. The second one feels a little bit unnatural. Two things: the onset, and after the movement has finished you feel a rotation component.*
Semifinal 2	B - O	*The first one has a pronounced after motion. What I miss in the second one is a really rapid onset. Here you have about the same response after the motion. The washout is also pretty pronounced here, it doesn't feel very natural.*
Final	E_m - B	*In the first condition you feel the washout. A lot going on after the aircraft has stopped moving. The second one has a nice and quick response, and even the washout is not disturbing although I notice it. Less disturbing than the previous one.*
World Cup (Single Blind)		
Stage	Pair	Subject Comments
Semifinal 1	B - O	*In the first condition I feel a little bit of a lag and after motion. Having said that the after motion coupled with the lag doesn't make it comfortable or natural. The second one is slow to pick up, but the washout seems a little bit more natural. On the first one I had better response, but less natural washout. Here I have a slower response, but a more natural washout.*
Semifinal 2	E_{ph} - E_m	*In the first condition it is difficult to explain what I'm feeling. Getting confused here, don't know what I'm feeling or seeing. A bit of a time delay but not too bad. The second condition feels more natural that the previous one. The motion and also the washout are in phase with what's going on outside.*
Final	B - E_m	*The first condition has a good response, the washout is not annoying, although I do feel some heave and rotation until well after the motion, but it doesn't bother me, it's not unnatural. For the second one it is the same. The motion is a bit less, and you feel the washout, but it's not out of phase or too annoying.*

Table F.12: Subject 5 – outcomes of both World Cup stages: double- and single-blind (winner shown in green)

F.2. Discussion on the time-specific pilot comments

Three of the pilots occasionally provided comments on their sensations of motion while they were controlling the aircraft. These pilots were Subjects 1,2, and 6. Since their voice was recorded for the entire experiment (with their explicit consent), the comments could be directly correlated to the time histories of the motion cues in the specific experiment runs and subsequently analyzed.

It must be stated that this is not a trivial undertaking, since it is difficult to pinpoint the exact time at which the subject experienced the cause of their remark. Therefore, the time interval which is investigated is taken from the starting time of the subject's comment to its end. In some instances this interval is approximately 10 seconds long. Furthermore, it is not always possible to find the cause of the pilots comment in this time window. This reason, combined with the contradictory nature of the comments between some subjects, makes it impossible to arrive at any concrete conclusion explaining the trends seen in the experiment results. Nevertheless, some of the time-specific comments are worth investigating, as they can lead to recommendations for any similar future experiments. These comments and their corresponding motion cue time histories are summarized below for Subjects 1,2, and 6. It must be stated that all presented comments in this section are taken verbatim from the voice recordings of the individual subjects.

When investigating the motion cue time histories, it is useful to have an indication of whether the subject actually perceived them. Therefore, several vestibular thresholds over a range of frequencies are overlain on top of the time histories. The frequency range is used since the exact frequency of the motion cues in the specific time windows is unknown. The vestibular threshold boundaries shown in the plots are taken from Heersipink [7], and Rodchenko et al. [14]. For the surge specific forces, the means of the lower thresholds (LT) for 1 rad/s and 2 rad/s are displayed. The lower thresholds are chosen, since they indicate the points

where the motion cue stops being perceived [7]. It must be noted that no direct values are given for the pitch rate thresholds by Heerspink. However, he does compare his findings with Rodchenko et al. and presents the outcomes in Fig. F.1. There it can be seen that there is little difference between the threshold values in the frequency range from 0.45 rad/s to 3 rad/s. Since, in the current context, the thresholds are not used for a detailed analysis of the time-domain motion cues but rather as an approximate indication, the Heerspink pitch rate threshold values in the previously specified frequency range are approximated as being constant. The values of all thresholds displayed in the time domain plots are summarized in Table F.13.

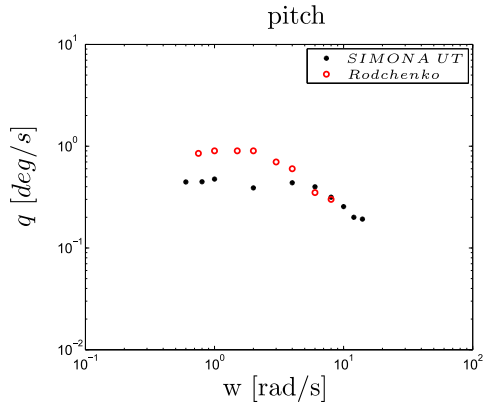

Figure F.1: Comparison between pitch rate vestibular thresholds measured by Heerspink and Rodchenko et al. [7]

Label	Theshold	Value
$LT_{[1rad/s]}$	Surge specific force lower threshold mean at 1 rad/s	0.052 [m/s^2]
$LT_{[2rad/s]}$	Surge specific force lower threshold mean at 2 rad/s	0.029 [m/s^2]
$H_{[0.5-4rad/s]}$	Approximate pitch rate threshold from 0.5 rad/s to 4 rad/s, measured by Heerspink	0.45 [deg/s]
$R_{[1rad/s]}$	Approximate pitch rate threshold at 1 rad/s, measured by Rodchenko et al.	0.90[deg/s]
$R_{[3rad/s]}$	Approximate pitch rate threshold at 3 rad/s, measured by Rodchenko et al.	0.70[deg/s]

Table F.13: Values for the vestibular threshold used in the time-specific pilot comment plots [7]

F.2.1. Subject 1

Pair $E_{ph} - O$

- Run 1 - configuration O (Fig. F.2):

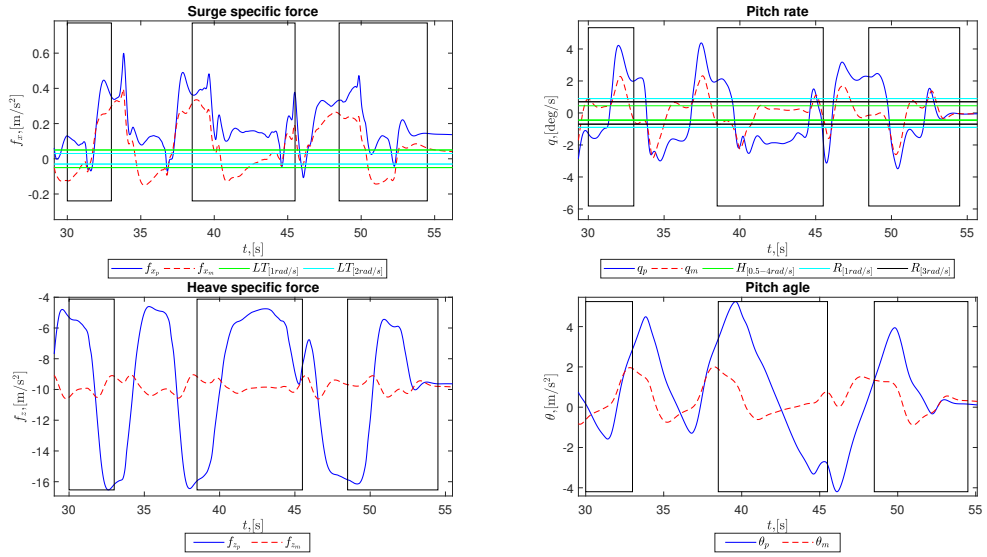

Figure F.2: Pair $E_{ph} - O$; time histories of the motion cues for Subject 1 during the first run with configuration O

  - (31s): *"No, there is a hesitation here."* The comment is made just at the intercept of $\theta_p = -2°$. Just before the intercept is made, there is a suppression of the oscillations of f_{x_p} by the MCS dynamics.
  - (39s-45s): *"There is a hesitation when you move from 5 up to 5 down, but there is a hesitation also in the visual."* The aircraft pitch rate levels at a relatively constant value for a few seconds. In the simulator, this is replicated, but at values that are most probably below the perceptual thresholds.
  - (49s-54s): *"I feel a hesitation in going up and down."* The simulator pitch rate goes in a region that falls below the thresholds. Additionally, f_{x_m} is dampened with respect to f_{x_p}. These two things might explain the reported 'hesitations'.

- Run 2 - configuration O (Fig. F.3)

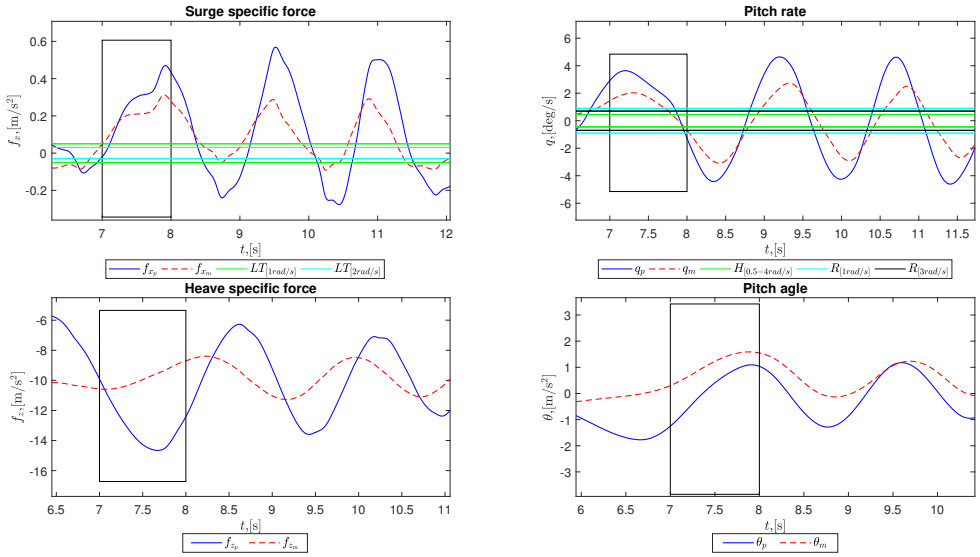

Figure F.3: Pair $E_{ph} - O$; time histories of the motion cues for Subject 1 during the second run with configuration O

– (21s): *"There is also a slowing down."* The simulator pitch rate goes below the perception thresholds.

- Run 2 - configuration E_{ph} (Fig. F.4)

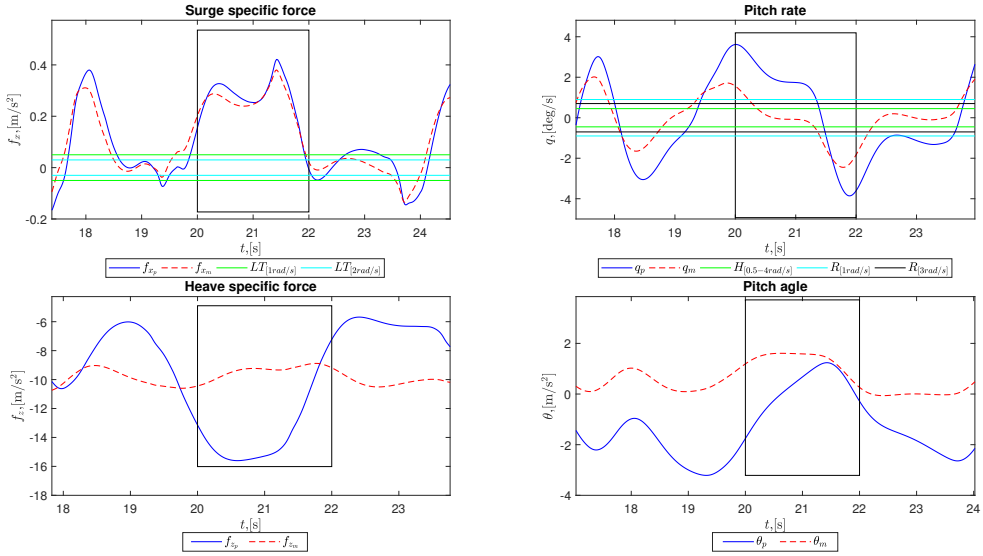

Figure F.4: Pair $E_{ph} - O$; time histories of the motion cues for Subject 1 during the second run with configuration E_{ph}

– (7.5s-8.5s): *"Also a hesitation."* The simulator surge specific force f_{x_m} levels off above the thresholds around that point; but f_{x_p} has a similar behavior. The pitch rate is above the thresholds for the time span of the comment.

Pair $B - O$

- Run 1 - configuration B (Fig. F.5)

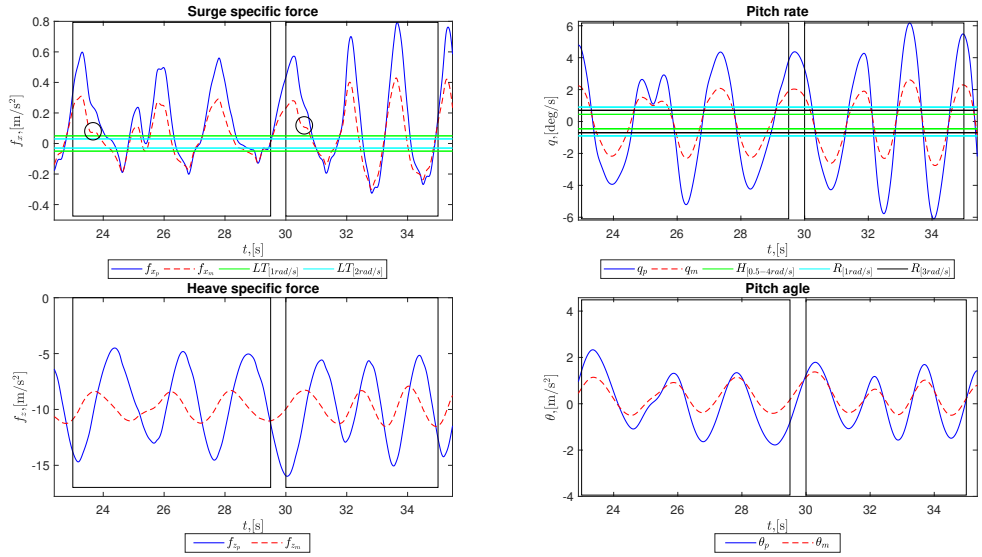

Figure F.5: Pair $B-O$; time histories of the motion cues for Subject 1 during the first run with configuration B

– (23s-28s): *"There is a small ripple when I hit the maximum speed, it felt like the last one."* There is an abrupt, but brief level-off in f_{x_m} at the 23s mark. There is a very subtle rate change of in the aircraft cue, which is exaggerated by the MCA. At that point the pitch rate cues are below the thresholds.

– (30s-35s): *"It's not fluid on the maximum, reversals are ok."* A similar behaviour of f_{x_m}, but less pronounced and barely visible, is seen at 30.6s.

- Run 1 - configuration O (Fig. F.6)

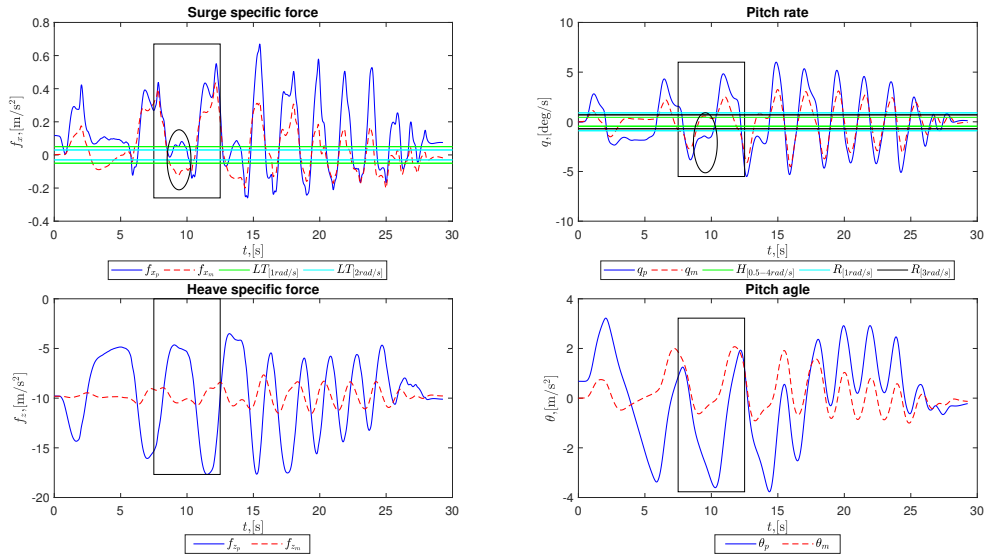

Figure F.6: Pair $B-O$; time histories of the motion cues for Subject 1 during the first run with configuration O

– (8s-10.5s): *"There is also a hesitation."* There is a dampening of f_{x_m} with respect to f_{x_p}, which is combined with a probable pitch rate cues that just go below the threshold (at the 9.4s mark).

- Run 2 - configuration O (Fig. F.7)

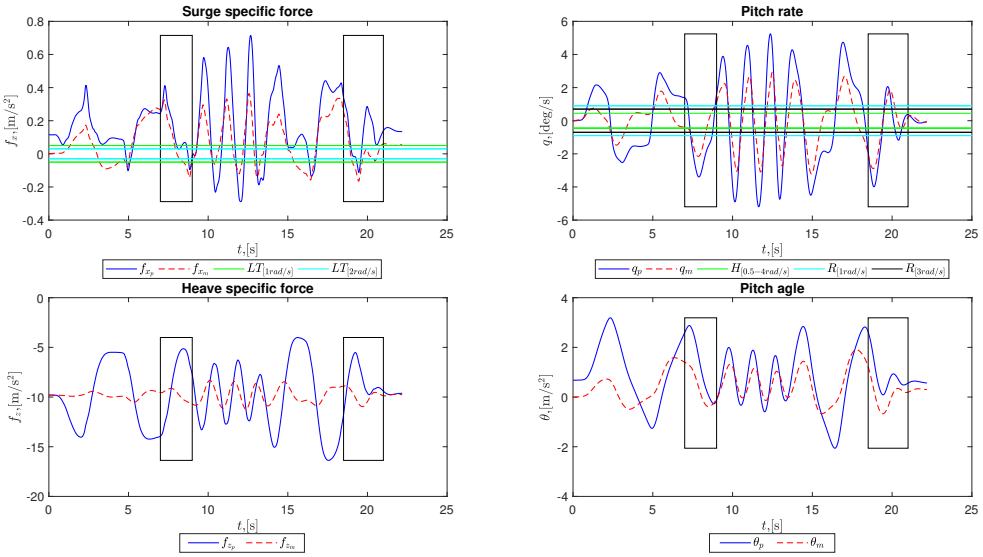

Figure F.7: Pair $B-O$; time histories of the motion cues for Subject 1 during the second run with configuration O

– (7.4s-8.8s): *"You already feel the hesitation."*; The f_{x_m} and q_m cues go in a region below the thresholds for a little bit when the the aircraft pitch angle is close to zero.

– (18.5-20.5s) *"Quite large hesitation."* Again the f_{x_m} and q_m cues are below the threshold. There is also a big phase mismatch in heave. Perhaps it is the reason for the experienced hesitation?

Pair $E_m - O$

- Run 1 - configuration E_m (Fig. F.8)

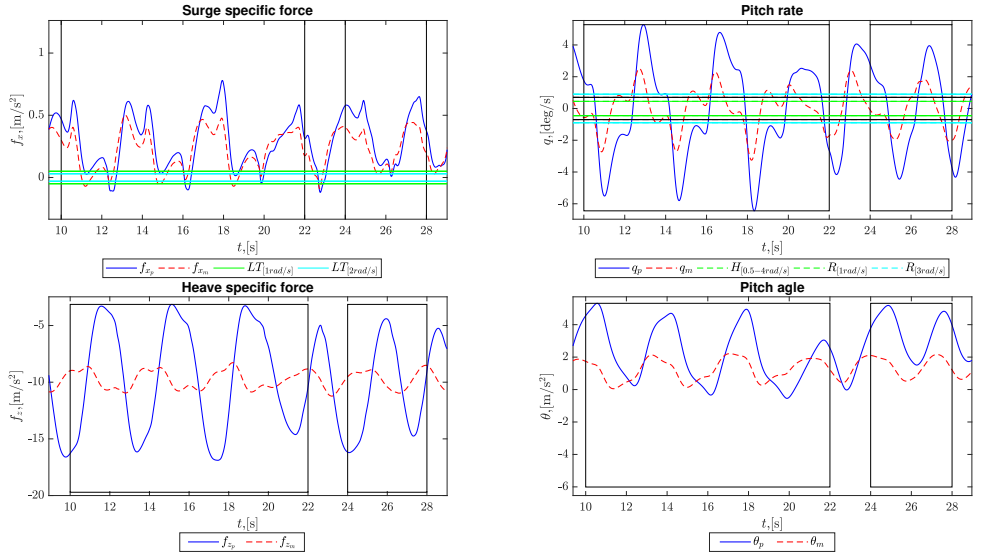

Figure F.8: Pair $E_m - O$; time histories of the motion cues for Subject 1 during the first run with configuration E_m

– (10s-22s): *"Here is the hesitation in motion. The visual is still moving and I feel it in the motion, it's not in line with the visual."* Both simulator cues, f_{x_m} and q_m, follow their aircraft references relatively well in phase. The pitch rate, however is close to the limits, while the surge specific force

is well pronounced. A probable reason for the experienced mismatch in motion is the dominant surge.

– (24s-28s): *"And there is the hesitation at many of the highest speeds."* There is a slight level-off in the pitch rate in the 24th second, which is most likely below the thresholds anyway. Around the 25th second, there is a short oscillation in surge, which is just at the threshold. It is present in the aircraft as well. I can't really say why he felt this oscillation here.

F.2.2. Subject 2

Pair $E_{ph} - O$ (Figs. F.9 and F.10)

- Run 1 - configuration E_{ph}

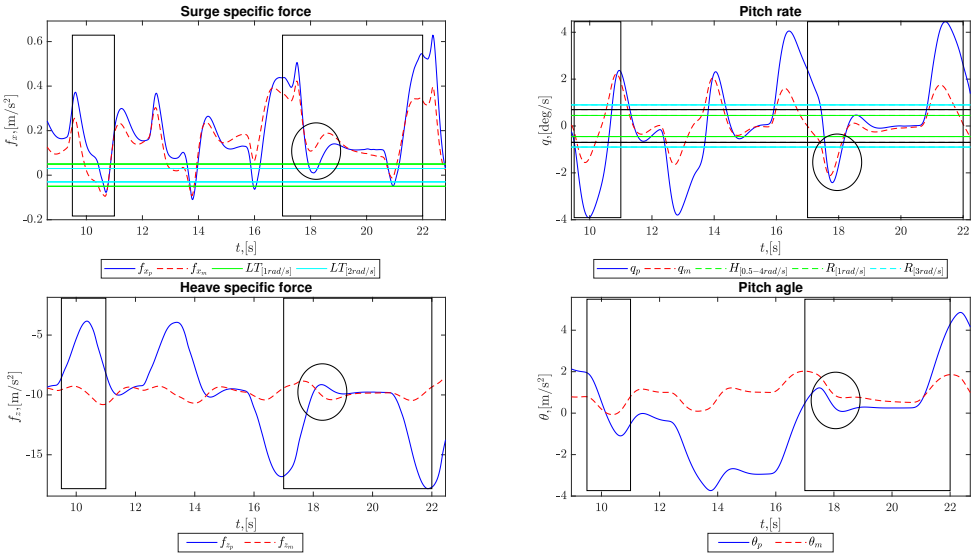

Figure F.9: Pair $E_{ph} - O$; Part 1 of the time histories of the motion cues for Subject 2 during the first run with configuration E_{ph}

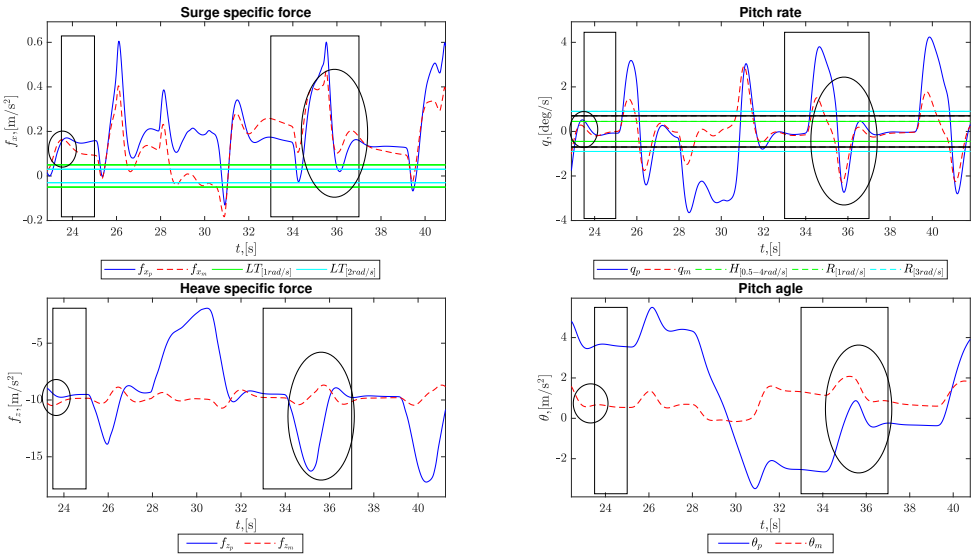

Figure F.10: Pair $E_{ph} - O$; Part 2 of the time histories of the motion cues for Subject 2 during the first run with configuration E_{ph}

– (9.8s-11s) *"This one has the wobble again."* In this time interval both the f_{x_m} and q_m cues go from a region below the perception thresholds to being just outside of them. This is a potential reason why the 'wobble' is registered.

– (17s-22s) *"It feels like the initial pitching is less pronounced than the first one, but the wobble is big."* The comment on the initial pitching makes a comparison with the previously flown configuration, which in this case is configuration O that has $|q|_{sp} = 1.83$. It is interesting to note that the subject managed to perceive a lower magnitude for the pitch cue in configuration E_{ph}, which agrees to the evaluation coming from the EMD analysis.

The second part of the comment once more refers to a big 'wobble'. When the subject made the comment, he was completing a pitch angle intercept of $\theta_p = 0°$. This is indicated with a circle in the time histories in the motion cues in Fig. F.9. It can be seen that the pitch angle intercept is done with some overshoot, which causes oscillations in all three motion cues in both the aircraft and simulator. Notice how for f_{x_p} the MCA attempts to replicate the behavior of the aircraft reference signal.

– (23.5s-25s) *"And the wobble is big."* The comment is once again made during a pitch angle intercept, indicated by the circled part in Fig. F.10. The simulator motion cues behave similarly to the previously discussed case, with the only difference being that the pitch rate is below the perceptual thresholds.

– (33s-37s) *"The pitching is less and when you release it the wobble is big."* The same behavior is observed again. Once more the aircraft surge specific force oscillates while the aircraft is stabilizing its pitch angle. The MCA replicates this behavior, as seen in Fig. F.10.

Pair $B - O$

- Repetition 1 - configuration O (Fig. F.11)

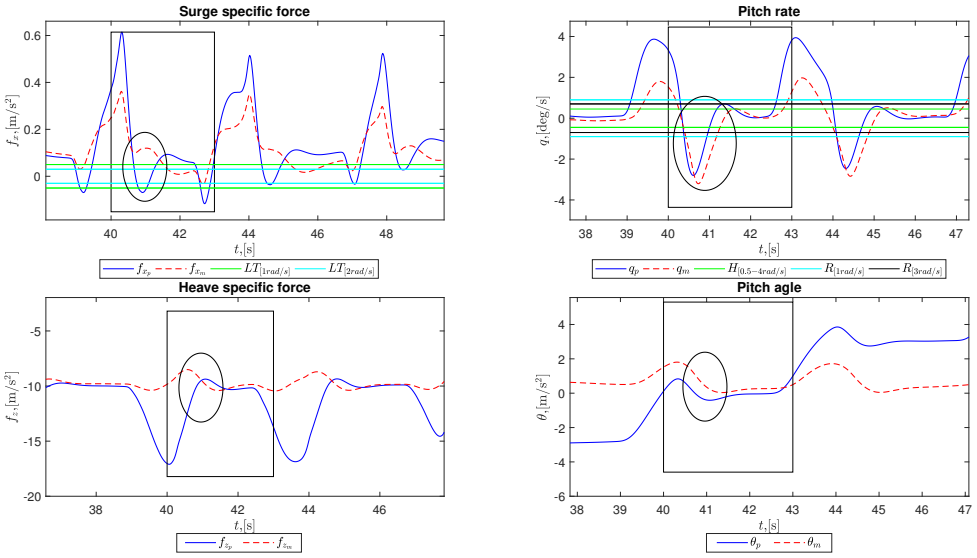

Figure F.11: Pair $E_{ph} - O$;time histories of the motion cues for Subject 2 during the first run with configuration O

– (40s-43s) *"Here pitch up and wobble down again."* The comment is made just as the subject is stabilizing at $\theta_p = 0°$. At this point, f_{x_m} is going out of phase with respect to the aircraft reference signal f_{x_p}. This is demonstrating the EMD evaluation of the phase distortion of f_x for this configuration, namely that $\angle f_{x_{sp}} = 152.1°$ lead.

F.2.3. Subject 6

Pair $E_{ph} - O$

- Repetition 2 - configuration O (Figs. F.12 and F.13)

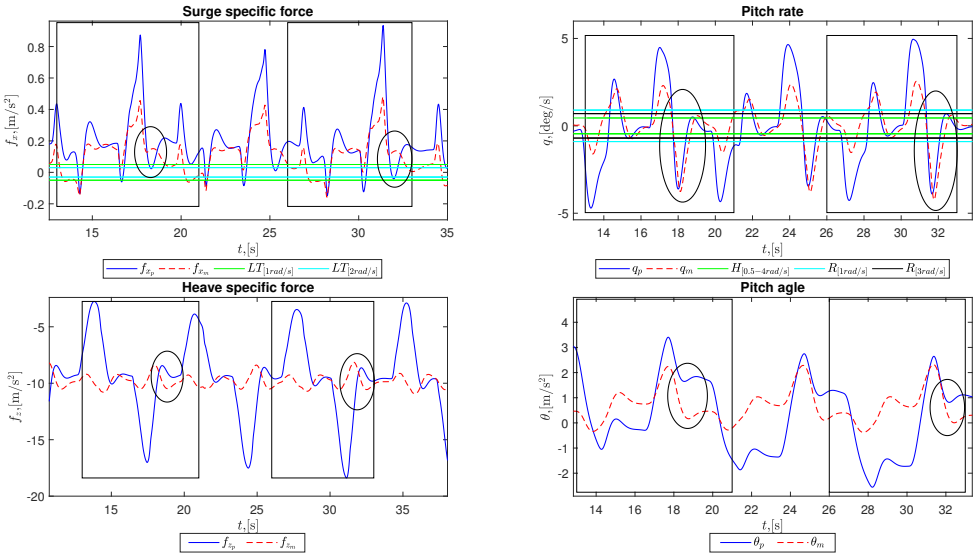

Figure F.12: Pair $E_{ph} - O$; Part 1 of the time histories of the motion cues for Subject 6 during the second run with configuration O

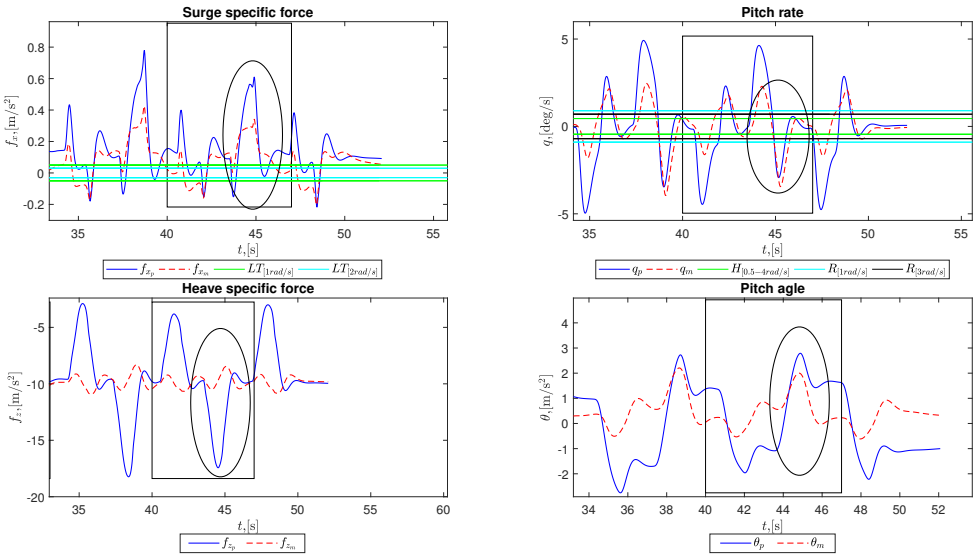

Figure F.13: Pair $E_{ph} - O$; Part 2 of the time histories of the motion cues for Subject 6 during the second run with configuration O

– (13s-21s) *"Here is after the motion a very pronounced feeling of washing out."* In this time interval, the subject performs two pitch angle intercepts: $\theta_p = 0°$ and $\theta_p \approx 3.5°$. After the second intercept (at $t \approx 18$s), in Fig. F.12 it can be seen that f_{x_m} goes out of phase with respect to f_{x_p}. This response is similar to the one observed in Fig. F.11, where the same CWA configuration is used. The simulator pitch rate q_m manages to follow its reference signal well, without showing any noticeable deficiencies.

– (26s-33s) *"That continues for almost a second after the motion."* The same remarks can be made

for the motion cues in this time interval as for the last. The pitch intercept is $\theta_p \approx 3°$ and happens at $t \approx 32$s.

– (40s-47s) *"The onset is pretty good, but the washout is really noticeable."* Once again a similar trend in the simulator motion cues can be seen after a pitch angle intercept of $\theta_p \approx 3°$ at $t \approx 45$s as seen in Fig. F.13. It is easy to see that the simulator specific force f_{x_m} behaves in the same way as in the earlier time intervals, because the pilot is very consistent in his strategy of exciting the aircraft. This consistency is clearly seen in Figs. F.12 and F.13.

It must be noted that Subject 6 made similar time-specific comments while again flying configuration O during the evaluation of the pair $B - O$.

Pair $E_{ph} - E_m$

- Repetition 1 - configuration E_{ph} (Figs. F.14 and F.15)

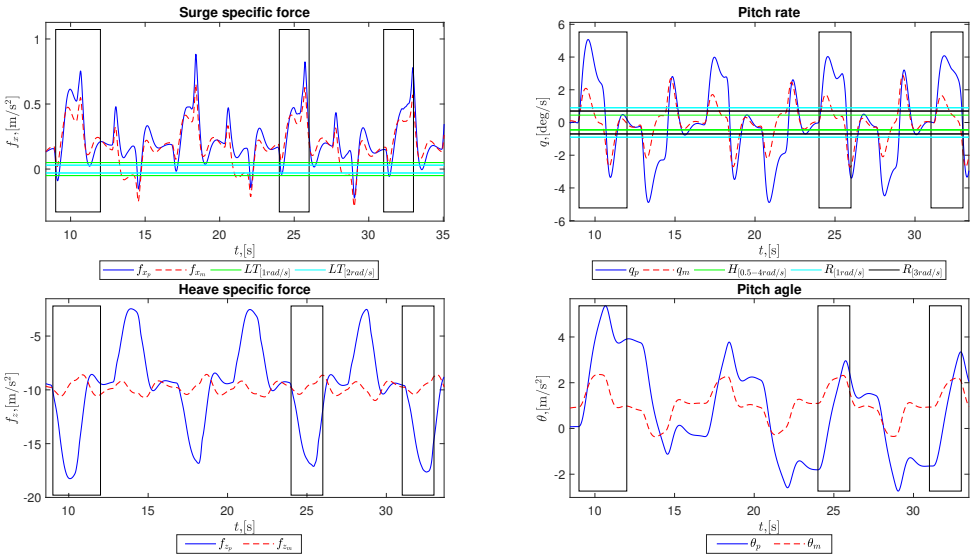

Figure F.14: Pair $E_{ph} - E_m$; Part 1 of the time histories of the motion cues for Subject 6 during the first run with configuration E_{ph}

– (10s; 25s) *"This is the one where I feel a little bit of after-motion, after the aircraft has stabilized."*; *"It is very pronounced."* The subject makes these comments while he is doing pitch angle intercepts of $\theta_p \approx 5°$ and $\theta_p \approx 5°$ respectively. The simulator motion cues for f_x and q manage to replicate their aircraft reference signals. The aircraft surge specific force f_{x_p} has two sharp oscillations at $t = 10$s, which are replicated by the simulator specific force f_{x_m} with a very small phase lag. This is a potential explanation why the subject complains about "after-motion". A similar behaviour is observed at $t = 25$s, as seen in Fig. F.14.

– (51s-53s) *"I don't like what happens when you release the stick."* From the motion cue time histories, visualized in Fig. F.15, it is not immediately clear what is the origin of the subject's complaints. In this interval, q_m is below the vestibular perception thresholds, while f_{x_m} is closely following the reference signal, which has a benign response. This is an example for the motion cue time histories are not always able to explain the time-specific comments.

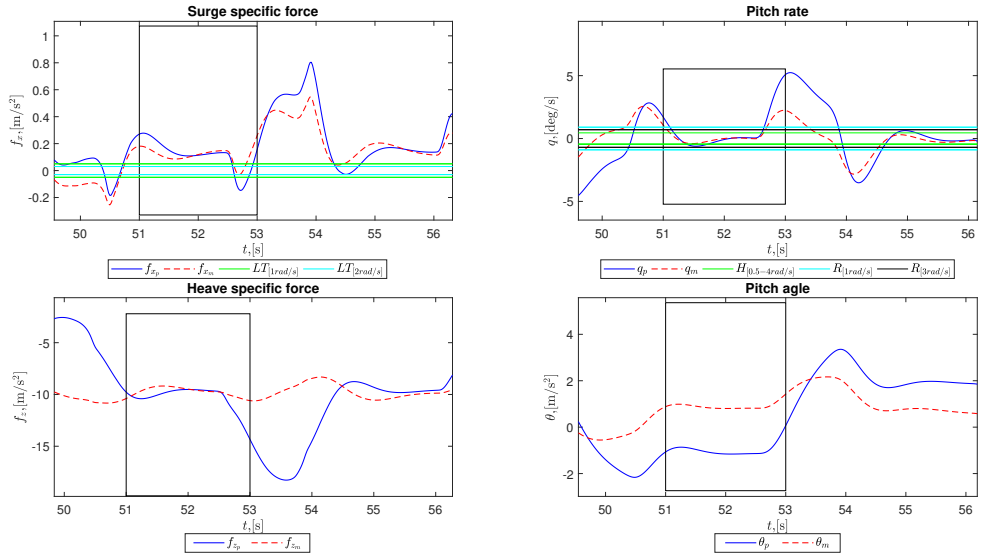

Figure F.15: Pair $E_{ph} - E_m$; Part 2 of the time histories of the motion cues for Subject 6 during the first run with configuration E_{ph}

- Repetition 1 - configuration E_m (Fig. F.16)

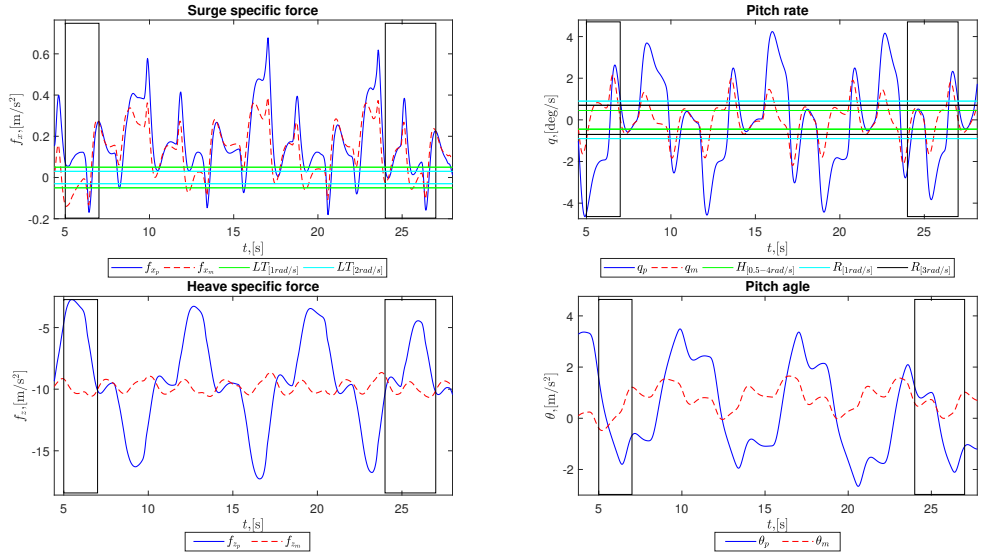

Figure F.16: Pair $E_{ph} - E_m$; time histories of the motion cues for Subject 6 during the first run with configuration E_m

  - (5s-7s) *"Very benign motion cues, I can hardly feel anything."* The motion cues are indeed close to the perceptual thresholds.

  - (24s-26s) *"No false cues from what I can see. Also a bit slower to react."* It is interesting to note that for f_{x_m}, at $t \approx 25$s, the oscillation falls below the perceptual thresholds and is very possibly not sensed by the pilot. Similar motion cues were present while the subject was flying with configuration E_{ph}, see Fig. F.14. There, the pilot was complaining about after motion. It is possible that these oscillations are perceived as false cues by the pilot, while in reality they closely represent the aircraft response.

- Repetition 2 - configuration E_m (Figs. F.17 and F.18)

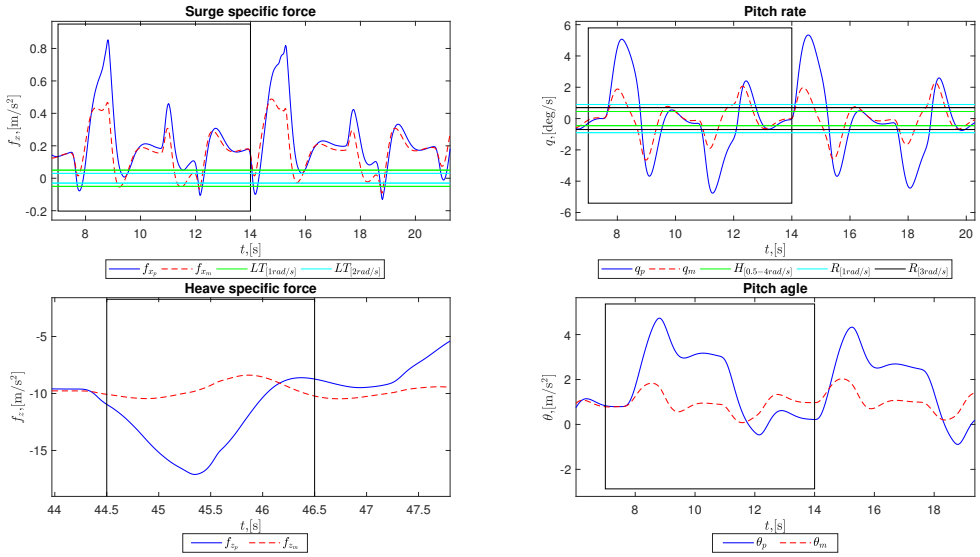

Figure F.17: Pair $E_{ph} - E_m$; Part 1 of the time histories of the motion cues for Subject 6 during the second run with configuration E_m

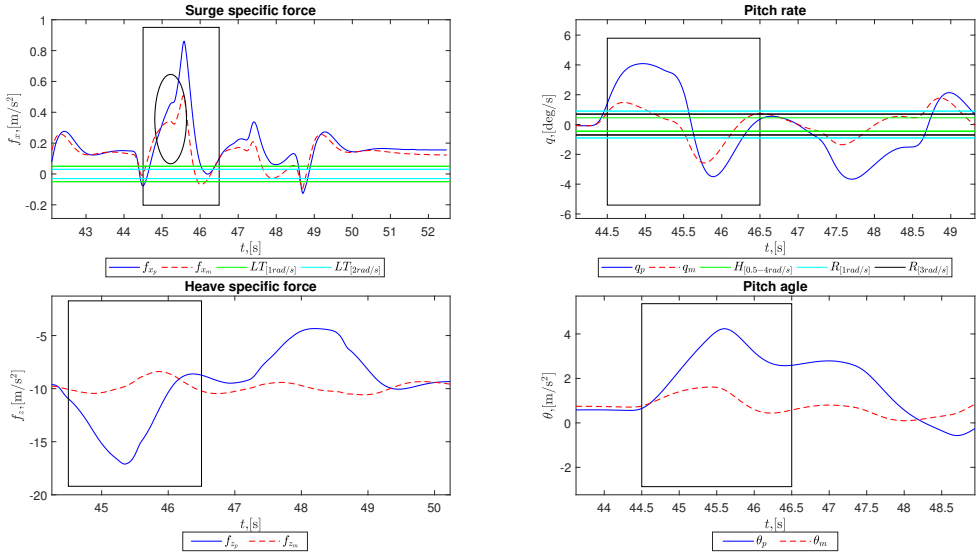

Figure F.18: Pair $E_{ph} - E_m$; Part 2 of the time histories of the motion cues for Subject 6 during the second run with configuration E_m

- (7s-14s) *"There is a lot going on in pitch. I can almost feel the fluids in my head turning."* In this time interval there are clearly instances of q_m being above the perceptual thresholds. However, it is interesting to note that the f_{x_m} is also very pronounced and is further away from its perceptual thresholds. This can be seen in Fig. F.17. Therefore, it may be possible that the subject was feeling more surge than pitch.

- (45s) *"The washout is pretty pronounced but not disturbing."* It is difficult to see in the time histories what the subject experienced as a washout. A possible explanation is a small oscillation in f_{x_m} at $t = 45$s, as seen in Fig. F.18.

Having observed the motion cue time histories of the time-specific pilot comments the following statements can be made. First, the effect of the magnitude and phase distortions, evaluated by EMD, could be seen. The differences between the conditions are most visible when looking at the time histories of Subject 6 due to his consistent nature of his inputs. For example, if time histories of configurations O and E_{ph} are compared by

using Figs. F.12 and F.14 respectively, it can be observed that configuration E_{ph} replicates the behaviour of f_{x_p} better than configuration O. The differences between the two are smaller when observing the pitch rate.

However, the closer replication of the aircraft motion cues is not a guarantee for success. It was sometimes the case that when parts of the aircraft surge specific force are accurately represented, they are perceived as false cues. This was observed for Subject 2 in his time-specific comments. On the other hand, the possibility exists that the used aircraft dynamics model is has deficiencies in its response, to which some pilots reacted.

Another factor responsible for the variation of the pilot feedback is that the deliberate excitation of the short period eigenmode is not an ordinary task that pilots perform. Therefore, it is possible that some of the pilots have not often experienced similar motion cues during real flight.

F.3. Recommendations for future experiments

Although the main recommendation is to pursue the investigation of objective methods for quantification and evaluation of the performance of objective metrics, such as EMD and OMCT, recommendations can also be made for improved experiments with a subjective element.

The first recommendation is to introduce a more specifically defined task. Based on the feedback and the control strategies of several pilots, it is recommended to have the test subjects perform a series of positive and negative pitch angle intercepts. A similar strategy was employed by Subjects 2 and 6, who are a part of the most within-pair consistent group. In order to ensure that all pilots perform the same set of intercepts, it is recommended to introduce a visual aid, which points them to the correct pitch angle. A possible solution is to overlay a Flight Director marker over the PFD.

In order to further decrease the possibility for variation in the evaluation of pilots, it is recommended to have test subjects fly the prescribed task in the real aircraft and then replicate it in the simulator as soon as possible. However, there are several complications with this proposed set-up. First, the amount of subjects will be limited, due to the immense costs in time and money involved in performing test flights. Furthermore, an accurate aircraft model must be available for the specific flight condition.

This proposal for the experiment design can be further refined. Instead of making pilots replicate the task in the simulator, they can observe the simulator's response to the aircraft motion cues that were recorded during the test flight. In order to bring the two tasks closer together, the simulator evaluation pilot can instead observe the aircraft motion cues and control inputs (which will also be recorded) during the test flight as well. As soon as possible, the same pilot repeats the same task in the simulator, with the same motion cues used as an input to the MCA and the same control inputs being played back. The advantage of this design is that there is no aircraft model running the simulation, which eliminates the possibility for deficiencies. In addition, it is possible for more than one evaluation pilot to perform the task during the test flight, since they are not the pilot in command. This can also, to a certain extent, mitigate the issue with the limited number of test subjects.

G

Statistical Analysis of Paired Comparisons Experiments

Statistical analysis is an integral part of any research that aims to prove a certain hypothesis. The correct application of the methods that can be used for it is heavily dependent on the experiment design and the measured data. While in the field of engineering research there is a plethora of examples on how the statistical analysis must be performed for experiments where either the independent variables or the dependent variables are continuous, there is a lack of studies where both variable types are categorical, such as in the case of paired comparisons experiment designs. The latter are however commonly used in psychometric studies, where various methods are employed for the statistical analysis.

The purpose of this appendix is to introduce the analysis of paired comparisons experiments to the field of flight simulation research. This is achieved by discussing the difficulties related to the analysis that result from the experiment design, giving a short summary on the main methods for analyzing paired comparisons data and the reasoning behind the choices made during the analysis of the results in this Master Thesis project.

The appendix is structured as follows. In Appendix G.1 arguments are given for supporting the choice of the paired comparisons design for recording subjective opinions. This is followed by a discussion on how to properly select widely used statistical tests in Appendix G.2. In Appendix G.3 the main methods that are tailored for analysis of paired comparisons data are presented. Finally, in Appendix G.4 the specifics of applying these methods in within-subject experiment designs are discussed and recommendations are given on how such analysis must be approached in future studies.

G.1. Why doing paired comparisons?

In the majority of studies that have an element of a subjective evaluation of fidelity (be it motion, vehicle model, etc.) rating scales, such as the Motion Fidelity Rating Scale (MFR) [8], are used to record the pilot opinion on the fidelity of the system. In general rating scales have some inherent drawbacks:

- Rating scales are prone to introduce inconsistencies in the data, due to how different subjects evaluate the scale levels - i.e. the obtained score is *relative* the subject giving it. This drawback is mitigated to a large extend in the MFR scale, as pilots arrive at every different level through a predefined evaluation process.

- There is the possibility that a subject gives scores depending on the context, such as the ordering of the presented conditions [2]. Therefore it is important to ensure that the various conditions are presented to the test subjects in a random order.

- The ratings given by pilots are in fact categorical in nature. However, they are often considered as interval or ratio data, causing the subsequent analysis to be unreliable [13].

While these scales are a valid metric for many experiment designs, they are not entirely suitable for cases where motion configurations of similar quality are compared. The reason is that all configurations are likely to receive very similar ratings, thus preventing any definitive distinction between them. Therefore in such scenarios a paired comparisons experiment proves to be a viable alternative. It enables subjects to give an absolute preference between any two conditions, which can in turn be used to create a ranking of all tested conditions, if this is required.

G.2. Which statistical test to choose?

The process of selecting the statistical tests that are used for testing the hypotheses starts in the experiment design phase. When researchers define the experiment set-up, they need to consider the data type of the used independent and dependent measures. This, together with whether the experiment has a within-subjects or a between-subjects design, determines the type of the statistical tests that can be used. A good starting point for selecting an appropriate statistical test is the statistical test decision tree by A. Field [5], shown in Fig. G.1.

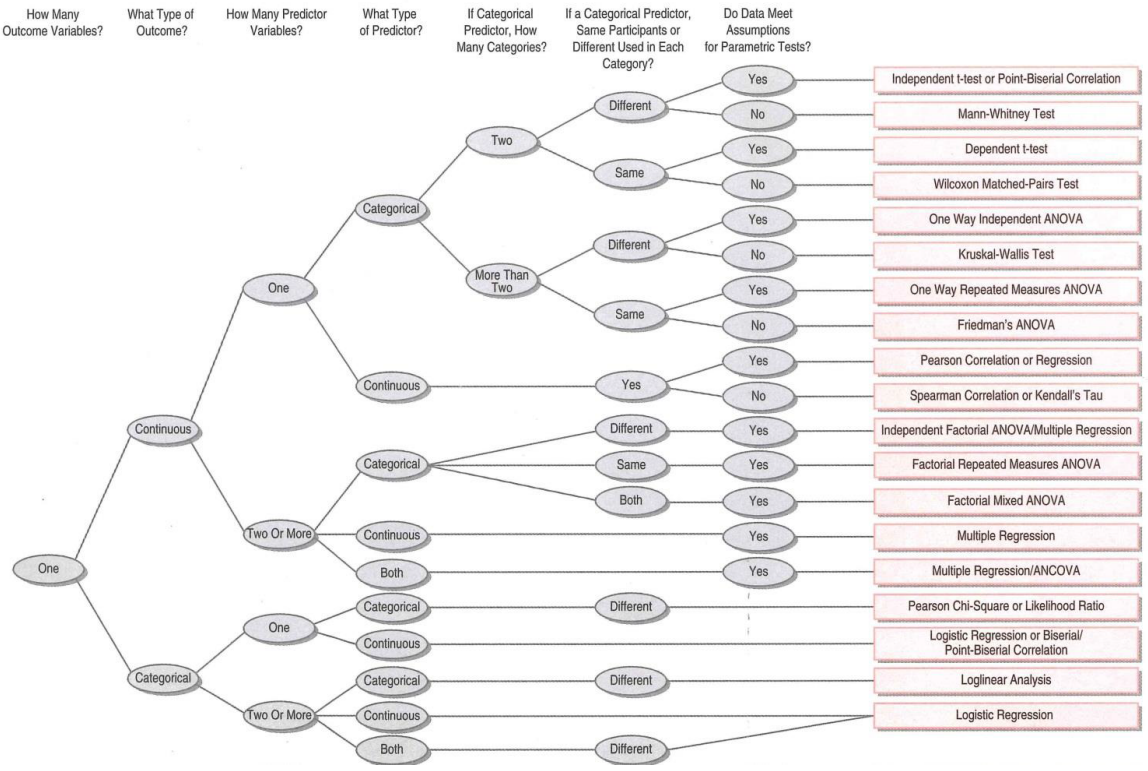

Figure G.1: Statistical test decision tree [5]

In most studies in the field of engineering, either the dependent measures, or the independent measures (or both) consists of continuous data types (which can be interval or ratio). This in turn leads to many possible choices for statistical tests, as seen in Fig. G.1. However, when the dependent and independent measures are both categorical, only two options remain: a Pearson's Chi Square or Likelihood ratio, when there is only one independent variable, and Loglinear Analysis in the case of multiple independent variables. Both of these statistical analysis methods are only applicable for between-subject experiment designs. Therefore, according to Fig. G.1 there is not a suitable statistical test for a within subjects experiment design with categorical dependent and independent measures.

In such cases the experiment design can be adapted to accommodate the formulation of a hypothesis that includes continuous dependent measures, which can be obtained from processed categorical dependent measures. This approach is taken in the current study. By using the paired comparison outcomes, the ratio of correct predictions to the CWA configuration rankings, based EMD and OMCT, are calculated for each subject. The result from doing this is the ability to perform either a One Way Repeated Measures ANOVA, or Friedmann's ANOVA if the data does not satisfy the normality and homogeneity of variance criteria. These methods can be used to test whether the subjective pilot evaluations conform more to the EMD or OMCT based rankings.

As already stated, this approach requires the processing of the paired comparison outcomes. However, it is also possible to directly use the recorded pilot evaluations to arrive at a ranking, which is based on them. The methods that are use for this purpose are presented in the next section.

G.3. Main methods for analysis of paired comparisons data

The two main methods that are used for the analysis of paired comparisons data are the Thurstone method [11] and the Bradley-Terry (BT) method [3]. Their main working principle is the same, and it is briefly explained below.

Consider that a person can choose between two options, or objects. The *quality* of each object can be modeled with a symmetric probability distribution, i.e. p_j and p_k for, respectively, Objects j and k. The two objects have a *worth*, which is equivalent to the expected values of their distributions: $E[p_j] = \mu_j$. To find the probability of Object j being preferred to Object k (π_{jk}), the Cumulative Distribution Function (CDF) of their worth difference is used:

$$\pi_{jk} = F(\mu_j - \mu_k) \tag{G.1}$$

The type of the CDF determines the method type and its specifics. The Thurstone method uses a Gaussian density and distribution functions to model the object worth μ and the probability of choice π. For the latter, a new variable for the object difference can be defined [12]:

$$\begin{aligned} jk &\sim N(\mu_{jk}, \sigma_{jk}) \\ \mu_{jk} &= \mu_j - \mu_k \\ \sigma^2_{jk} &= \sigma^2_j + \sigma^2_k + 2\rho_{jk}\sigma_j\sigma_k \end{aligned} \tag{G.2}$$

Here the term ρ_{jk} represents the correlation coefficient between Objects j and k, while μ_{jk} is the mean relative difference between the two objects. If μ_{jk} is positive, then Object j is preferred to Object k. It can be derived that μ_{jk} can be calculated with Eq. (G.3):

$$\mu_{jk} = \sigma_{jk} F^{-1}(p_j - p_k) \tag{G.3}$$

It is seen that the joint standard deviation has to be known in order to obtain μ_{jk}. This is not a trivial task and some assumptions must be made. Thurstone identified five base cases [11]. They were later expanded upon and new approaches have been used to adapt the base method for more specific applications, including cases for dependent data [4].

In the case of the Bradley-Terry model, the used CDF is a logistic cumulative distribution function. In its base form, the probability of Object j being preferred to Object k, π_{jk}, is calculated with Eq. (G.4):

$$\pi_{jk} = \frac{\pi_j}{\pi_j + \pi_k} \tag{G.4}$$

Here π_j and π_k are the *worth parameters*, defined as $\pi_j = \exp \mu_j$. In this form, the BT model assumes that the two objects are independent. Both the Thurstone and BT models can be applied to data consisting of paired comparisons between N objects and S subjects, or people making the choices. In both cases, there is a total of N worth parameters, for which $\sum_{i=1}^{N} \pi_i = 1$ is valid. The two models can also be extended to calculate the outcome probability of simultaneously comparing more than two objects [4].

G.4. Analysis of within-subject paired comparisons experiments

The BT and Thurstone models can be adapted for use with data, which is not completely satisfying the independence assumption. There have been many studies in this field, which are often addressing a specific application. They have been summarized and reviewed by Cattelan [4]. One thing common among most models for dependent paired comparisons data analysis is that their implementation is non-trivial and complex, since they are tailored for specific uses [4].

There are some software packages, however, which can perform such an analysis. In this study, the *R* package **`prefmod`**, developed by Hatzinger and Dittrich [6], is used. This package employs a loglinear representation of the BT model, which can also be executed in a pattern, i.e. simultaneously modeling all pairwise responses. The pattern model also has the distinct advantage that it can include the influence of dependence between the different comparisons for a single subject [6]. Therefore it is more suitable for the analysis of within-subject experiments. Furthermore, it can also work with ranking-type and rating-type data. Both the loglinear and pattern BT models can be subjected to several extensions:

- Including undecided responses (ties) - The outcomes of the pairwise comparison between objects j and k are now three: $j > k$, $j < k$, and $j = k$. This extension enables the analysis of more complex experiment designs and is useful when subjects could not provide a definitive response, as is the case for Subject 1 for the comparison of $B - E_m$.

- Introducing subject covariates (categorical, numerical) - The use of categorical covariates enables a comparative analysis between different categories of the test subjects (i.e. experience level, gender, etc.). They are not particularly useful for within-subject experiment designs, since there the subjects are usually selected to represent a sample of a single group pool. The numerical covariates are better suited for this use, since they can be used to model specific characteristics of each subject, such as their level of consistency.

- Introducing object specific covariates - Similar to the categorical subject covariates.

If no subject or object covariates are used, the data can be easily analyzed with the function `pattPC.fit` which directly uses the matrix with all pairwise comparison outcomes for all subjects. This function can also model the dependence between the outcomes of each subject. However, it can not account for the repeated measures made by every subject. The approach that is taken in the current study is to include the repeated measures as new subjects that are treated separately by the function, i.e. as far as it is concerned, there are twelve test subjects instead of six. Therefore the outcomes of the analysis will not be completely accurate. It is thus recommended to investigate alternative approaches to work with repeated measures data. The worth parameters that result from the analysis with dependence between the outcomes and the ones from the independent analysis are presented, respectively, in Eq. (G.5) and Eq. (G.6) and are visualized in Fig. G.2. It can be seen that while the ordering of the four conditions is the same in both cases, for the dependent case the worths of B and E_{ph} are closer to one another than in the independent case.

$$\begin{bmatrix} \pi_B & \pi_{E_{ph}} & \pi_{E_m} & \pi_O \end{bmatrix} = \begin{bmatrix} 0.348 & 0.335 & 0.174 & 0.143 \end{bmatrix} \tag{G.5}$$

$$\begin{bmatrix} \pi_B & \pi_{E_{ph}} & \pi_{E_m} & \pi_O \end{bmatrix} = \begin{bmatrix} 0.366 & 0.281 & 0.200 & 0.153 \end{bmatrix} \tag{G.6}$$

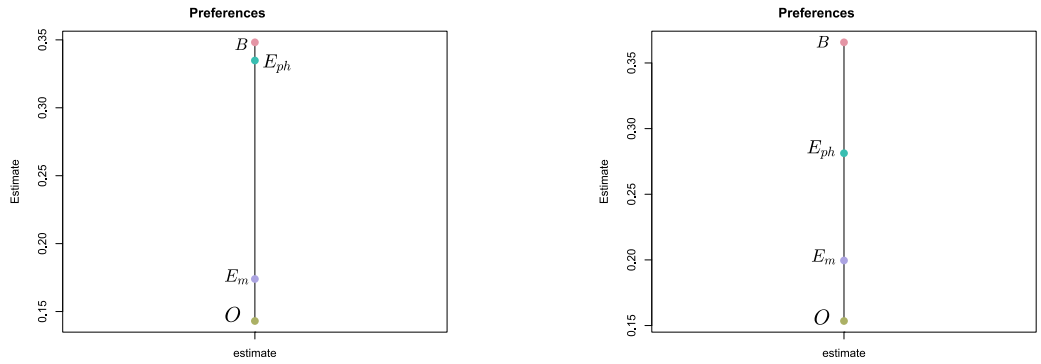

(a) Worth parameters from the dependent analysis

(b) Worth parameters from the independent analysis

Figure G.2: Comparison of the outputs from dependent and independent analysis of the `pattPC.fit` function

In the case of including subject or object covariates in the statistical modeling, a design matrix needs to be made, which includes the covariates together with the matrix of the pairwise comparison outcomes. The creation of the design matrix goes beyond the scope of this appendix. The reader is referred to the paper by Hatzinger and Dittrich [6] that describes the package functionality and their course given at WU Vienna *"Paired Comparison Preference Models"* [1]. There the underlying theory used in the **`prefmod`** package is presented together with many examples on how to use the different functions and extensions.

[1]The course material – lecture slides, homework assignments, and supporting code – is available on-line at: `http://statmath.wu-wien.ac.at/people/hatz/preference/`

Bibliography

[1] Sunjoo K. Advani. *The Kinematic Design of Flight Simulator Motion-Bases*. PhD thesis, Faculty of Aerospace Engineering, Delft University of Technology, 1998.

[2] Ammar Ammar and Devavrat Shah. Ranking: Compare, don't score. In *2011 49th Annual Allerton Conference on Communication, Control, and Computing, Allerton 2011*, pages 776–783. IEEE, sep 2011. ISBN 9781457718168. doi: 10.1109/Allerton.2011.6120246.

[3] Ralph Allan Bradley and Milton E Terry. Rank analysis of incomplete block designs: I. the method of paired comparisons. *Biometrika*, 39(3/4):324–345, 1952.

[4] Manuela Cattelan. Models for paired comparison data: A review with emphasis on dependent data. *Statistical Science*, pages 412–433, 2012.

[5] Andy Field. *Discovering Statistics Using SPSS*. ISM Introducing Statistical Methods. SAGE Publications Ltd., second edition, 2005. ISBN 10 0-7619-4451-6.

[6] Reinhold Hatzinger and Regina Dittrich. Prefmod: An r package for modeling preferences based on paired comparisons, rankings, or ratings. *Journal of Statistical Software*, 48(10):1–31, 2012.

[7] Harm M. Heerspink, Walter R. Berkouwer, Olaf Stroosma, Marinus M. van Paassen, Max Mulder, and Jan A. Mulder. Evaluation of Vestibular Thresholds for Motion Detection in the SIMONA Research Simulator. In *Proceedings of the AIAA Modeling and Simulation Technologies Conference and Exhibit, August 15–18, San Francisco (CA)*, number AIAA-2005-6502, 2005.

[8] SJ Hodge, P Perfect, GD Padfield, and MD White. Optimising the vestibular cues available from a short stroke hexapod motion platform. In *Proceedings of the 67th Ann Forum Am Helicopter Soc, Virginia Beach, VA*, 2011.

[9] J.A Mulder and A.C. in 't Veld. *Flight Dynamics Assignment AE3212-II*. Faculty of Aerospace Engineering, Delft University of Technology, January 2018.

[10] J.A Mulder, W.H.J.J van Staveren, J.C. van der Vaart, E. de Weerdt, C.C. de Visser, A.C. in 't Veld, and E. Mooij. *Lecture notes in Flight Dynamics*. Faculty of Aerospace Engineering, Delft University of Technology, March 2013.

[11] Louis L Thurstone. A law of comparative judgment. *Psychological review*, 34(4):273, 1927.

[12] Kristi Tsukida and Maya R Gupta. How to analyze paired comparison data. Technical report, Washington University Seattle Department of Electrical Engineering, 2011.

[13] Georgios N. Yannakakis and Héctor P. Martínez. Ratings are Overrated! *Frontiers in ICT*, 2:13, jul 2015. ISSN 2297-198X. doi: 10.3389/fict.2015.00013.

[14] L. E. Zaichik, V. V. Rodchenko, I. V. Rufov, Y. P. Yashin, and A. D. White. Acceleration Perception. In *Proceedings of the AIAA Modeling and Simulation Technologies Conference and Exhibit, Portland (OR)*, number AIAA-1999-4334, 1999.